Introduction to Nuclear Fusion as An Energy Source

Po-Yu Chang

Institute of Space and Plasma Sciences, National Cheng Kung University

Lecture 11

2026 spring semester

Tuesday 9:00-12:00

Materials:

https://capst.ncku.edu.tw/PGS/index.php/teaching/

Online courses:

https://reurl.cc/GaLmxA (Google meet)

2026/5/21 updated

Pitch angle = 0°

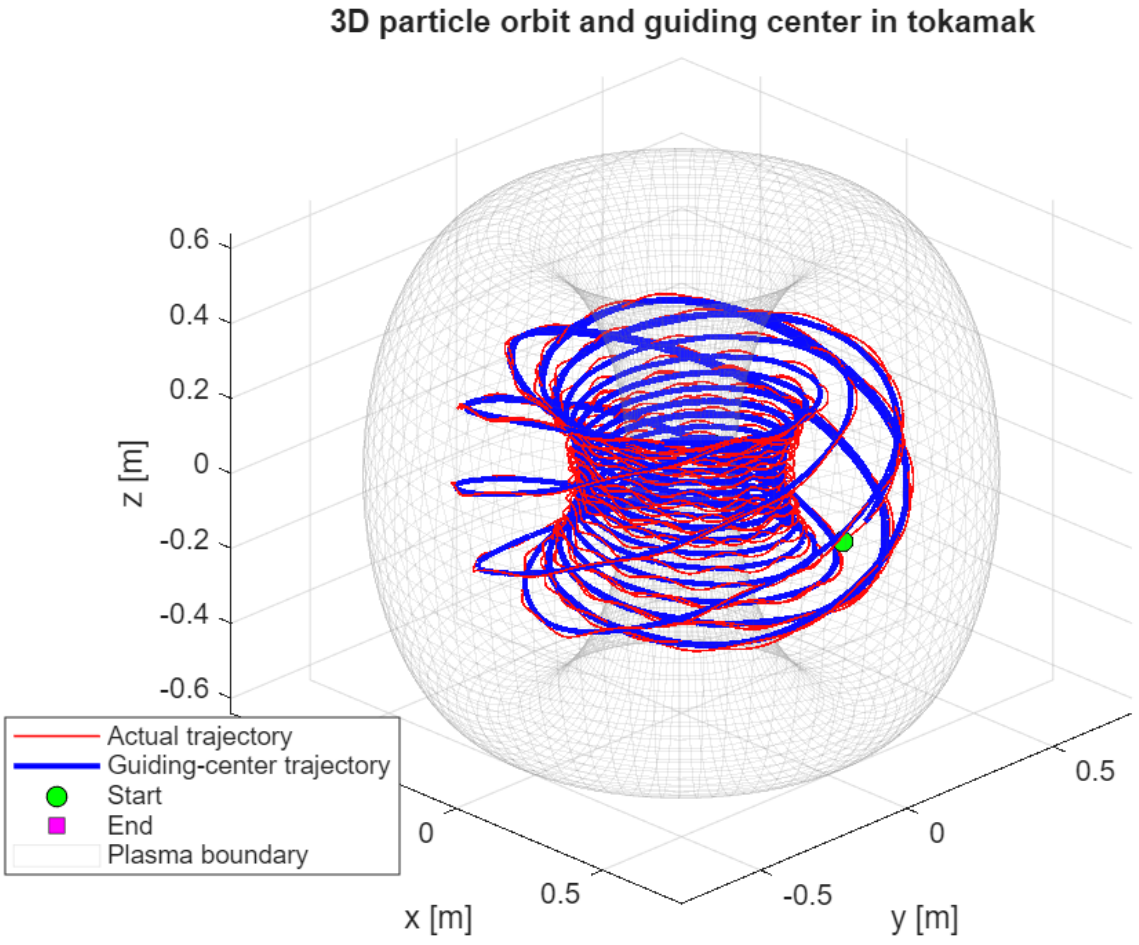

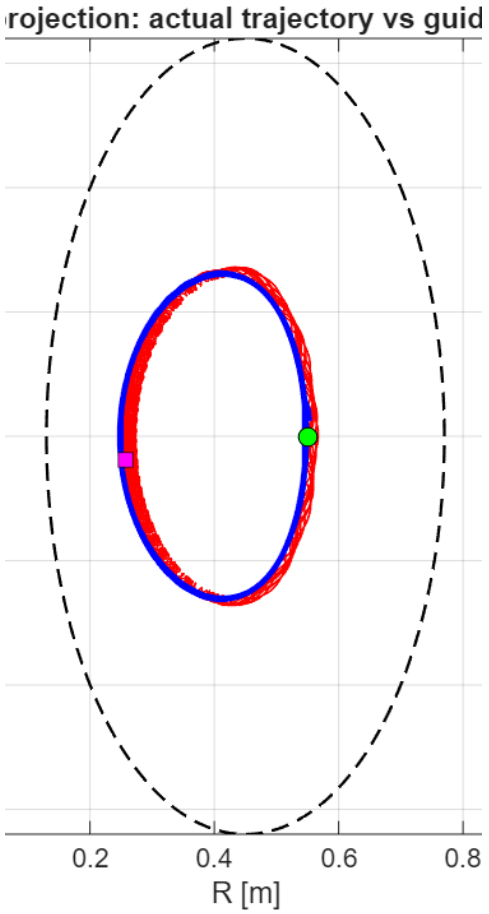

Pitch angle = 0°

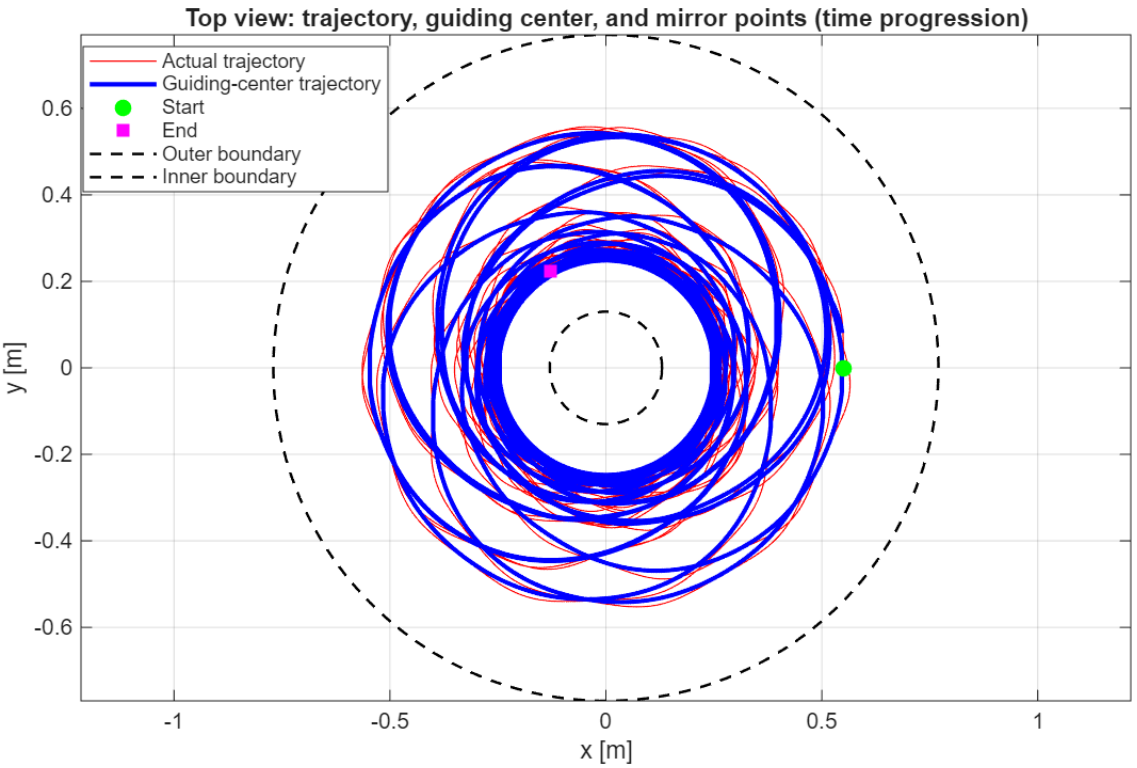

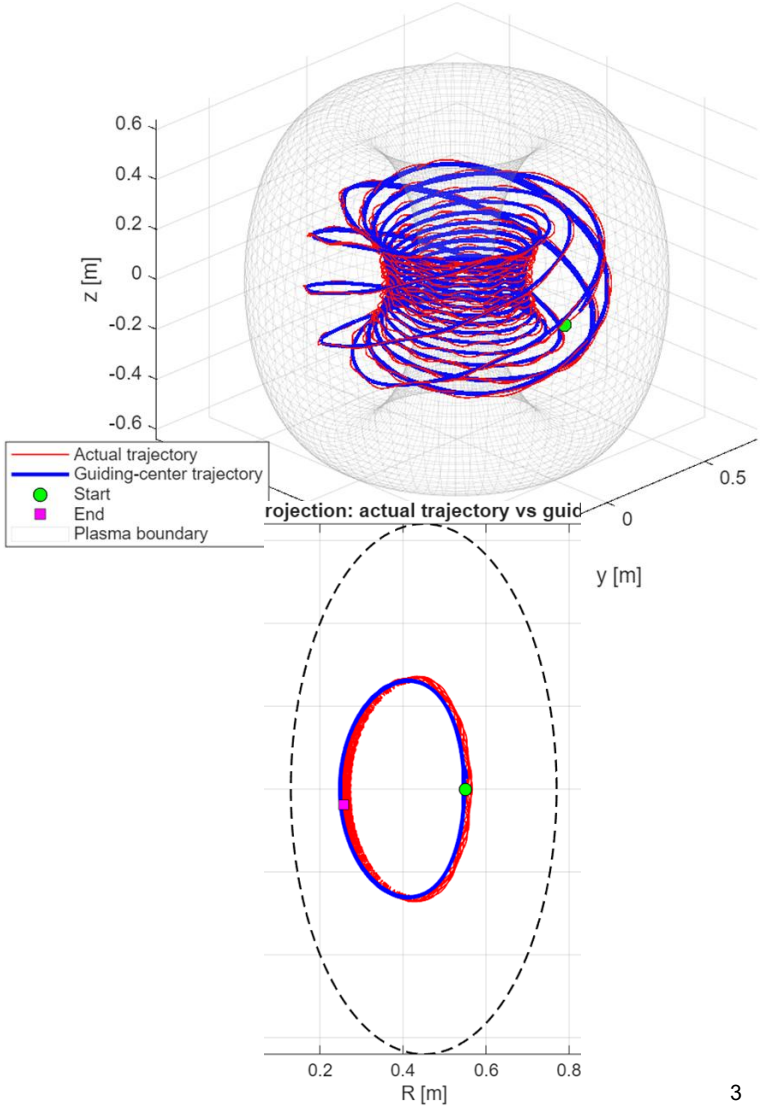

Pitch angle = 0°

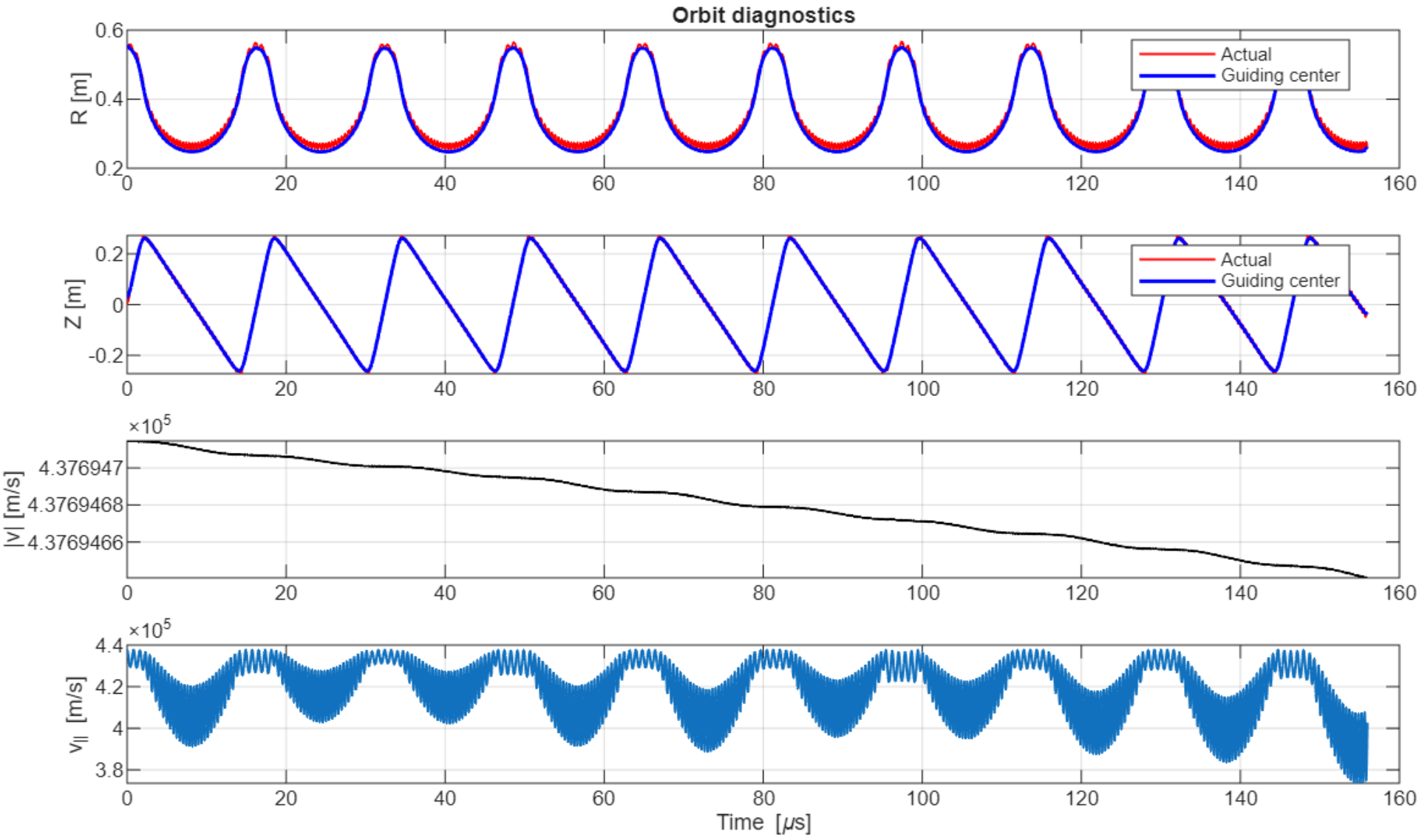

Pitch angle = 15°

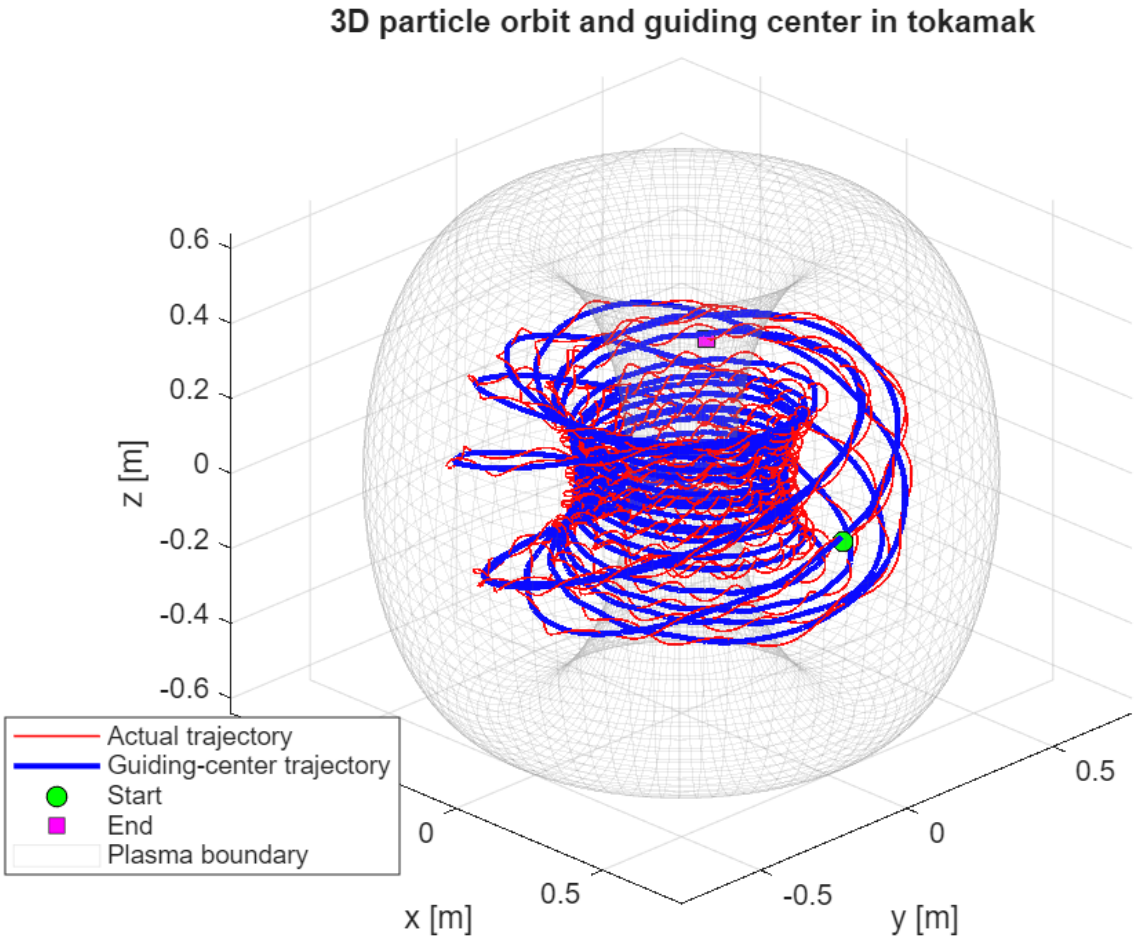

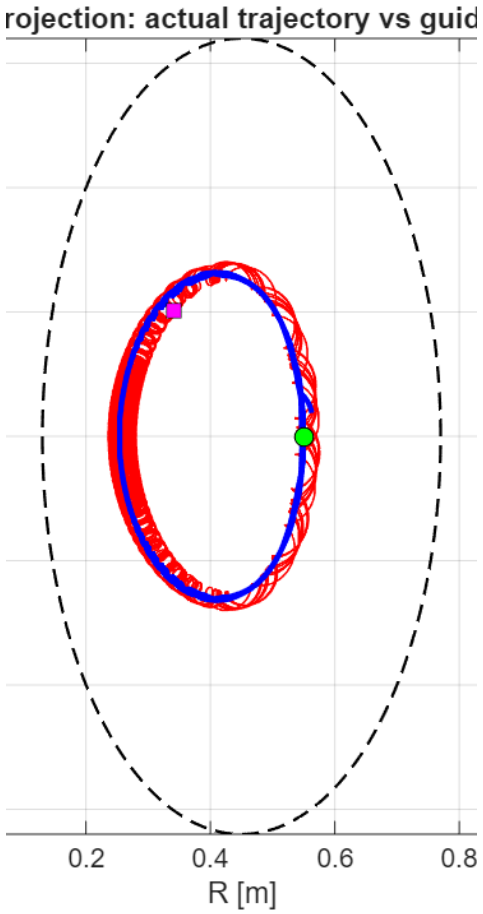

Pitch angle = 15°

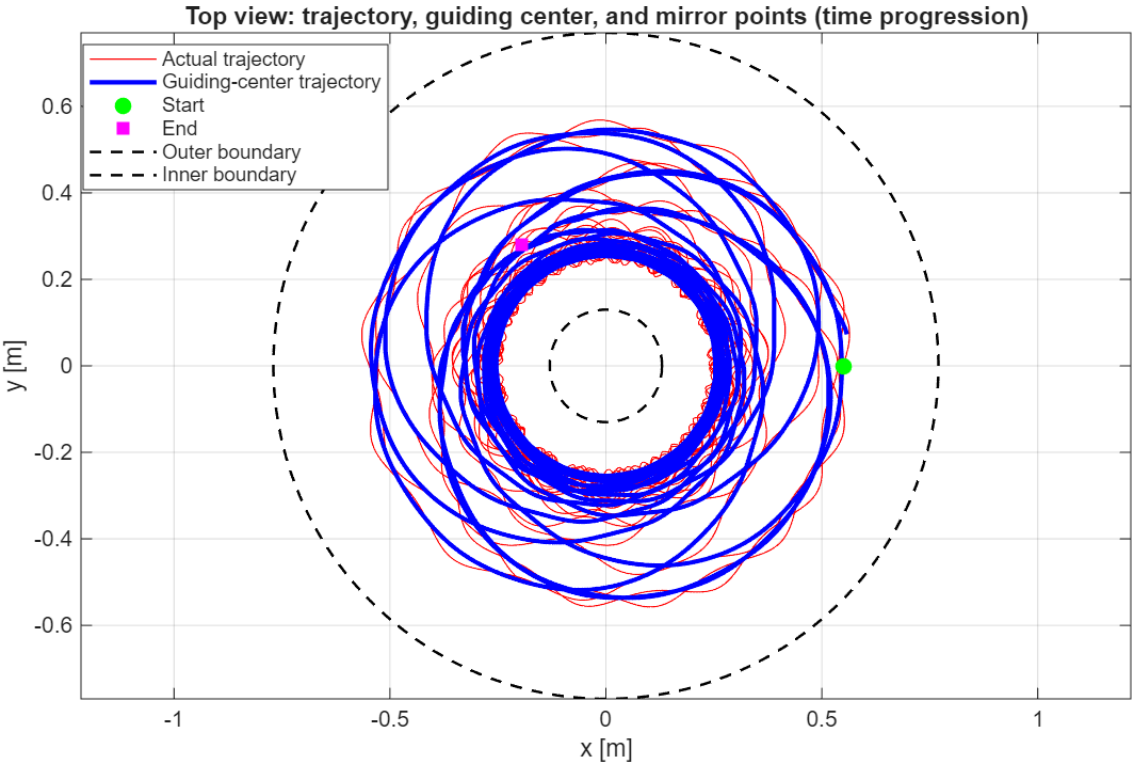

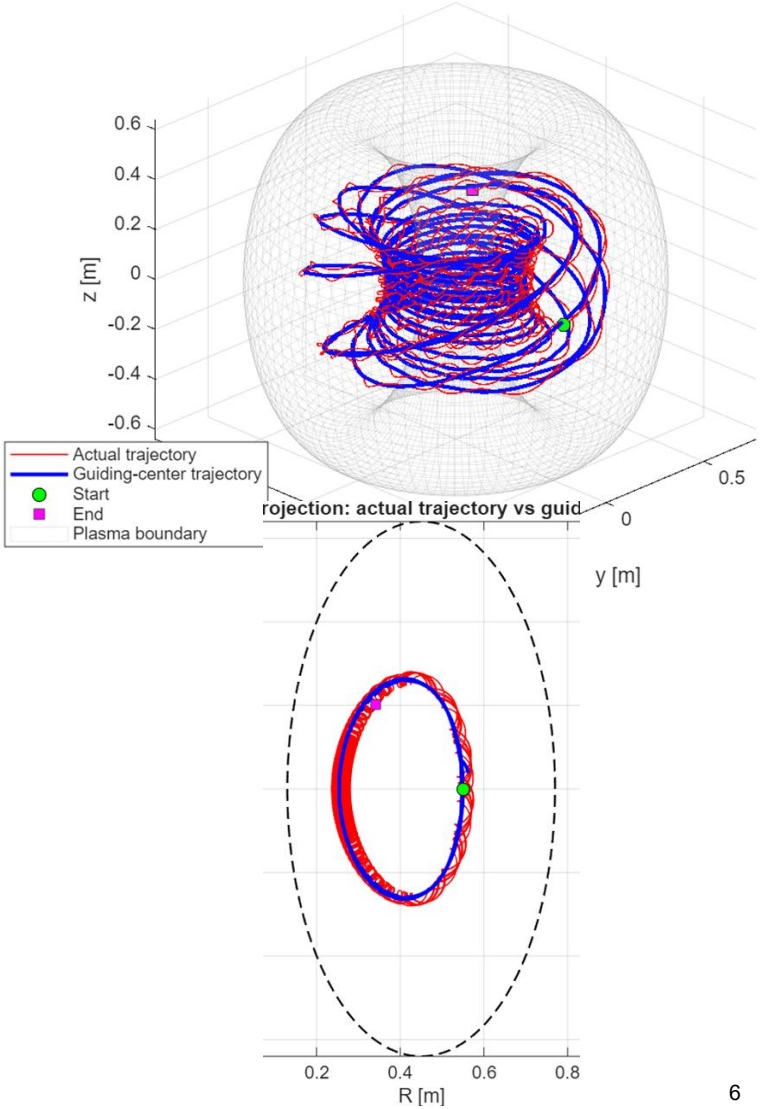

Pitch angle = 15°

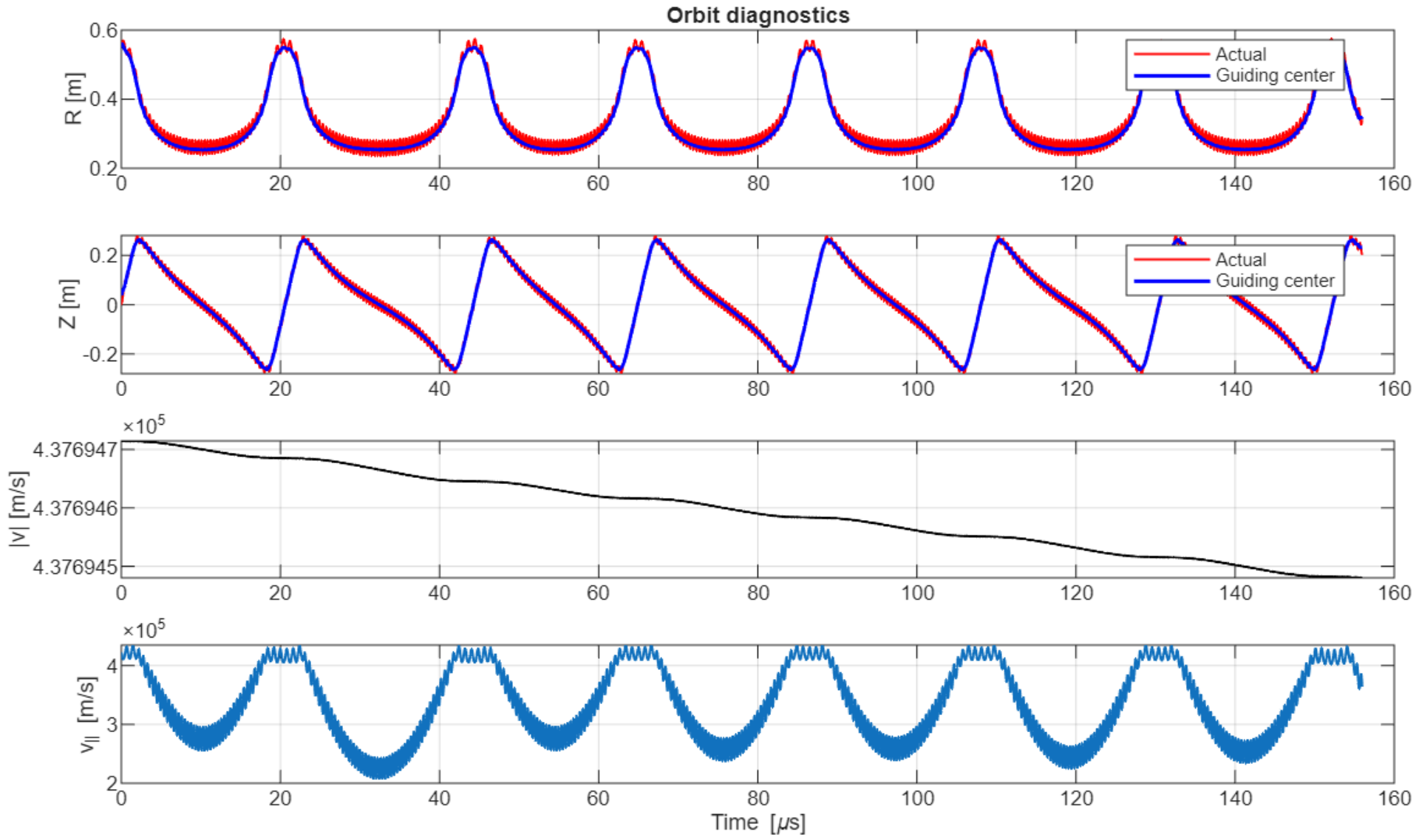

Pitch angle = 30°

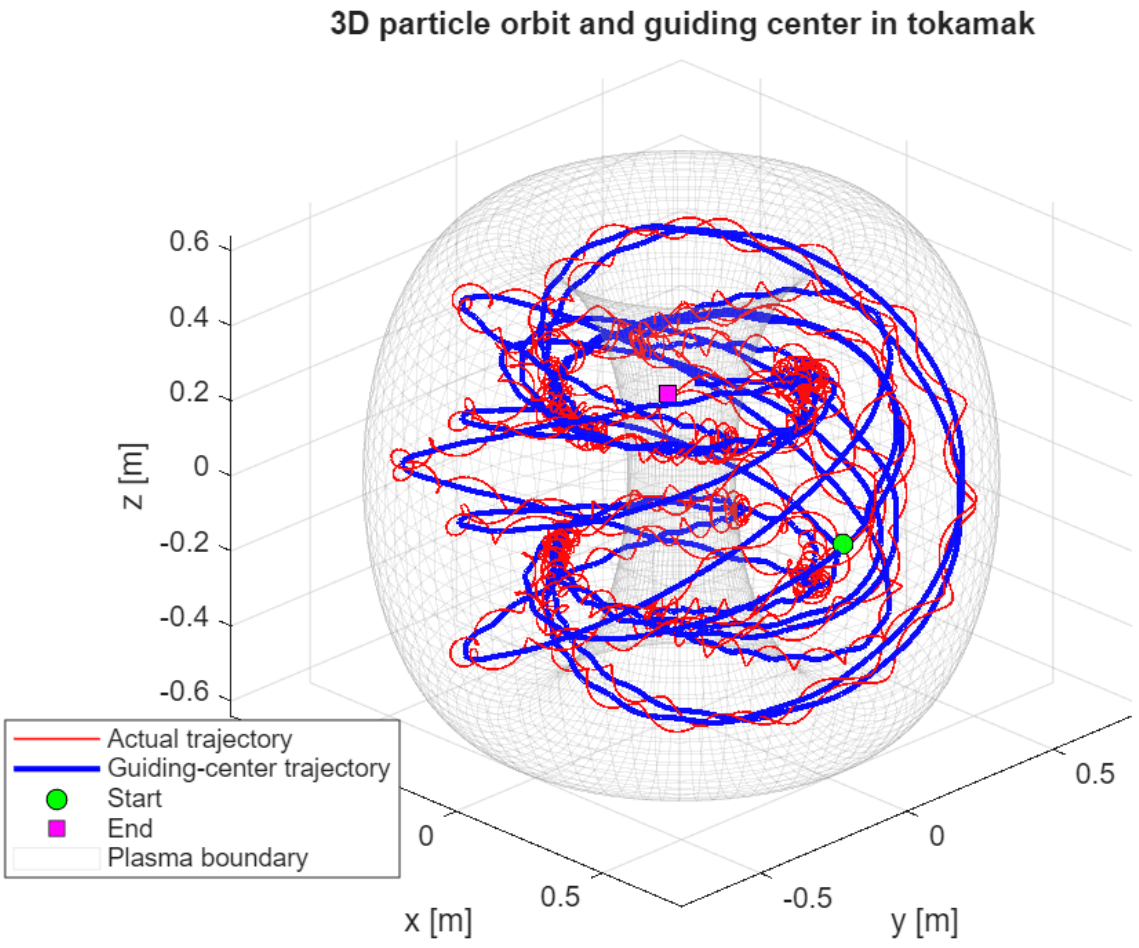

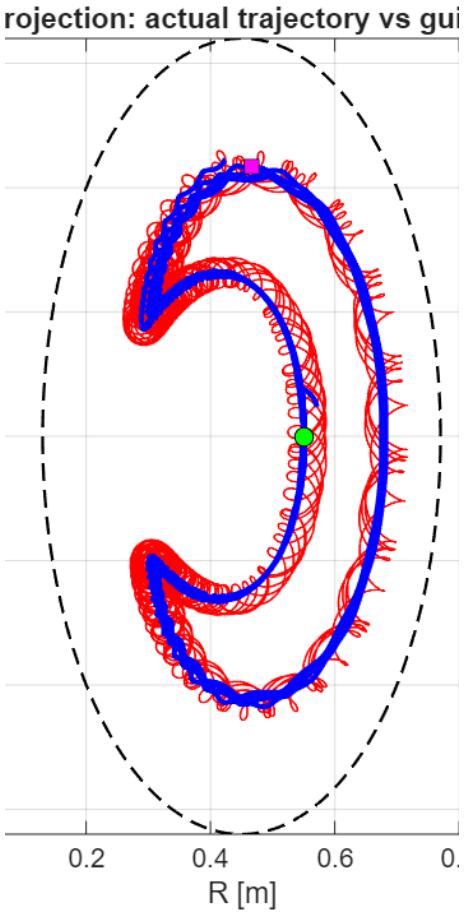

Pitch angle = 30°

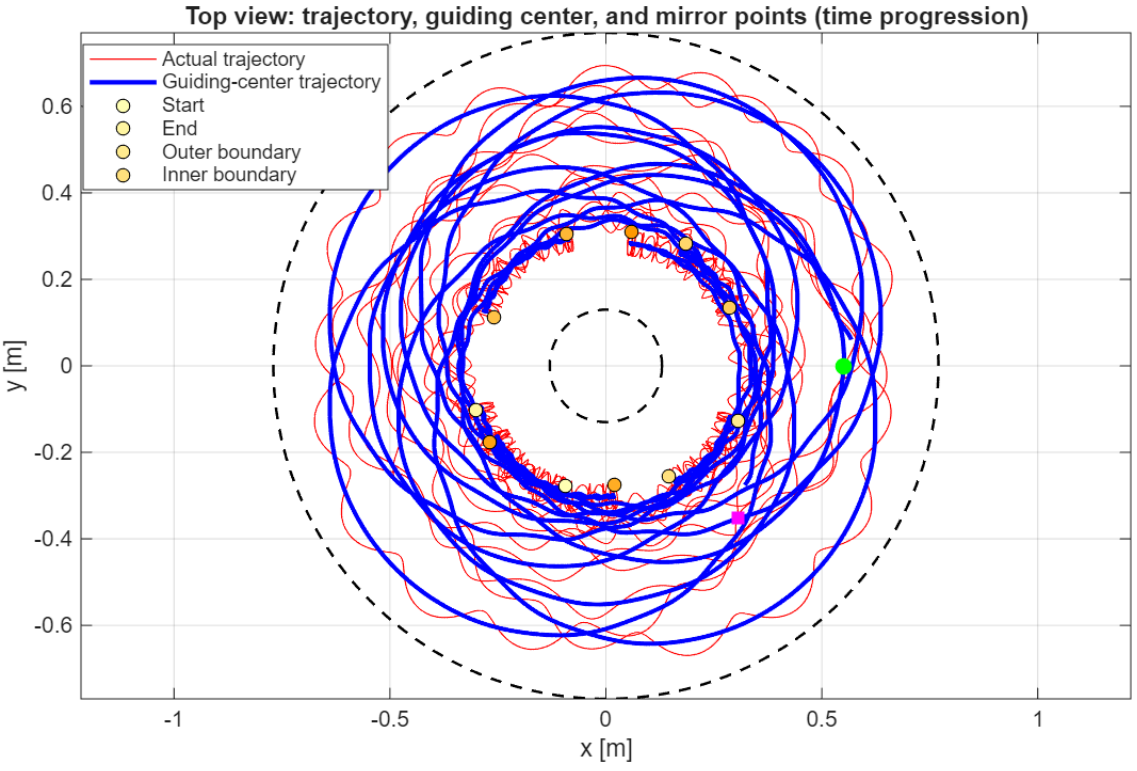

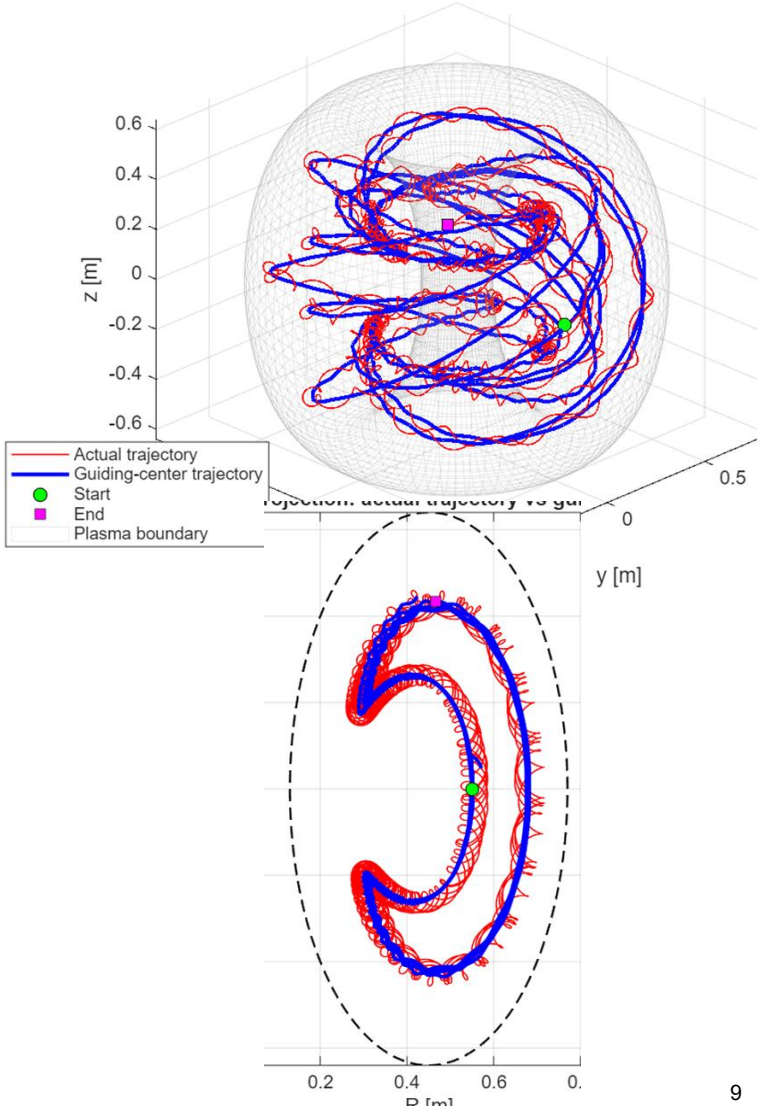

Pitch angle = 30°

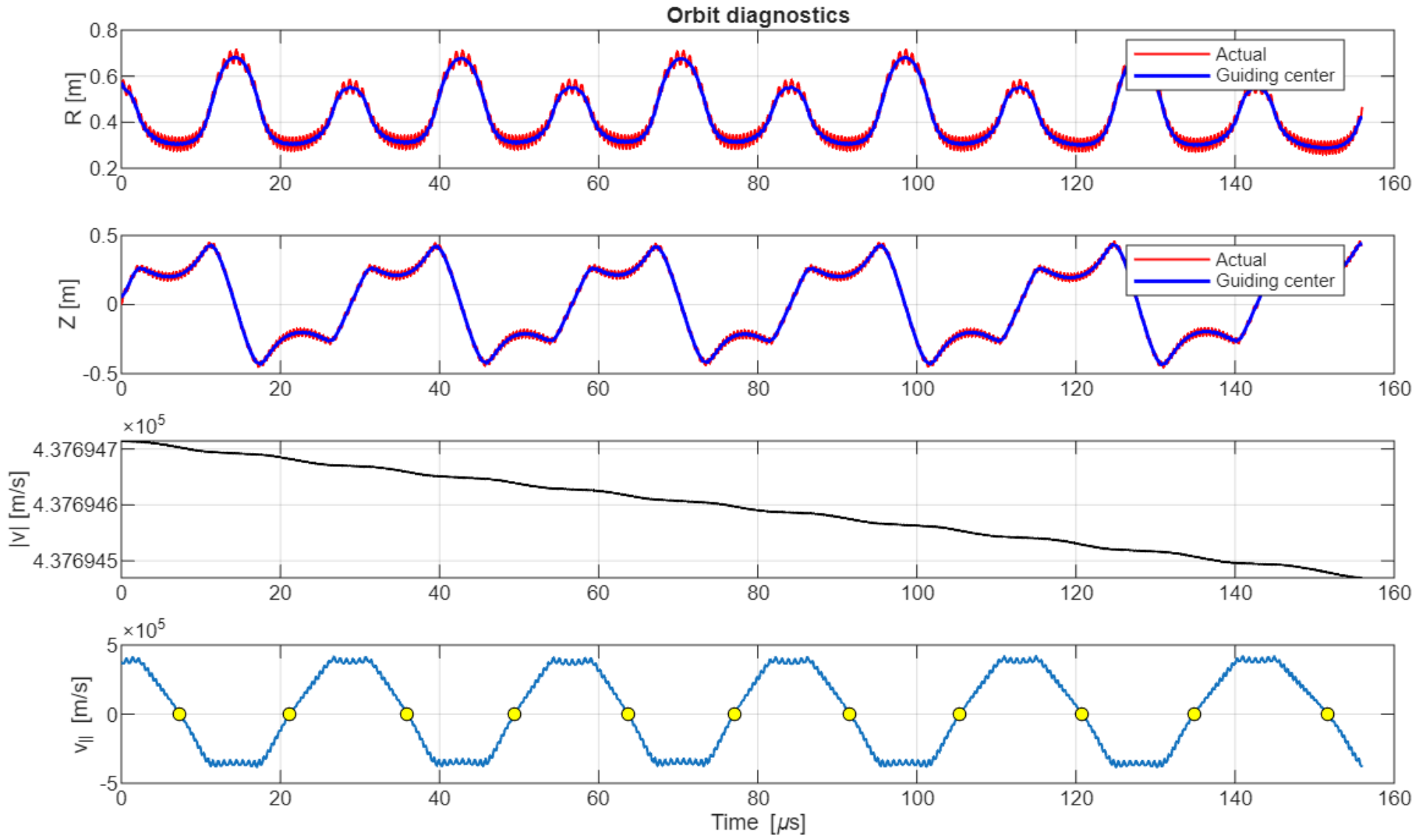

Pitch angle = 45°

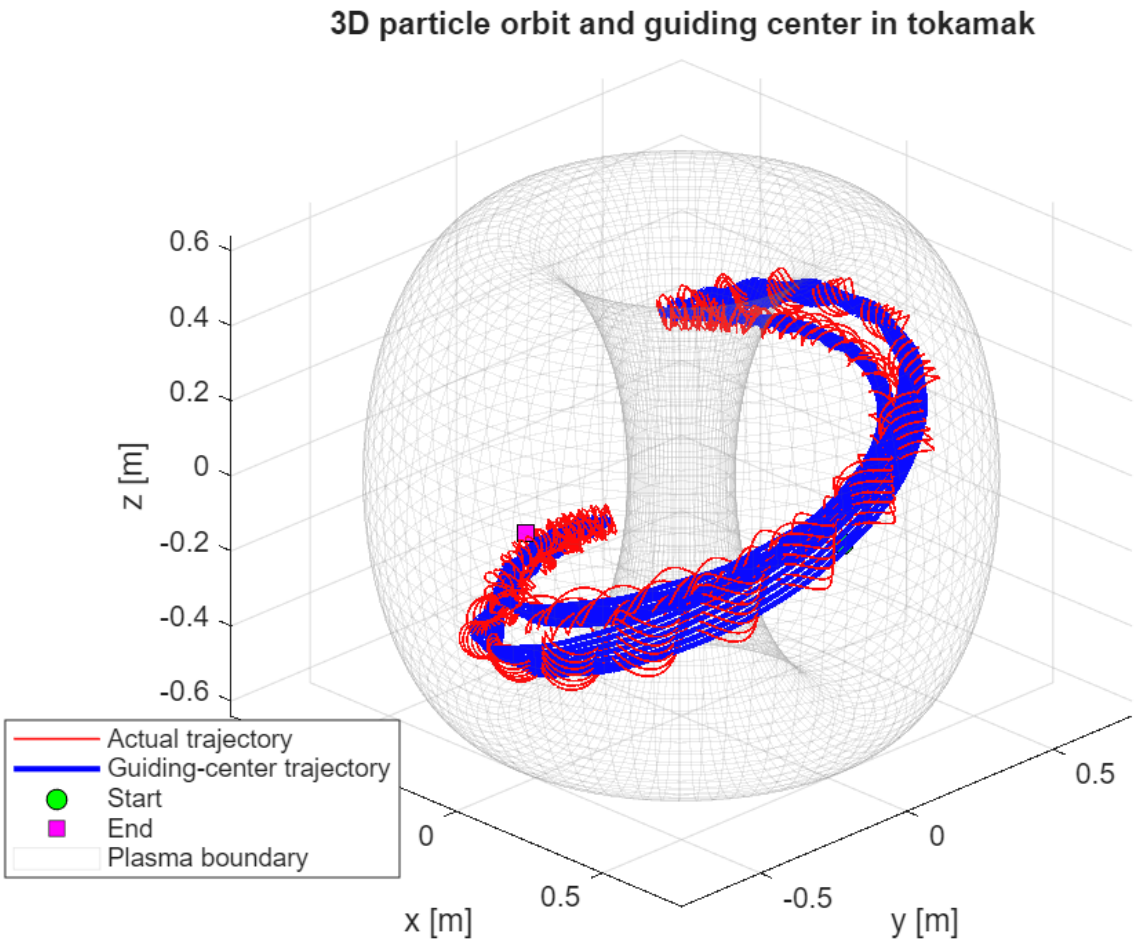

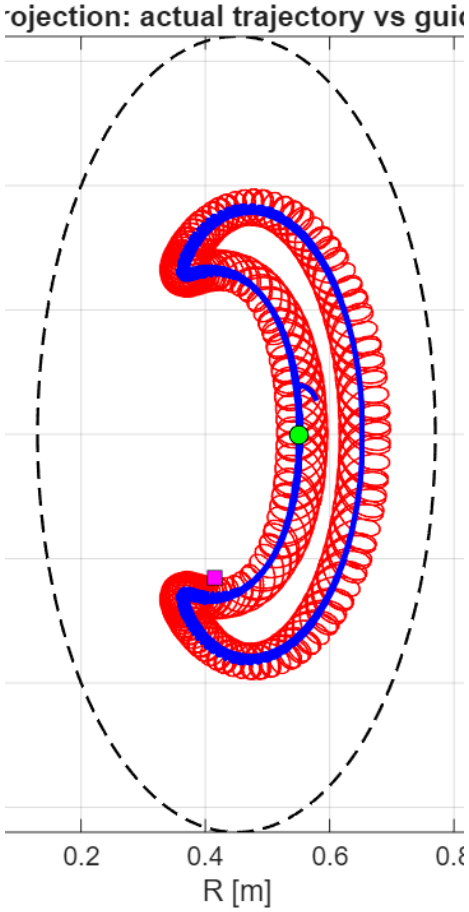

Pitch angle = 45°

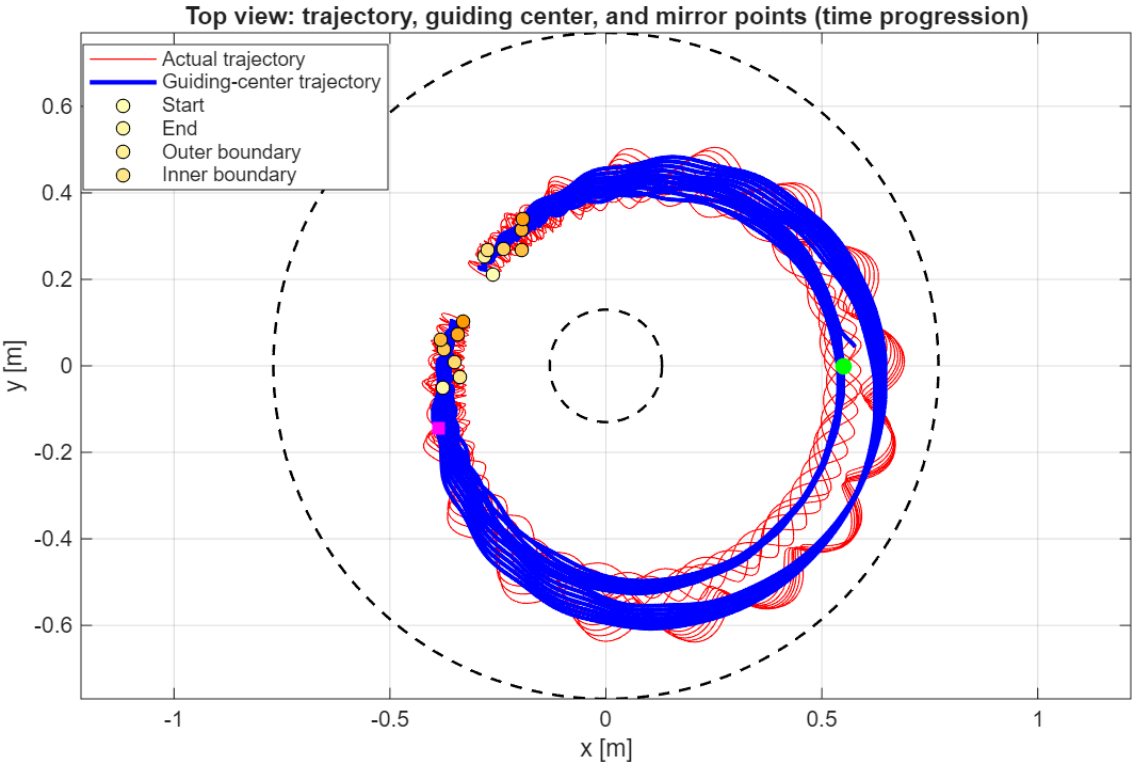

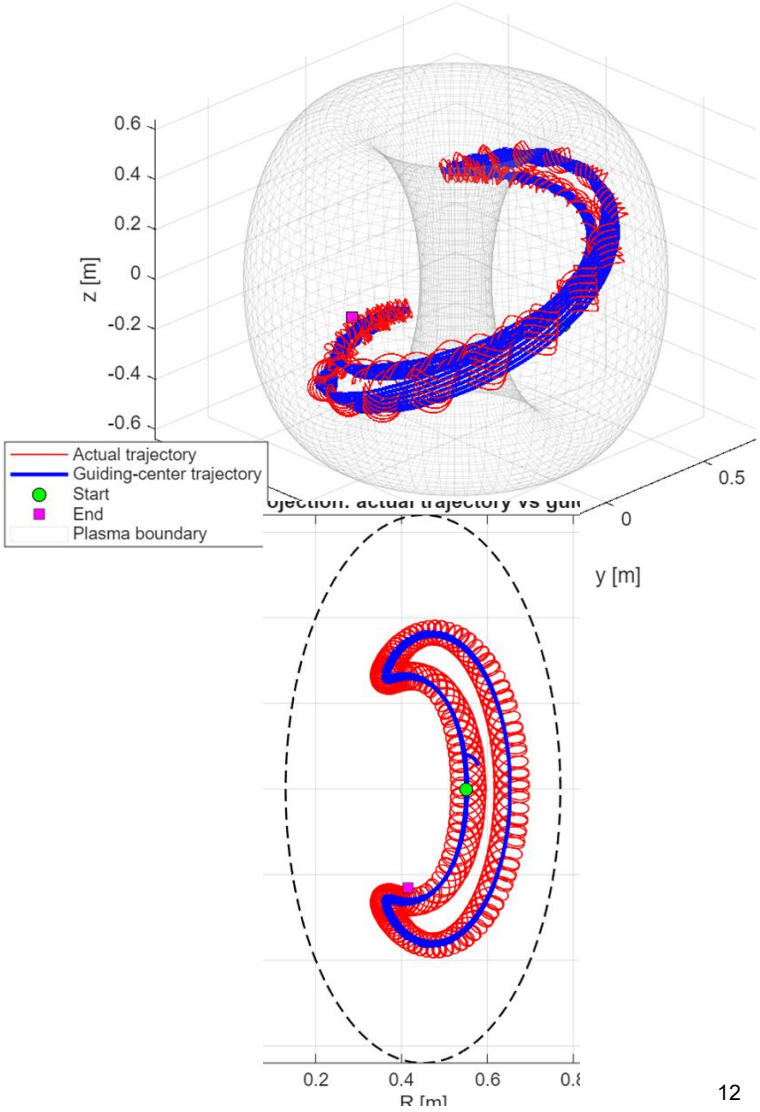

Pitch angle = 45°

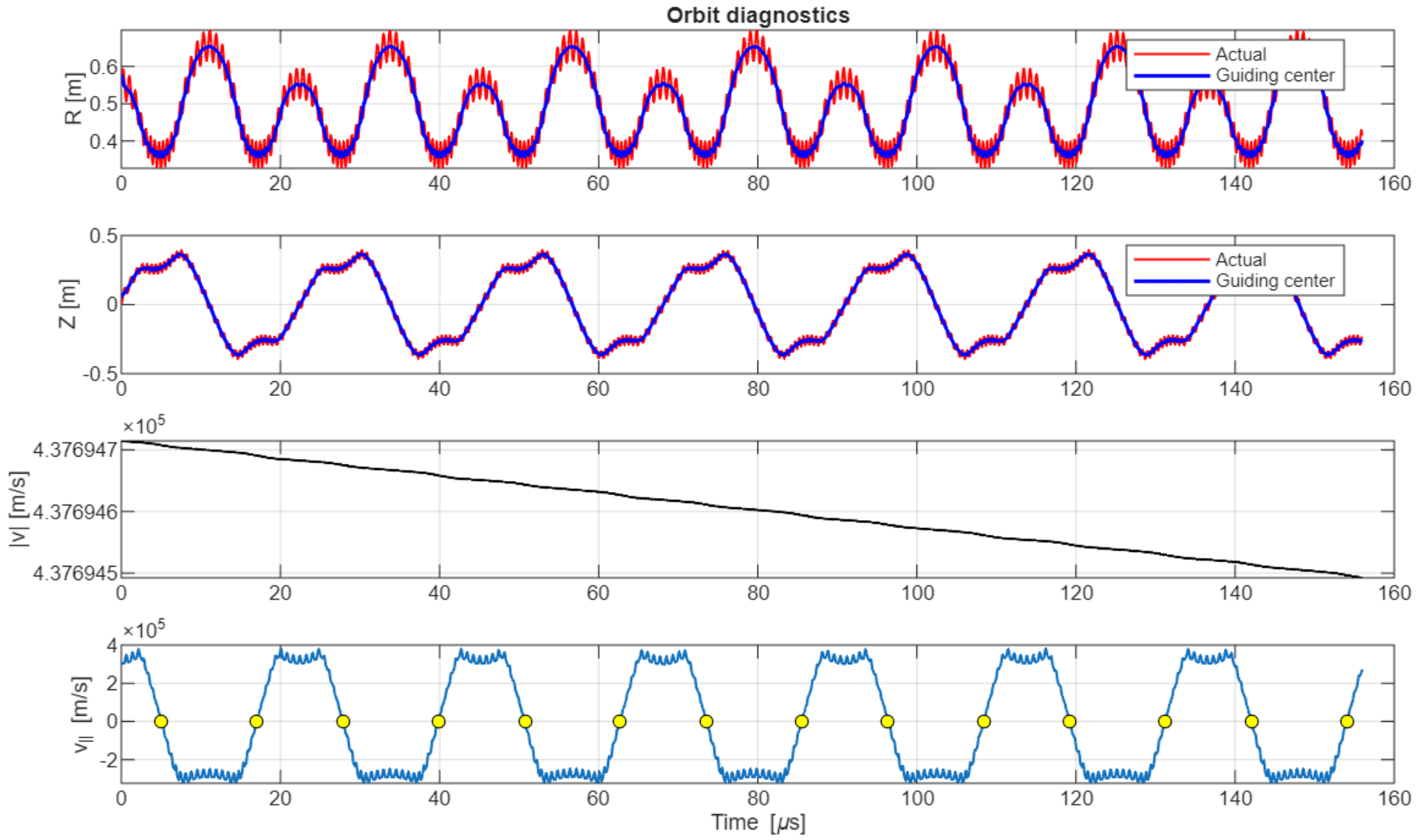

Pitch angle = 60°

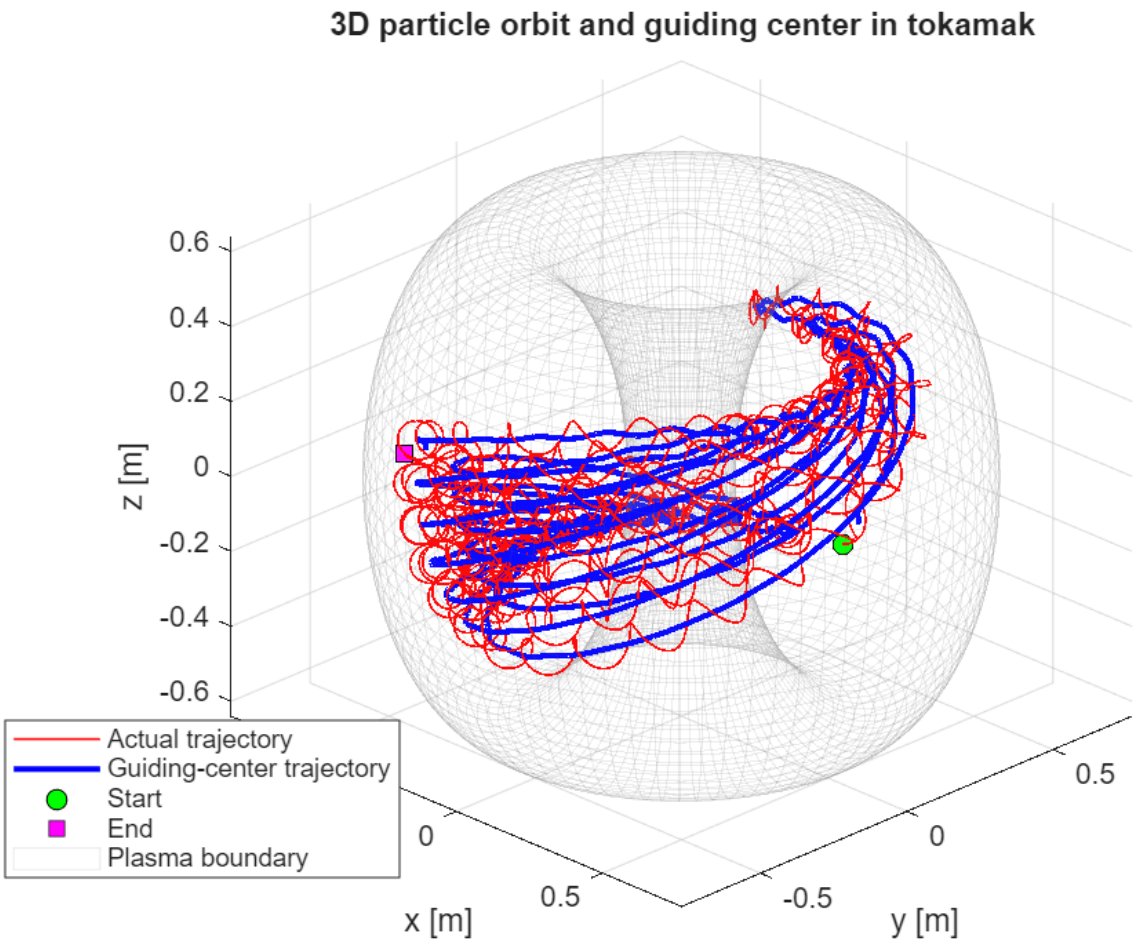

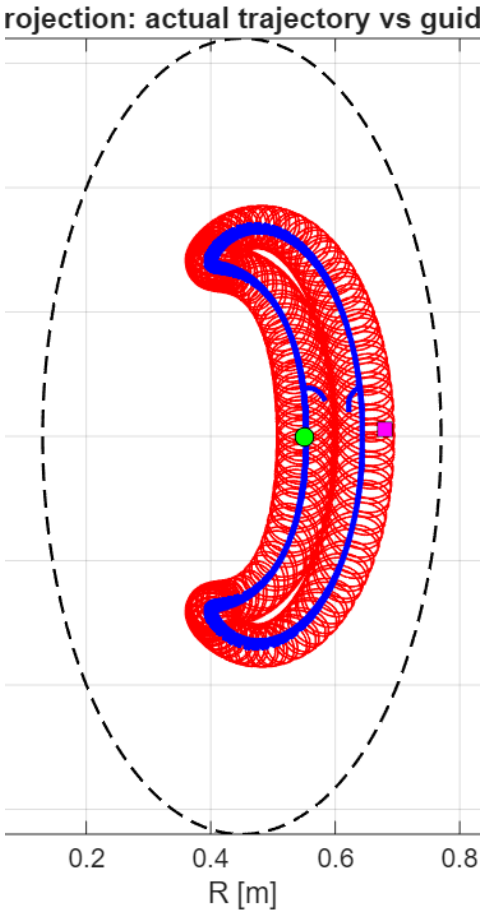

Pitch angle = 60°

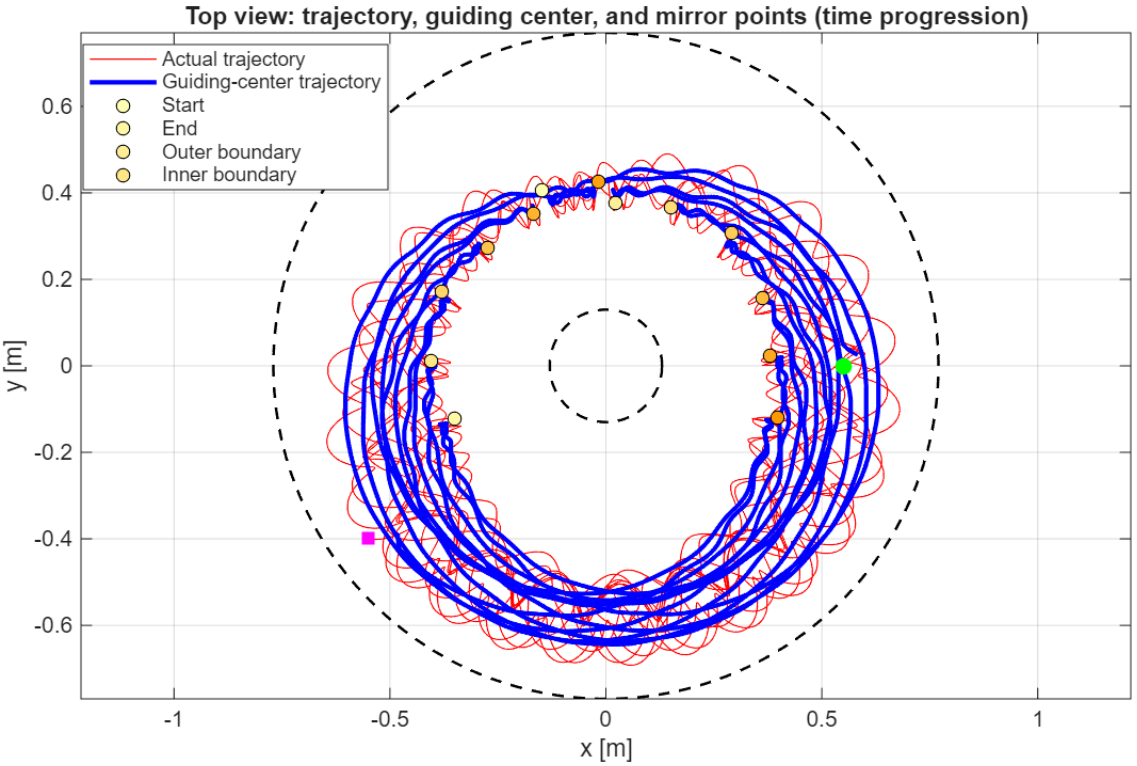

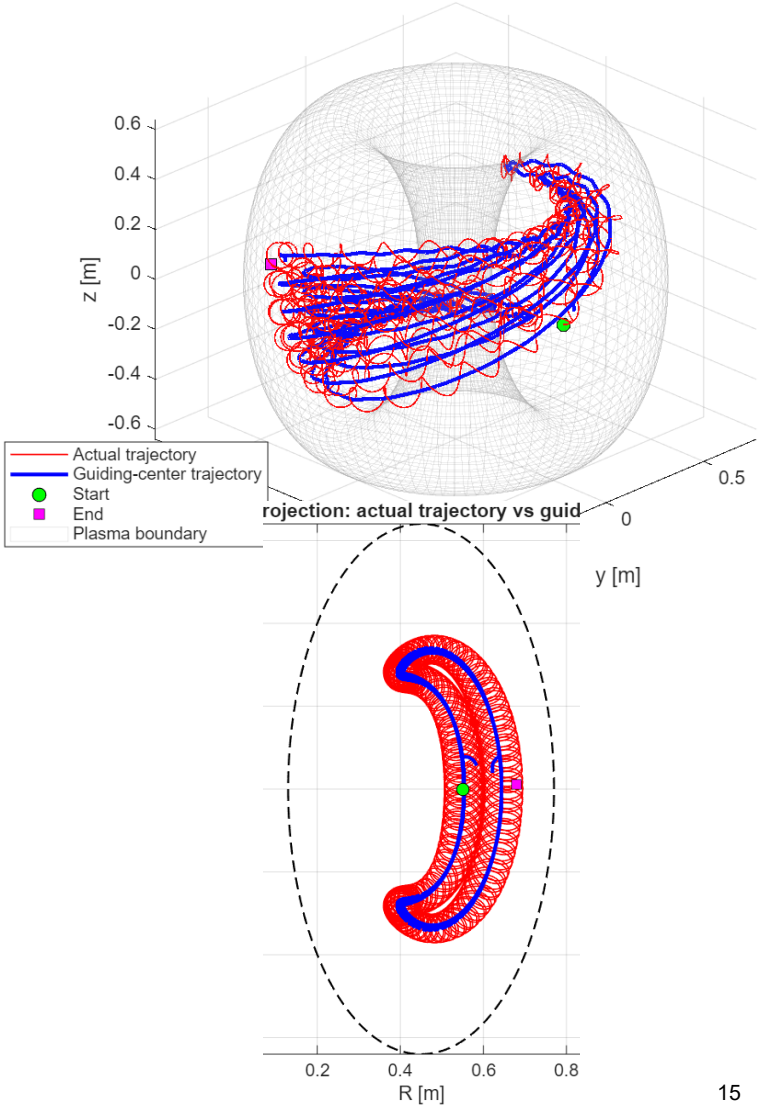

Pitch angle = 60°

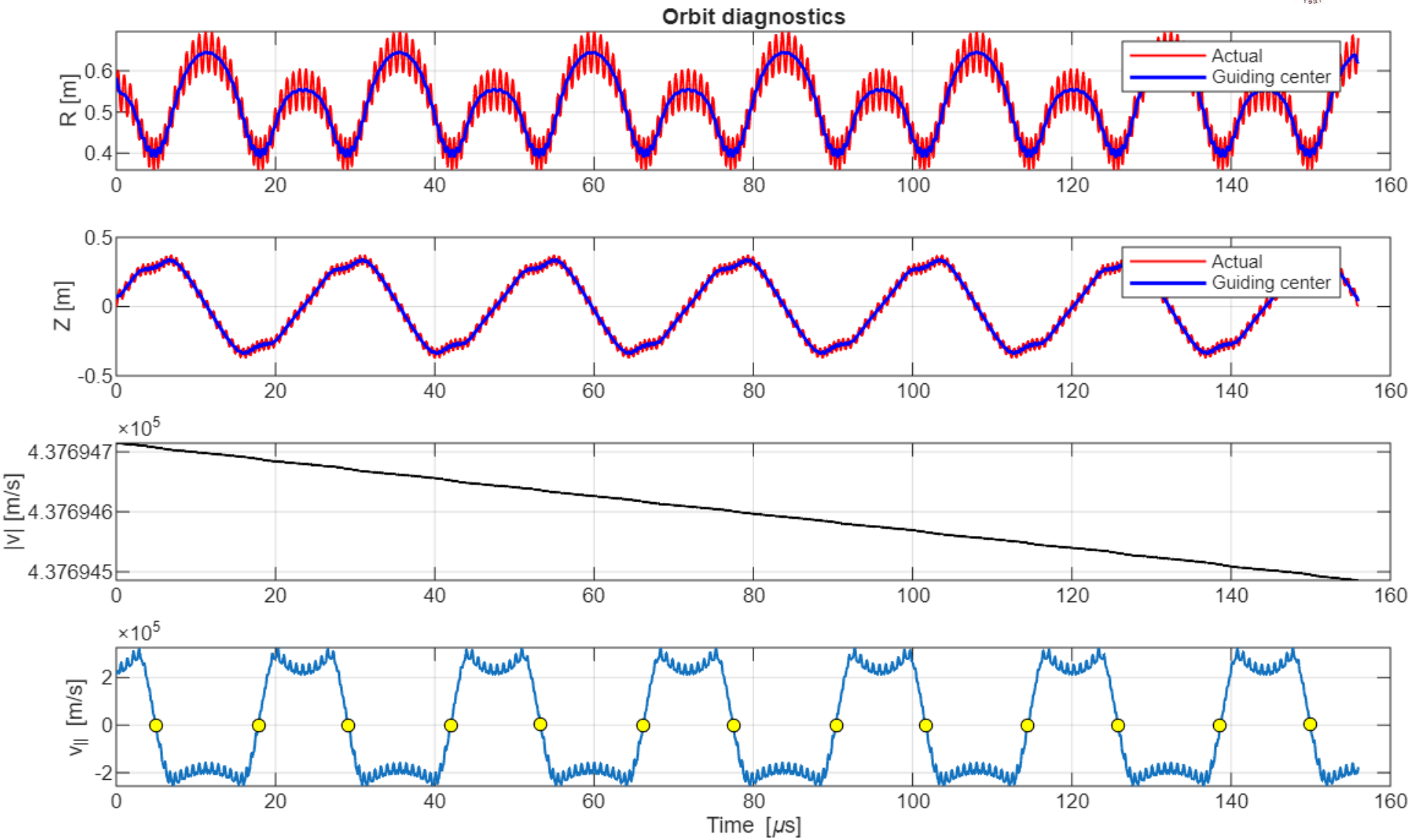

Pitch angle = 75°

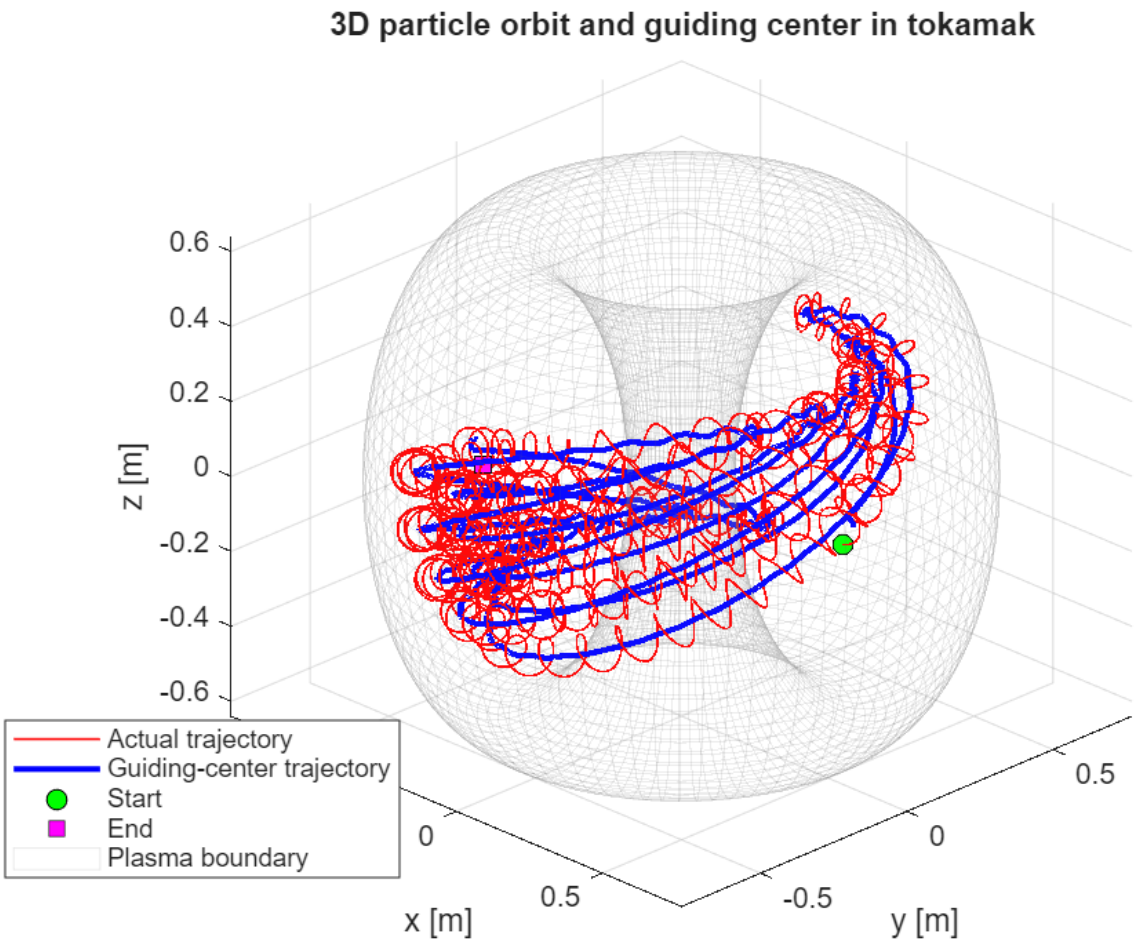

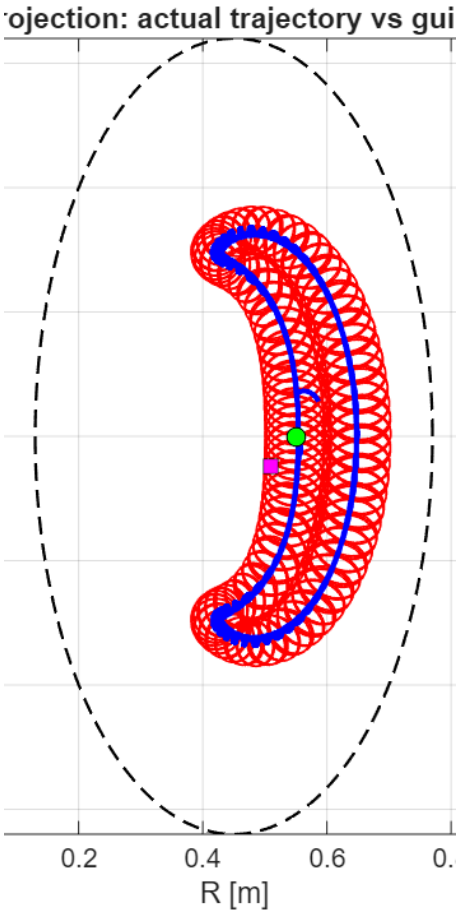

Pitch angle = 75°

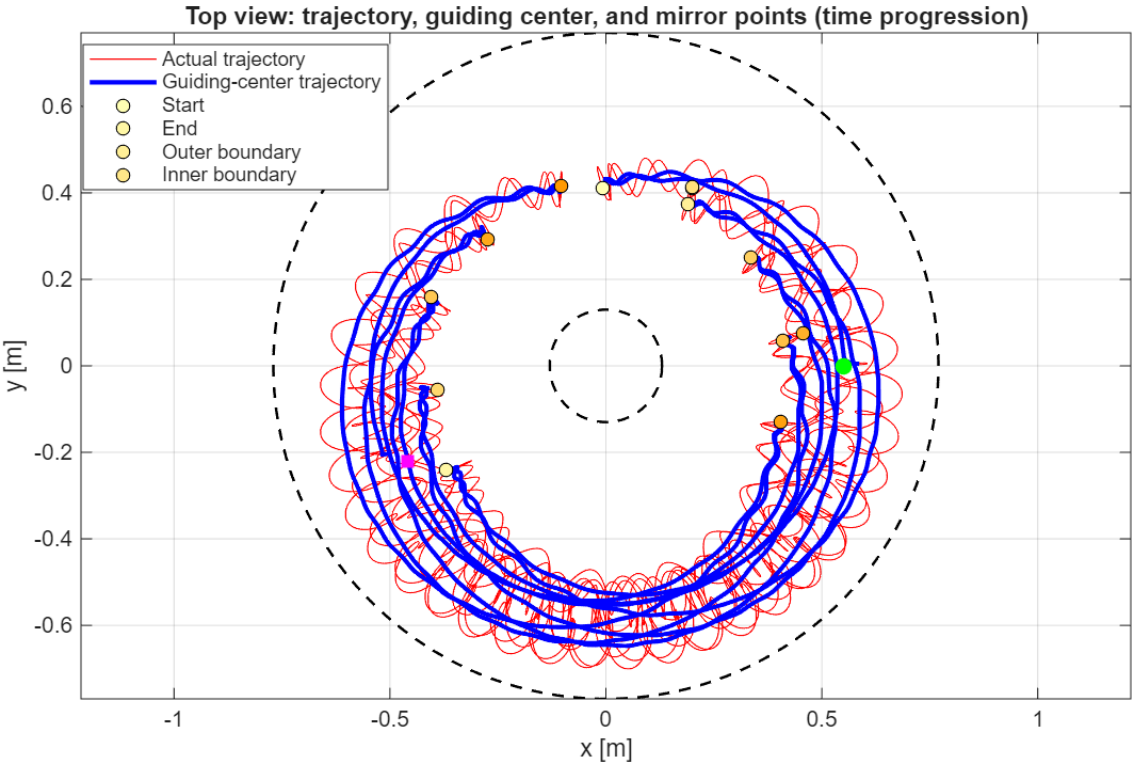

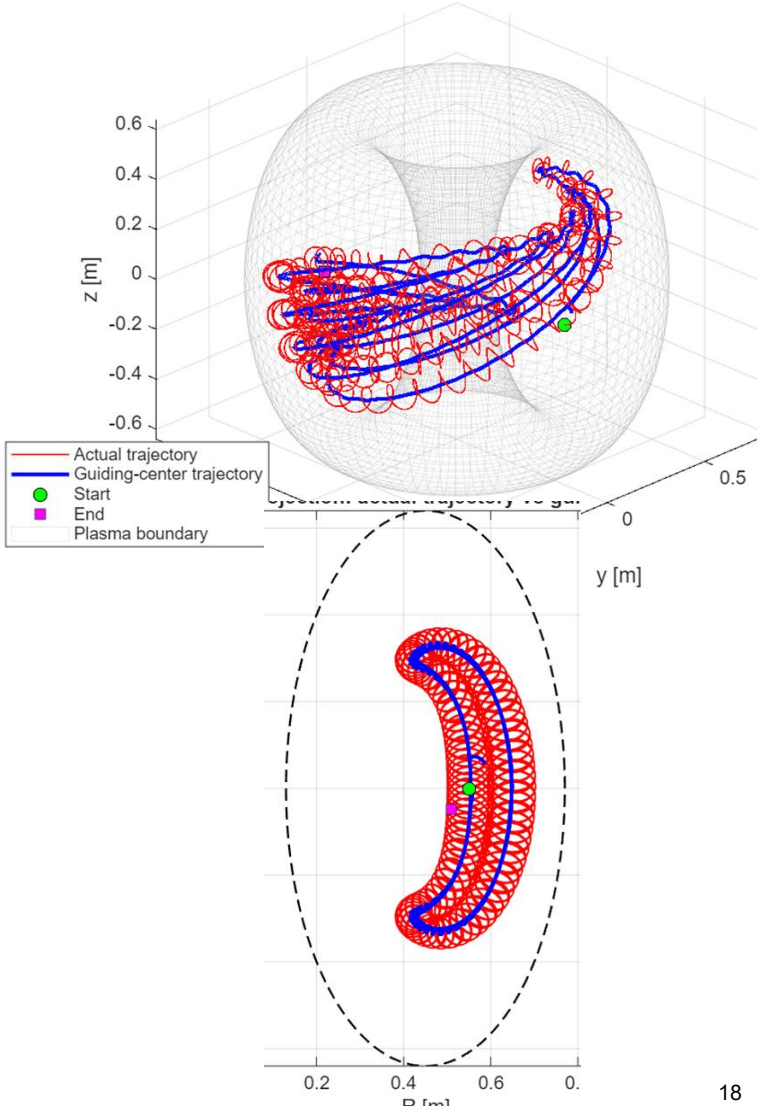

Pitch angle = 75°

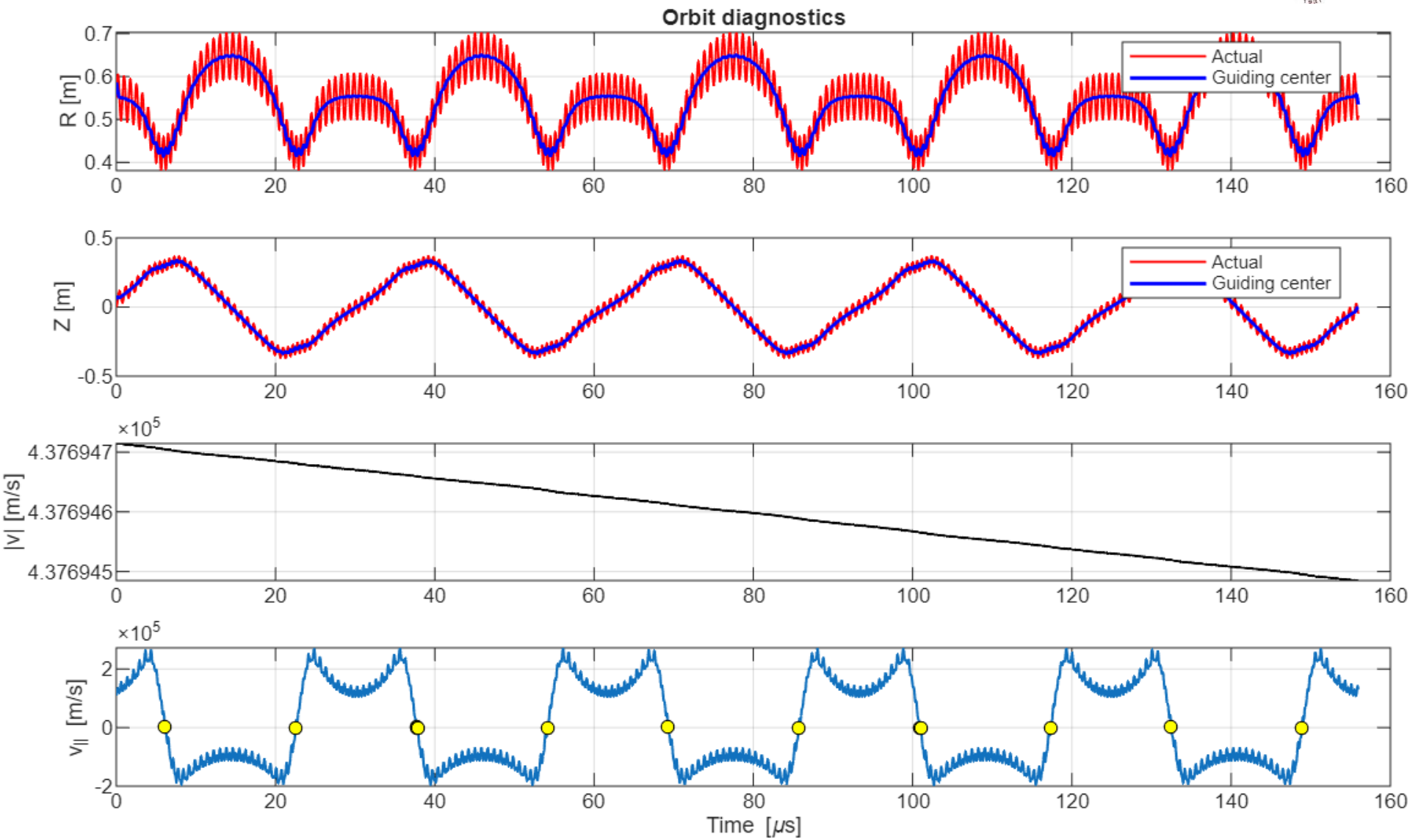

Pitch angle = 90°

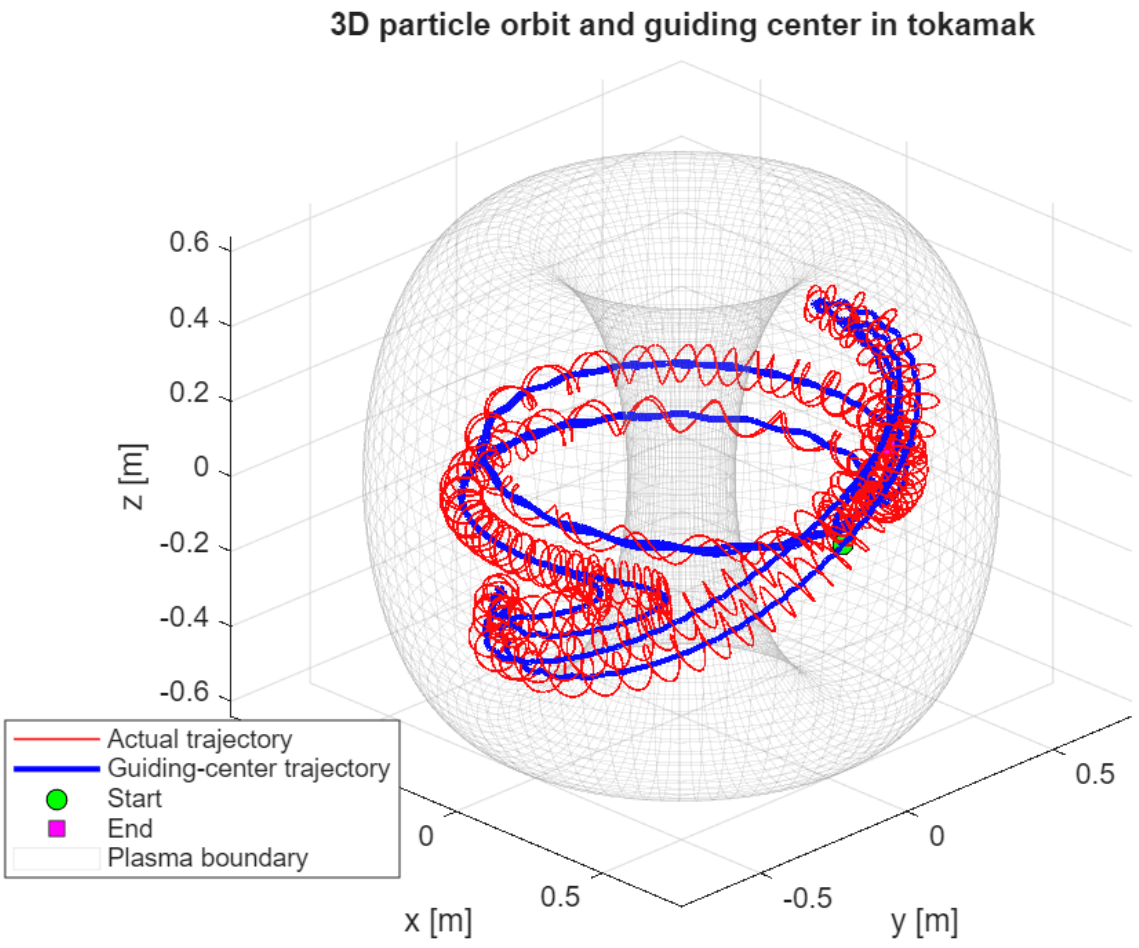

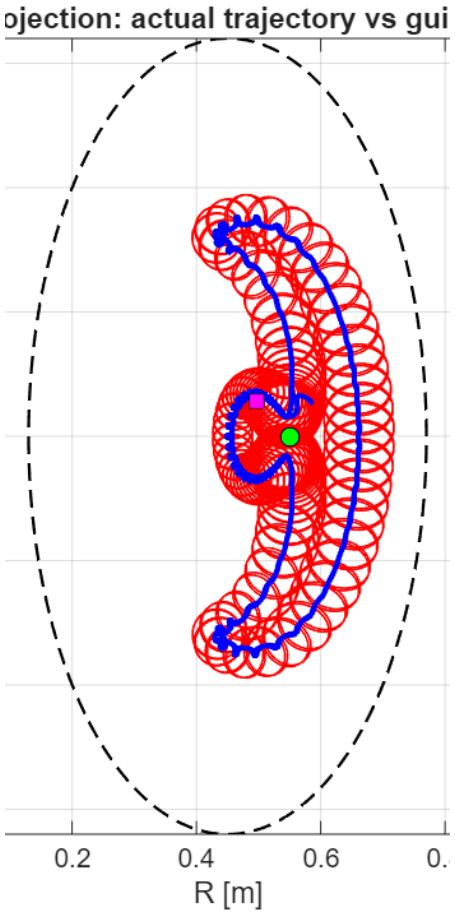

Pitch angle = 90°

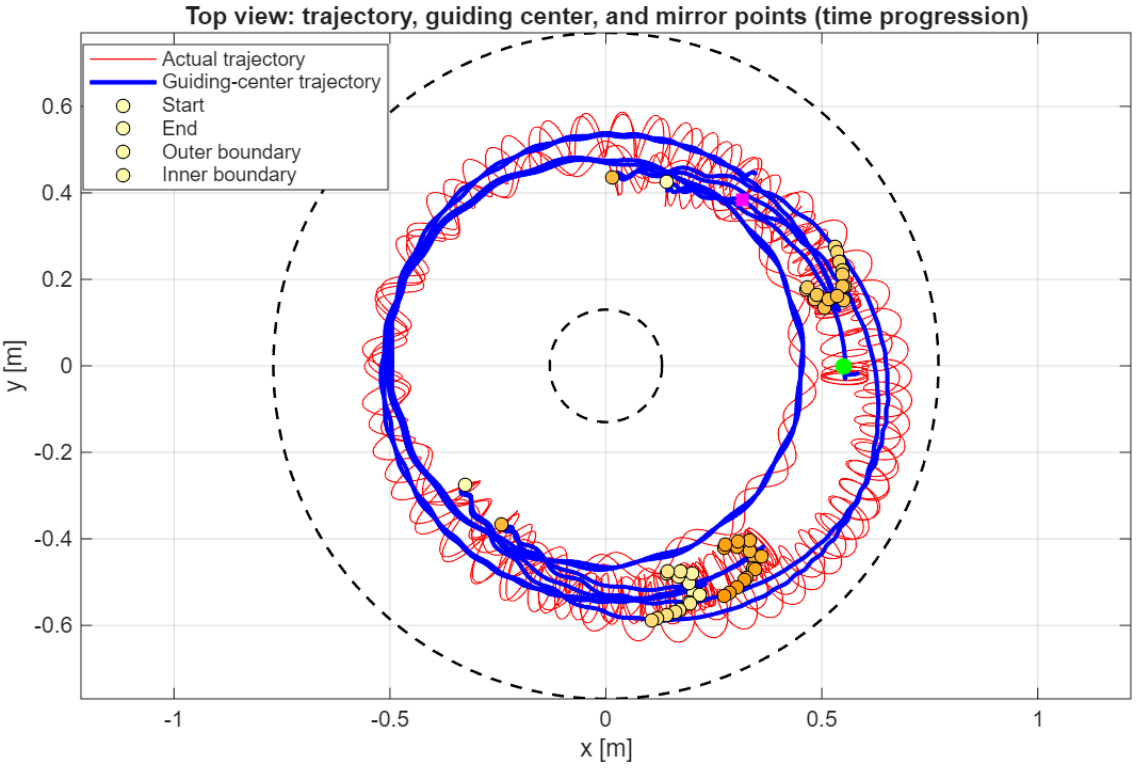

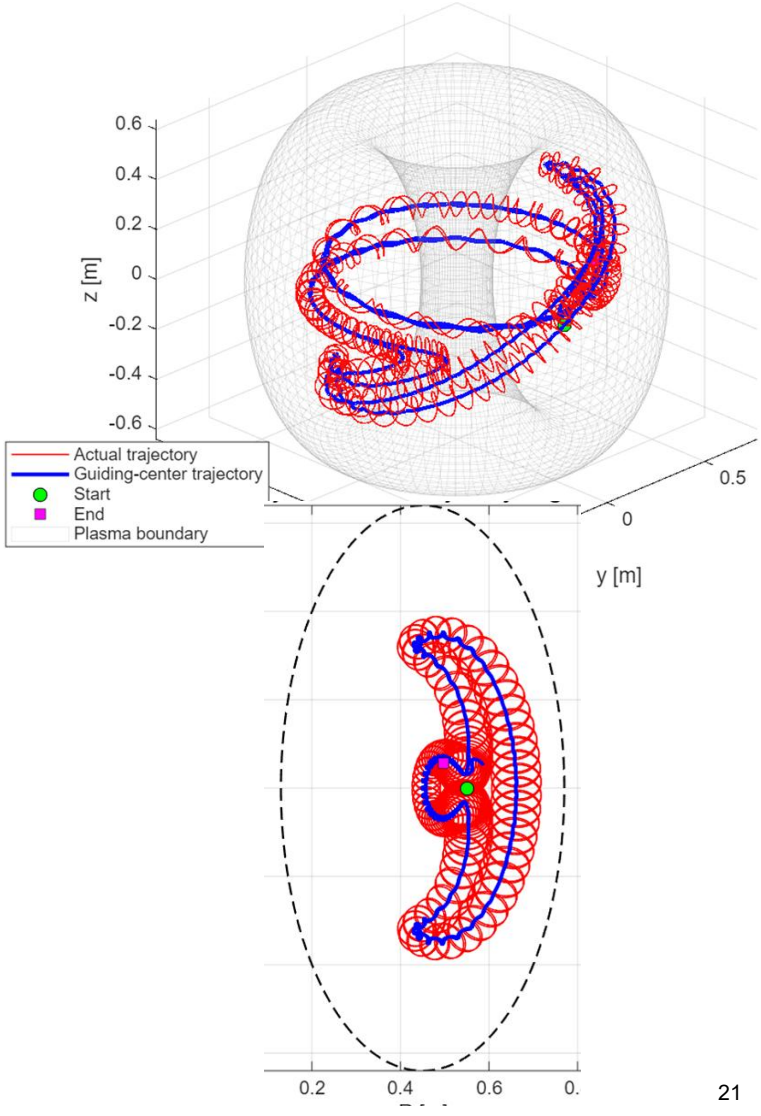

Pitch angle = 90°

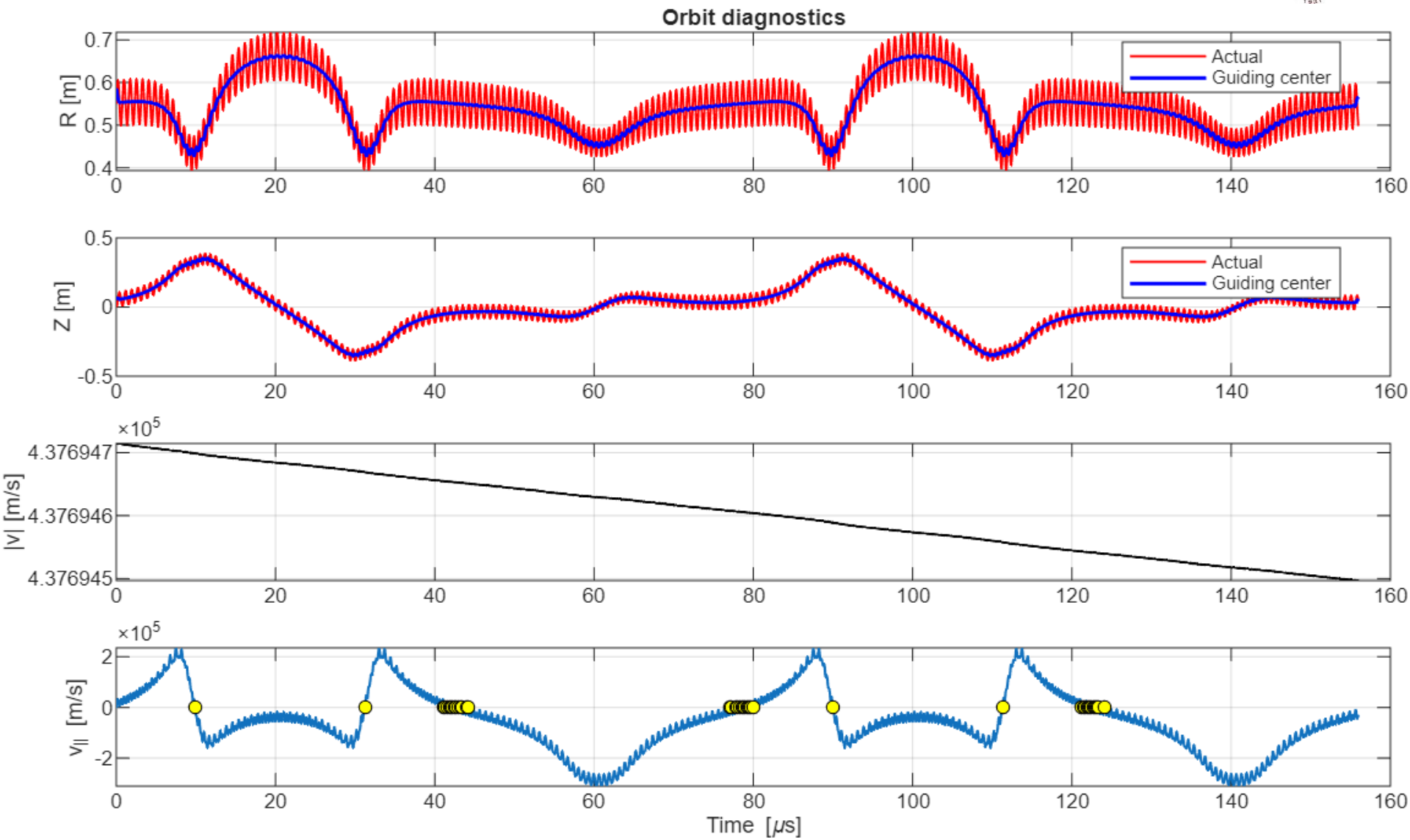

When forces are balances, the system is in the equilibrium state, or called “Magnetohydrostatics”

- **Equilibrium state:**

$$\rho_{\mathrm{m}}\left[\frac{\partial \vec{v}}{\partial t}+(\vec{v}\cdot\nabla)\,\vec{v}\right]=\vec{j}\times\vec{B}-\nabla p\equiv 0$$

$$\vec{j}\times\vec{B}=\nabla p$$

$$\nabla\times\vec{B}=\mu_{\mathrm{o}}\,\vec{j}$$

$$\vec{j}\times\vec{B}=\frac{1}{\mu_{\mathrm{o}}}(\vec{\nabla}\times\vec{B})\times\vec{B}=\frac{1}{\mu_{\mathrm{o}}}\left[(\vec{B}\cdot\vec{\nabla})\,\vec{B}-\frac{1}{2}\,\vec{\nabla}\,B^{2}\right]=\nabla p$$

$$\nabla\left(P+\frac{B^{2}}{2\mu_{\mathrm{o}}}\right)=\frac{1}{\mu_{o}}(\vec{B}\cdot\vec{\nabla})\,\vec{B}$$

Magnetic pressure — Magnetic tension ← Forces caused by curvature of the field lines

$$\vec{j}\perp\nabla p \qquad \vec{B}\perp\nabla p \quad\Rightarrow\quad \vec{j}\cdot\nabla p=0 \qquad \vec{B}\cdot\nabla p=0$$

- **The surfaces with p = constant are both magnetic surfaces (i.e., they are made up of magnetic field lines) and current surfaces (i.e., they are made of current flow lines).**

Grad-Shafranov equation

$$\Delta^*\psi = -\mu_0 R^2 \frac{dp}{d\psi} - \frac{1}{2}\frac{dF^2}{d\psi} \quad \text{where } \Delta^*\psi = R^2 \nabla \cdot \left(\frac{\nabla\psi}{R^2}\right) \qquad \psi \equiv \frac{1}{2\pi}\int \vec{B}\cdot d\vec{S} = RA_\phi$$

$$\mu_0 j_R = -\frac{1}{R}\frac{\partial F}{\partial z} \qquad \mu_0 j_z = \frac{1}{R}\frac{\partial F}{\partial R} \qquad \mu_0 j_\phi = -\frac{1}{R}\Delta^*\psi \qquad F \equiv RB_\phi$$

$$B_R = -\frac{1}{R}\frac{\partial \psi}{\partial z} \qquad B_z = \frac{1}{R}\frac{\partial \psi}{\partial R} \qquad B_\phi = \frac{F(\psi)}{R}$$

$$\vec{B} = \underbrace{\left(\frac{\nabla\psi}{R}\right)\times\hat{\phi}}_{\vec{B}_P} + \underbrace{\frac{F(\psi)}{R}\hat{\phi}}_{\vec{B}_T} \qquad \vec{j} = \underbrace{\frac{1}{\mu_0}\left(\frac{\nabla F}{R}\right)\times\hat{\phi}}_{\vec{I}_P} + \underbrace{\left(-\frac{1}{\mu_0}\frac{1}{R}\Delta^*\psi\right)\hat{\phi}}_{\vec{I}_T}$$

Poloidal component $\vec{B}_P$

Toroidal component $\vec{B}_T$

Poloidal component $\vec{I}_P$

Toroidal component (Plasma current) $\vec{I}_T$

$$I_P = \int \vec{j}_P \cdot d\vec{S} = -2\pi F(\psi)$$

$$\vec{S} = S\hat{z}$$

$$d\vec{l} = dl\hat{\phi}$$

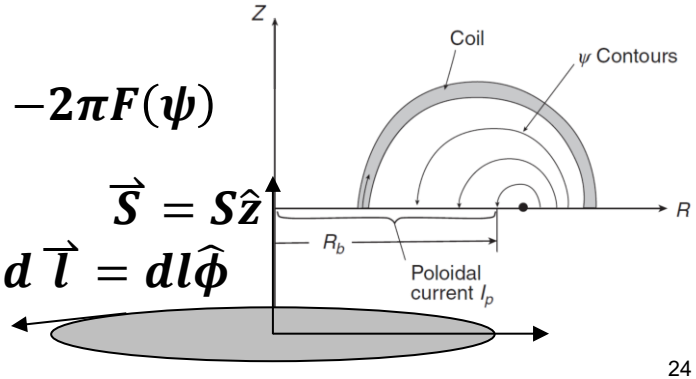

Plasma condition can be obtained by solving Grad-Shafranov equation

$$\Delta^*\psi = -\mu_0 R^2 \frac{dp}{d\psi} - \frac{1}{2}\frac{dF^2}{d\psi} \qquad \text{where } \Delta^*\psi = R^2 \nabla \cdot \left(\frac{\nabla\psi}{R^2}\right) \qquad \mu_0 j_\phi = -\frac{1}{R}\Delta^*\psi$$

$$j_\phi = R\frac{dp}{d\psi} + \frac{1}{2\mu_0 R}\frac{dF^2}{d\psi}$$

- The usual strategy to solve the Grad-Shafranov equation:
  1. Specify two free functions, the plasma pressure $p = p(\psi)$ and the toroidal field function $F = F(\psi)$.
  2. Solve the equation with specified boundary conditions to determine the flux function $\psi(R, z)$.
  3. Calculation the magnetic field using the following equations:

$$B_R = -\frac{1}{R}\frac{\partial\psi}{\partial z} \qquad B_\phi = \frac{F(\psi)}{R} \qquad B_z = \frac{1}{R}\frac{\partial\psi}{\partial R}$$

  4. The pressure profile can then be obtained from $p = p\big(\psi(R, z)\big)$.

Application of solving Grad-Shafranov equation for designing a tokamak

- Given I_{plasma}, $p(\psi)$, $I(\psi)$, I_{coils}, free boundary of plasma, perfect conductor as the chamber.
- Given I_{plasma}, $p(\psi)$, $I(\psi)$, I_{coils}, free boundary of plasma, insulator chamber.
- Given I_{plasma}, $p(\psi)$, $I(\psi)$, I_{coils}, free boundary of plasma, chamber with eddy current.
- Given I_{plasma}, $p(\psi)$, $I(\psi)$, fixed boundary of plasma. Then, use I_{coils}, free boundary of plasma and match the plasma shape calculated in the fixed boundary condition.

$$\Delta^*\psi = -\mu_0 R^2 \frac{dp}{d\psi} - \frac{1}{2}\frac{dF^2}{d\psi} \qquad \text{where } \Delta^*\psi = R^2 \nabla \cdot \left(\frac{\nabla\psi}{R^2}\right)$$

$$j_\phi = R\frac{dp}{d\psi} + \frac{1}{2\mu_0 R}\frac{dF^2}{d\psi} \qquad I_P = -2\pi F(\psi)$$

$$\mu_0 \vec{j} = \left(\frac{\nabla F}{R}\right) \times \hat{\phi} + \left(-\frac{1}{R}\Delta^*\psi\right)\hat{\phi} \qquad \vec{B} = \left(\frac{\nabla\psi}{R}\right) \times \hat{\phi} + \frac{F(\psi)}{R}\hat{\phi}$$

Example: design a spherical tokamak

- $R_o = 0.45$ m
- $a = 0.32$ m
- $\kappa = 2.4$
- $\delta = 0.5$
- $I_p = 100$ kA

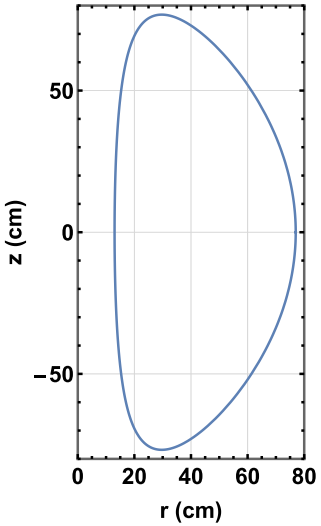

- **Step 1: Choose target plasma boundary**

$$r = R + a\mathrm{Cos}\left(\theta + \delta\mathrm{Sin}(\theta)\right)$$

$$z = a\kappa\mathrm{Sin}(\theta)$$

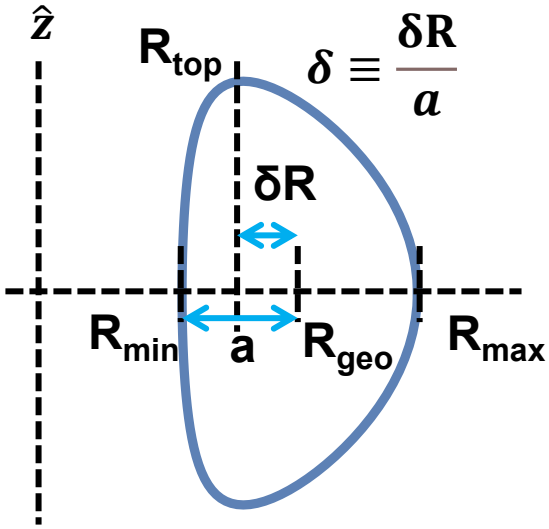

- **The goal is to find:**
  - **plasma shape**
  - **magnetic axis position**
  - **LCFS (Last closed flux surface)**
  - **poloidal field coil currents**
  - **safety factor profile q(ψ)**
  - **pressure and current profiles**
  - **whether the equilibrium is physically reasonable**

Example: design a spherical tokamak

- **Step 2: Choose pressure and toroidal-field profiles**

$$p(\psi) = p_o(1-\psi_N)^{\alpha}$$

$$F(\psi) = F_o\left[1 + c_F(1-\psi_N)^{\beta}\right]$$

$$\psi_N = \frac{\psi - \psi_{axis}}{\psi_{LCFS} - \psi_{axis}}$$

$$\alpha = 1.5\sim 2 \qquad \beta = 1\sim 2$$

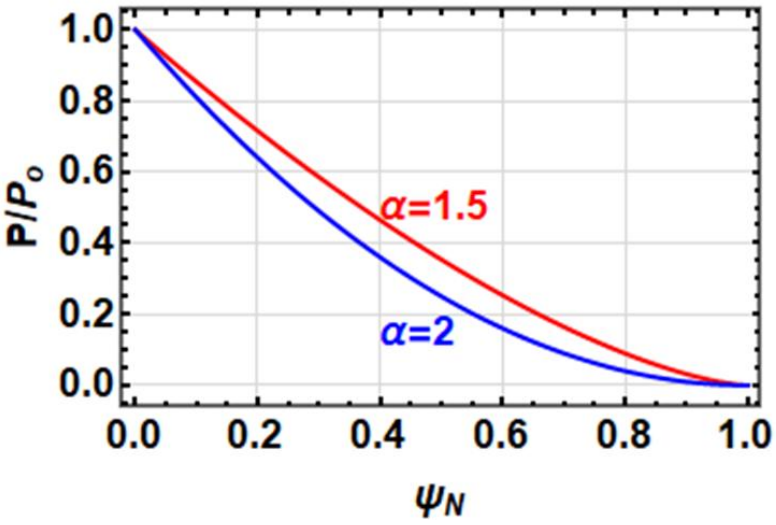

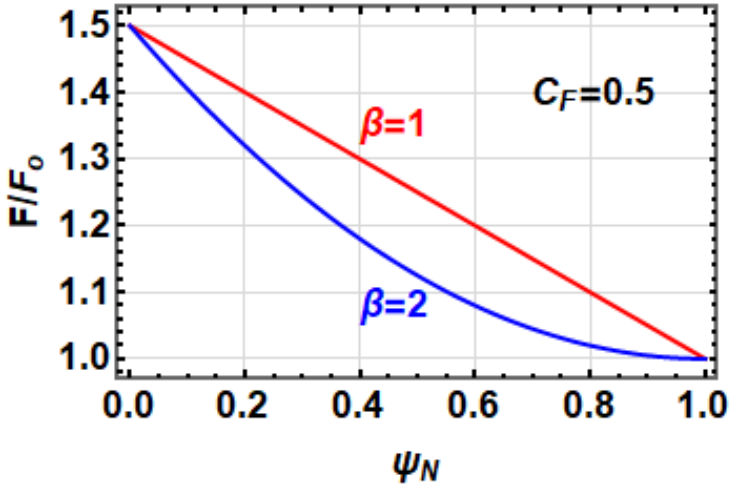

Example: design a spherical tokamak

- **Step 3: solve a fixed-boundary equilibrium**

$$\Delta^{*}\psi = -\mu_{o} R^{2} \frac{dp}{d\psi} - \frac{1}{2} \frac{dF^{2}}{d\psi}$$

$$p(\psi) = p_{o}(1 - \psi_{N})^{1.5}$$

$$F(\psi) = F_{o}$$

- **Input (known):**
  - R_{LCFS}, Z_{LCFS}
  - $p(\psi)$
  - $F(\psi)$
  - I_{p}
- **Output:**
  - $\psi(R, Z)$
- **Calculate:**

$$R = 45 + 32\mathrm{Cos}\left(\theta + 0.5\mathrm{Sin}(\theta)\right)$$

$$Z = 32 \times 2.4\mathrm{Sin}(\theta)$$

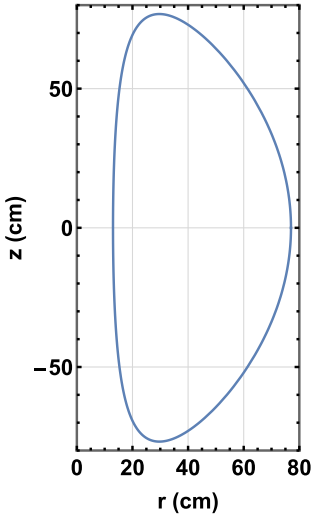

$$B_{R} = -\frac{1}{R} \frac{\partial \psi}{\partial z} \qquad B_{\phi} = \frac{F(\psi)}{R} \qquad B_{z} = \frac{1}{R} \frac{\partial \psi}{\partial R}$$

$$j_{\phi} = R \frac{dp}{d\psi} + \frac{1}{2\mu_{o} R} \frac{dF^{2}}{d\psi}$$

$$p = p[\psi(R, z)]$$

Example: design a spherical tokamak

- **Step 4: check the equilibrium equality**
  - $q(\psi)$
  - β_{p}
  - β_{N}
  - l_{i}
- **Example:**
  - $q_{\mathrm{o}} > 1$?

Example: design a spherical tokamak

- Step 5: move to free-boundary equilibrium

- Input (known):
  - PF coil positions
  - PF coils currents
  - Conducting wall/chamber
  - Plasma current profile
  - Total plasma current
- Total flux:

$$\psi_{\text{total}} = \psi_{\text{plasma}} + \psi_{\text{coils}} + \psi_{\text{wall}}$$

j_{eddy}

$$j_\phi = R\frac{dp}{d\psi} + \frac{1}{2\mu_o R}\frac{dF^2}{d\psi}$$

$$\psi_{\text{coil}}(R,Z) = \sum_i G(R,Z;R_i,Z_i)I_i = \sum_i M(R,Z;R_i,Z_i)I_i$$

$$\mu_o j_\phi = -\frac{1}{R}\Delta^*\psi$$

- Adjust coil currents until the calculated LCFS matches the target LCFS.

Example: design a spherical tokamak

- **Step 6: optimize PF coil currents**

- **Typical constraints:**

$$B_R(R_{\text{axis}}, Z_{\text{axis}}) \approx 0$$
$$B_Z(R_{\text{axis}}, Z_{\text{axis}}) \approx 0$$

- **Desired x-point:**

$$\nabla\psi(R_X, Z_X) = 0$$

- **Require the LCFS to match the design boundary.**
- **Optimization problem (least-squares equilibrium fitting problem):**

$$\min_{I_{\text{coil}}} \left[w_1 \left(\psi_{\text{target}} - \psi_{\text{calc}} \right)^2 + w_2 (\nabla\psi_{\text{x}})^2 + w_3 \left(R_{\text{axis}} - R_{\text{axis,target}} \right)^2 \right]$$

Plasma boundary | **X-point condition** | **Magnetic-axis location**

Example: design a spherical tokamak

- Step 7: Engineering check

- Check:
  - Coil current limits
  - Coil forces
  - Vertical stability
  - Wall clearance
  - Divertor strike points
  - Available loop voltage
  - Pulse duration
  - Heat load
- If one fails, go back and modify

$$R_0, a, \kappa, \delta, I_p, p(\psi), F(\psi)$$

Or the PF coil positions.

Example of the analytical solution of the Grad-Shafranov equation

$$\Delta^{*}\psi = -\mu_0 R^2 \frac{dp}{d\psi} - \frac{1}{2}\frac{dF^2}{d\psi}$$

$$C_1 = 1$$

$$C_2 = -8$$

$$C_3 = -20$$

$$C_4 = 20$$

$$C_5 = 0.2$$

- For $\mu_0 \frac{dp}{d\psi} = -C_2$ $\quad \frac{1}{2}\frac{dF^2}{d\psi} = C_1$

$$\psi(R,z) = -\frac{C_1}{2}z^2 + \frac{C_2}{8}R^4 + C_3 + C_4R^2 + C_5\left(R^4 - 4R^2z^2\right)$$

$$B_R(R,z) = -\frac{1}{R}\left(-C_1 z - 8C_5R^2z\right) \qquad B_z(R,z) = \frac{1}{R}\left(\frac{C_2}{2}R^3 + 2C_4R + C_5\left(4R^3 - 8Rz^2\right)\right)$$

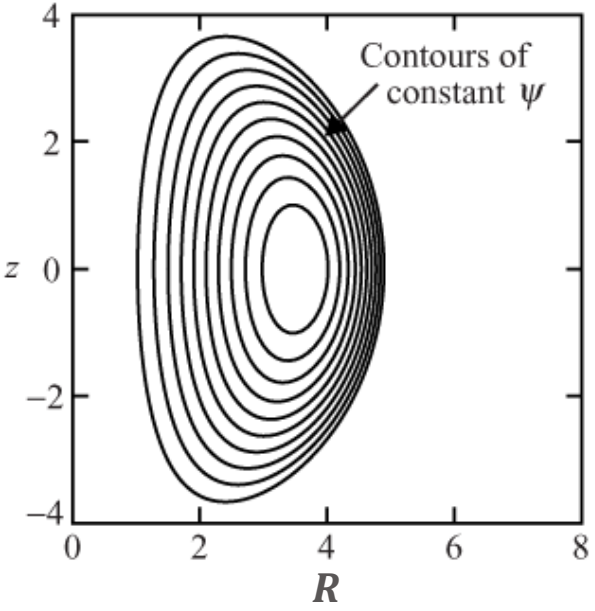

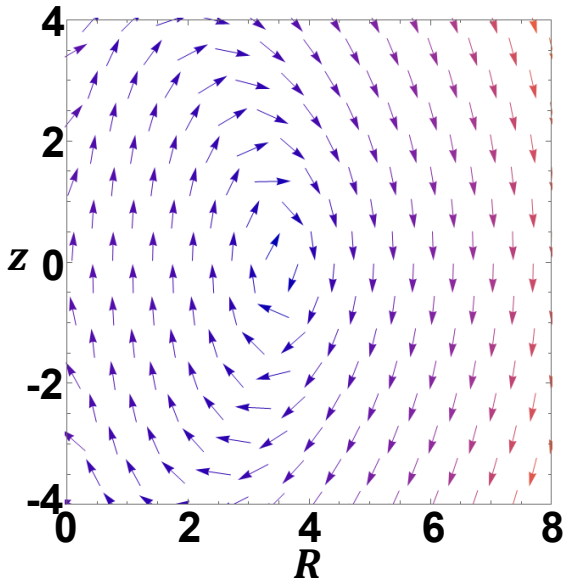

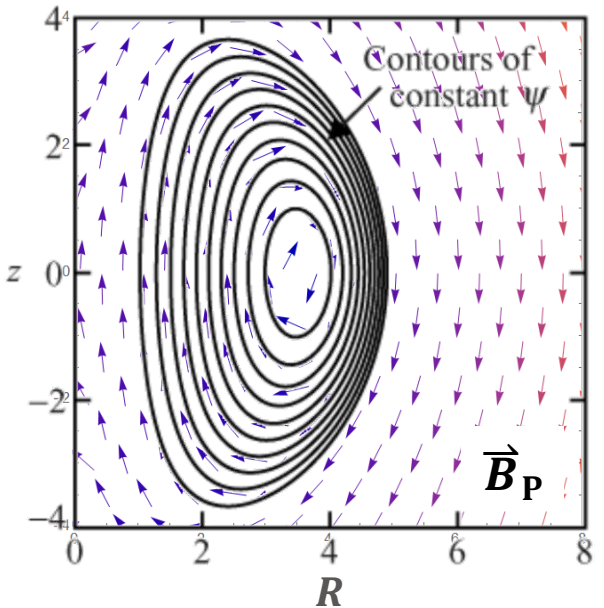

Examples: Large Aspect Ratio Tokamak

$$\Delta^*\psi = -\mu_o R^2 \frac{dp}{d\psi} - \frac{1}{2}\frac{dF^2}{d\psi}$$

$$j_\phi = R\frac{dp}{d\psi} + \frac{1}{2\mu_o R}\frac{dF^2}{d\psi}$$

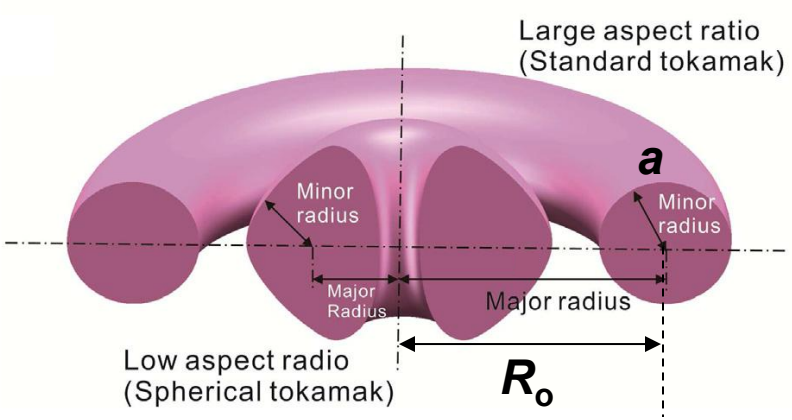

- **Assuming:**
  - $R_o >> a$
  - $j_\Phi = j_o = \text{constant}$
  - $F(\psi) = B_o R_o = \text{constant}$

$$\Delta^*\psi = R^2\nabla\cdot\left(\frac{\nabla\psi}{R^2}\right) = \frac{\partial^2\psi}{\partial z^2} + R\frac{\partial}{\partial R}\left(\frac{1}{R}\frac{\partial\psi}{\partial R}\right)$$

$$\Rightarrow \frac{dp}{d\psi} = \text{const} \qquad \mu_o j_\phi = -\frac{1}{R}\Delta^*\psi \Rightarrow -\mu_o R j_o = \frac{\partial^2\psi}{\partial z^2} + R\frac{\partial}{\partial R}\left(\frac{1}{R}\frac{\partial\psi}{\partial R}\right)$$

$$\psi(R,Z) = \frac{1}{2}A\left(R^2 - {R_o}^2\right) + \frac{1}{2}BZ^2 \qquad \Delta^*\psi = A + B = -\mu_o R j_o$$

$$\text{Let } A = B \equiv -\frac{\mu_o j_o}{2} \qquad \psi(R,Z) = -\frac{\mu_o j_o}{4}\left[\left(R^2 - {R_o}^2\right) + Z^2\right]$$

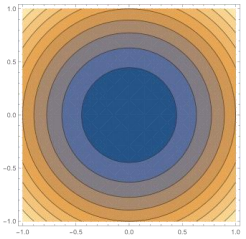

Application of solving Grad-Shafranov equation for reconstructing a tokamak equilibrium state

- **Measure**
  - **boundary conditions, including ψ, B, etc., on the wall (using flux loop and B-dot probe).**
  - **Pressure.**
  - **Plasma current (using Rogowski coil).**
- **Reconstruct $\psi(r,z)$, j, $p(\psi)$, $I(\psi)$, etc.**

$$\Delta^*\psi = -\mu_0 R^2 \frac{dp}{d\psi} - \frac{1}{2}\frac{dF^2}{d\psi} \qquad \text{where } \Delta^*\psi = R^2 \nabla \cdot \left(\frac{\nabla\psi}{R^2}\right)$$

$$I_P = -2\pi F(\psi)$$

$$\mu_0 \vec{j} = \left(\frac{\nabla F}{R}\right) \times \hat{\phi} + \left(-\frac{1}{R}\Delta^*\psi\right)\hat{\phi} \qquad \vec{B} = \left(\frac{\nabla\psi}{R}\right) \times \hat{\phi} + \frac{F(\psi)}{R}\hat{\phi}$$

Equilibrium reconstruction

- **Magnetic Diagnostics (Essential for the Grad-Shafranov equation)**
  - **Magnetic flux loops: Measure poloidal flux ψ at different locations.**
  - **Poloidal field (PF) probes: Measure B_p.**
  - **Toroidal field (TF) coils: Provide information on B_ϕ.**
  - **Rogowski coils: Measure total plasma current I_p.**
  - **Hall probes: Measure local magnetic fields.**
- **Interferometry & Thomson Scattering - Provide electron density profile $n_e(r)$.**
- **X-ray & Spectroscopy - Measure soft X-ray emission, used to infer internal plasma profiles.**
- **Motional Stark Effect (MSE) & Polarimetry - Measure the pitch angle of the magnetic field, used to infer the safety factor profile $q(\psi)$.**
- **Soft X-ray and ECE Imaging - Can give additional constraints on plasma shape and profiles.**

Equilibrium reconstruction – conti.

$$\Delta^* \psi = -\mu_0 R^2 \frac{dp}{d\psi} - \frac{1}{2}\frac{dF^2}{d\psi} \qquad j_\phi = R\frac{dp}{d\psi} + \frac{1}{2\mu_0 R}\frac{dF^2}{d\psi}$$

$j_\phi(\psi)$ $p(\psi)$ $F(\psi)$ **<= They are constrained with each other. When two are given, the third can be calculated.**

- **Adjustable functions:** $F(\psi)$ **and** $p(\psi)$ **are written in analytical forms.**
- **Solve Grad-Shafranov for** $\psi(R,Z)$
- **Compute derived quantities (flux loops, magnetic probes, pitch angles)**
- **Compare to diagnostics**
- **Adjust profile parameters**
- **Repeat until residuals are minimized**
- **Calculate** $j_\phi(\psi)$

Equilibrium reconstruction - process

- Step 1: collect experimental measurements
  - Magnetic probes: B_R, B_Z
    - Plasma boundary
    - Edge current distribution
  - Flux loops: ψ
    - Total flux distribution
    - LCFS position
  - Rogowski coil: I_p
    - Total plasma current
  - Current in coils:
    - Determine ψ_{coils}
  - Pressure diagnostics:
    - Thomson scattering (T, n)
    - CXRS (x-ray radiation)
    - Interferometer (n)
    - Infer $p(\psi)$

Equilibrium reconstruction - process

- **Step 2: Initial equilibrium guess**

$$p(\psi) = p_o(1-\psi_N)^{\alpha}$$

$$F(\psi) = F_o\left[1 + c_F(1-\psi_N)^{\beta}\right]$$

$$\psi_N = \frac{\psi - \psi_{axis}}{\psi_{LCFS} - \psi_{axis}}$$

$$\alpha = 1.5\sim 2 \qquad \beta = 1\sim 2$$

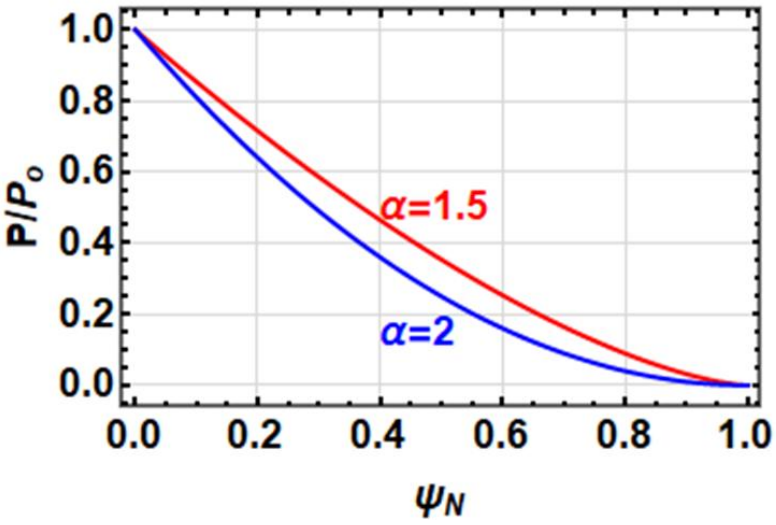

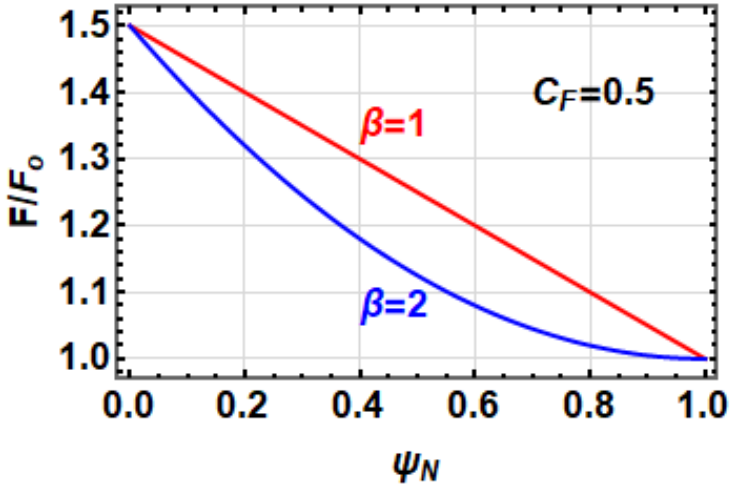

Equilibrium reconstruction - process

- **Step 3: calculate guessed current density**

$$j_\phi = R\frac{dp}{d\psi} + \frac{1}{2\mu_o R}\frac{dF^2}{d\psi}$$

- **Step 4: calculate guessed ψ_{plasma}**

$$\mu_o j_\phi = -\frac{1}{R}\Delta^*\psi$$

$$\psi_{total} = \psi_{plasma} + \psi_{coils} + \psi_{wall}$$

j_{eddy}

$$\psi_{coil}(R,Z) = \sum_i G(R,Z;R_i,Z_i)I_i = \sum_i M(R,Z;R_i,Z_i)I_i$$

- **Step 5: calculate synthetic diagnostics**

Equilibrium reconstruction - process

- Step 5: calculate synthetic diagnostics
  - Magnetic probes: B_R, B_Z
  - Flux loops: ψ
  - Rogowski coil: I_p
- Step 6: compare with experiment
  - Fitting error

$$\chi^2 = \sum_i w_i \left(y_i^{\text{measure}} - y_i^{\text{guessed}} \right)^2$$

- Adjust profiles till χ^2 is minimum.

$$p(\psi) = p_0 (1 - \psi_N)^{\alpha}$$
$$F(\psi) = F_0 \left[1 + c_F (1 - \psi_N)^{\beta} \right]$$

- All quantities can be retrieved by the best fitting profiles $p(\psi)$ and $F(\psi)$.

Magnetically confined toroidal equilibrium

1. **Radial pressure balance in the poloidal plan needs to be provided so that the pressure contours form closed nested surfaces. Both toroidal and poloidal fields can readily accomplish this task.**
2. **The radially outward expansion force inherent in all toroidal geometries needs to be balanced without sacrificing stability.**

- **Forces associated with toroidal force balance are usually than those corresponding to radial pressure balance. However, they are more difficult to compensate.**

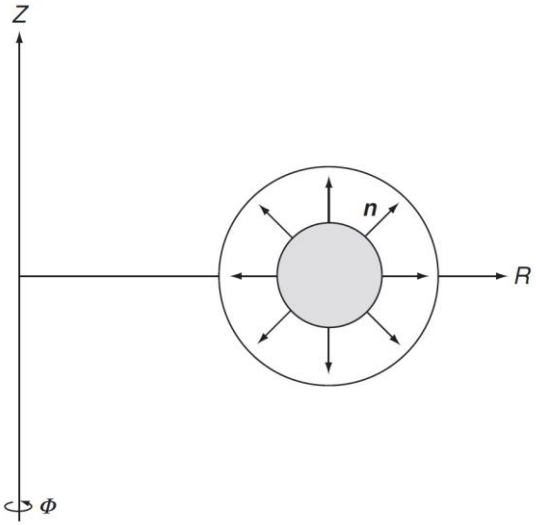

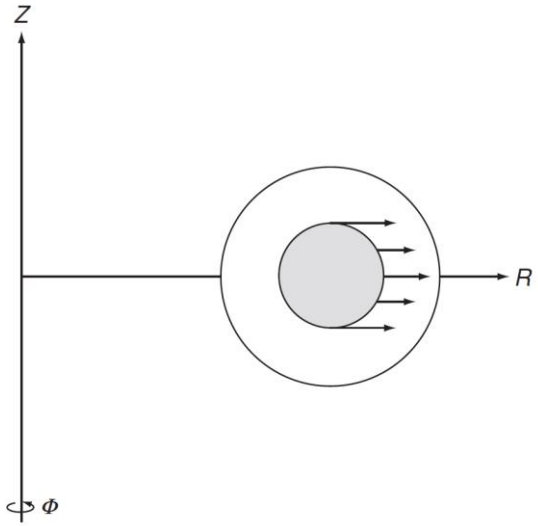

Toroidal configuration with a purely poloidal magnetic field

- **Hoop force:**

$$\psi_1 = \psi_2 \equiv \psi$$

$$S_1 < S_2 \quad B_1 > B_2$$

$$\vec{F}_{H,R} \propto \hat{e}_R \frac{B_1{}^2 S_1 - B_2{}^2 S_2}{2\mu_o} > 0$$

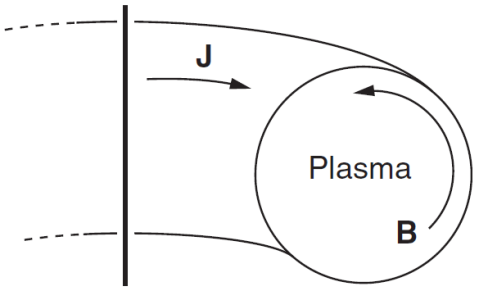

- **Tire tube force**

$$p_1 = p_2 \equiv p$$

$$S_1 < S_2$$

$$\vec{F}_{T,R} \propto -\hat{e}_R(pS_1 - pS_2) > 0$$

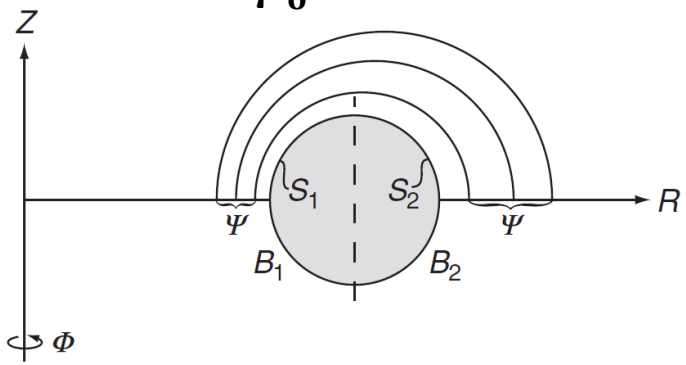

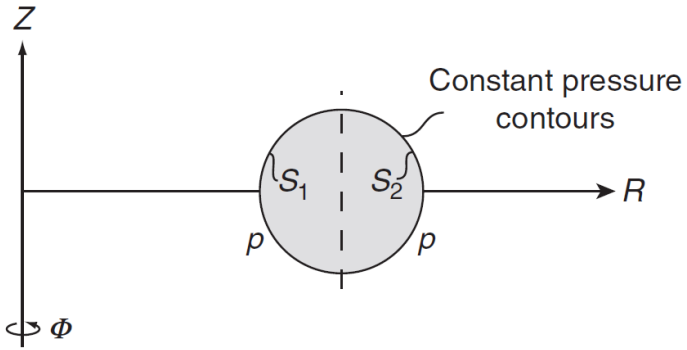

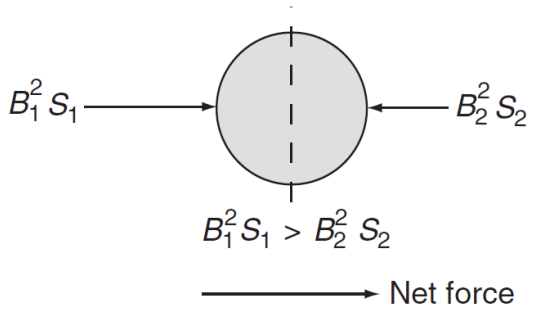

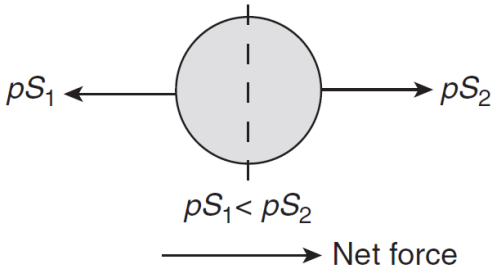

The outward force can be compensated by either a perfectly conducting shell or externally applied vertical field

- **Perfectly conducting shell**

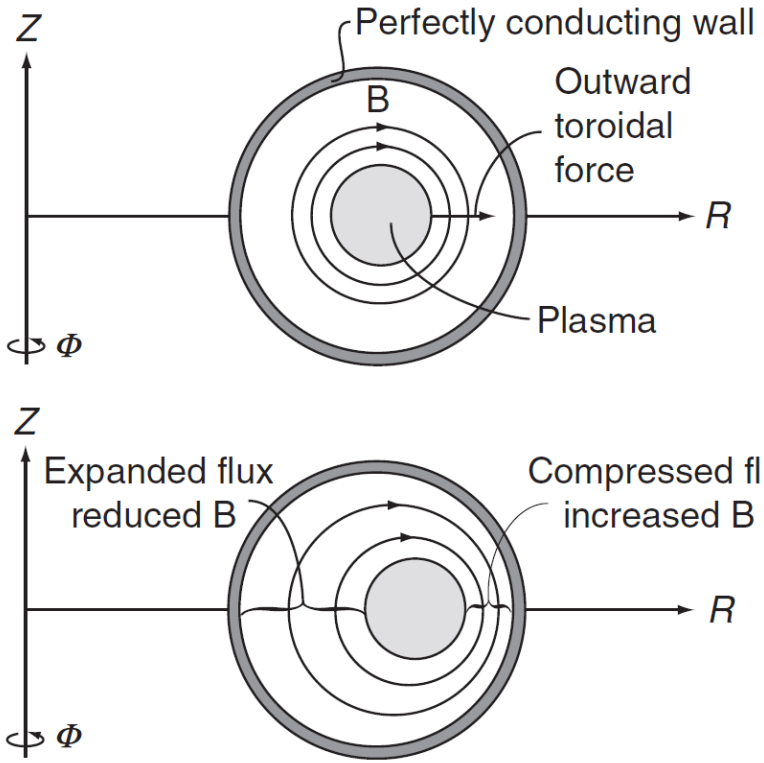

- **Externally applied vertical field**

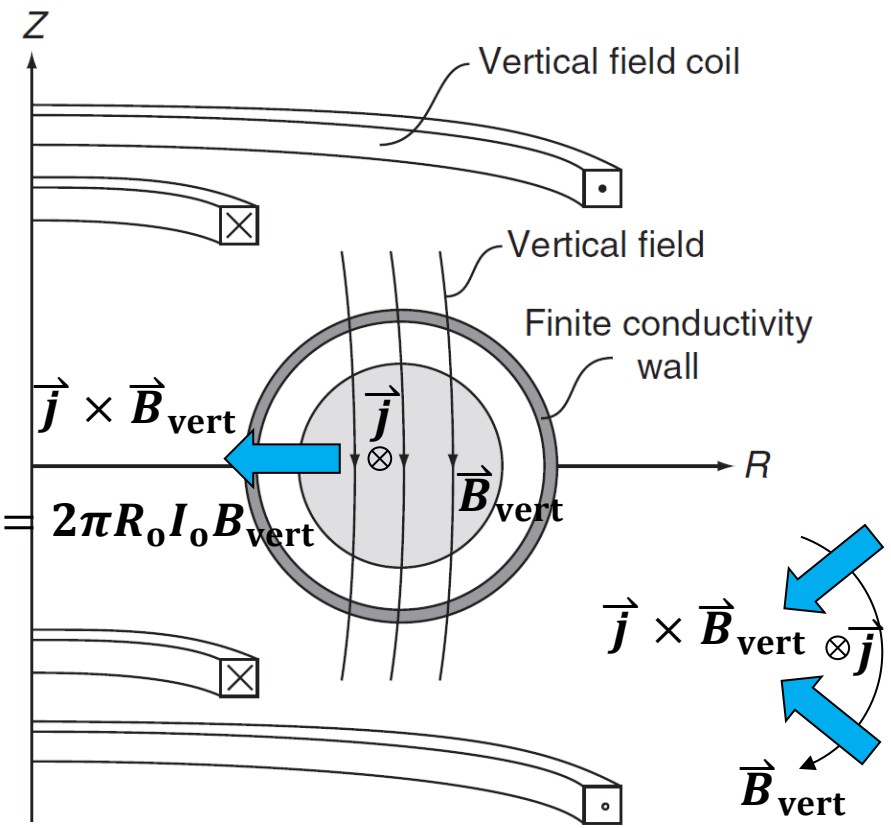

- **With a finite conductivity wall, flux can only remain compressed for about a skin time.**
- **This configuration develops disastrous MHD instabilities (z pinch).**

Toroidal configuration with a purely toroidal magnetic field, stable but NOT balanced

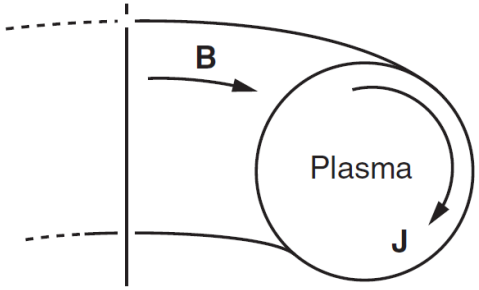

$$\vec{B} = B_\phi \hat{e}_\phi \qquad B_\phi = B_o \frac{R_o}{R} \qquad B_o = \frac{\mu_o I_c}{2\pi R_o}$$

$$\vec{F}_R \propto \hat{e}_R \frac{(B_{a1}{}^2 - B_{i1}{}^2)S_1 - (B_{a2}{}^2 - B_{i2}{}^2)S_2}{2\mu_o} > 0$$

Plasma is diamagnetic

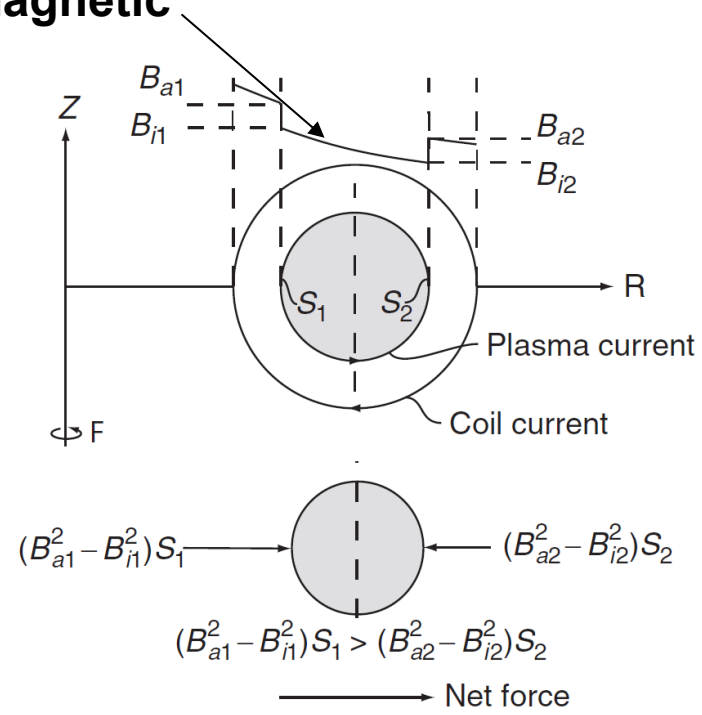

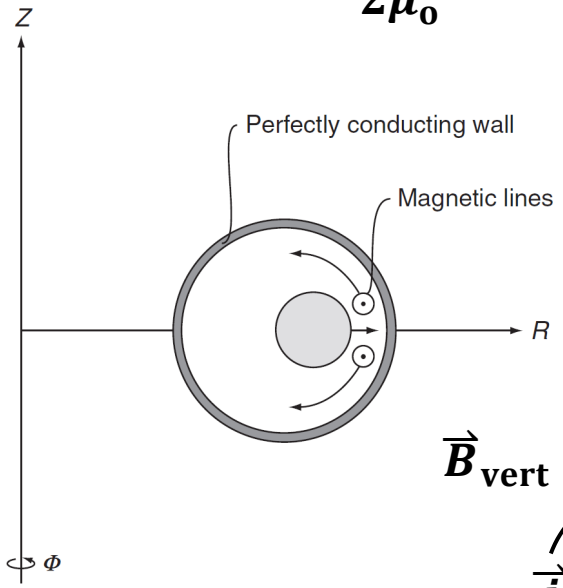

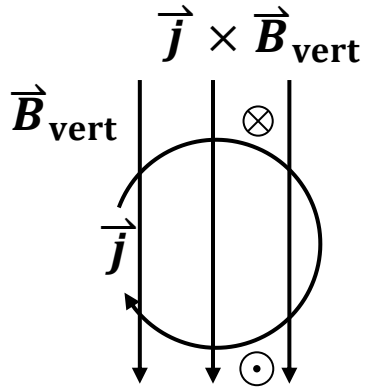

$\vec{j} \times \vec{B}_{vert}$ **is not pointed along** $\hat{e}_R$

Coils in a tokamak

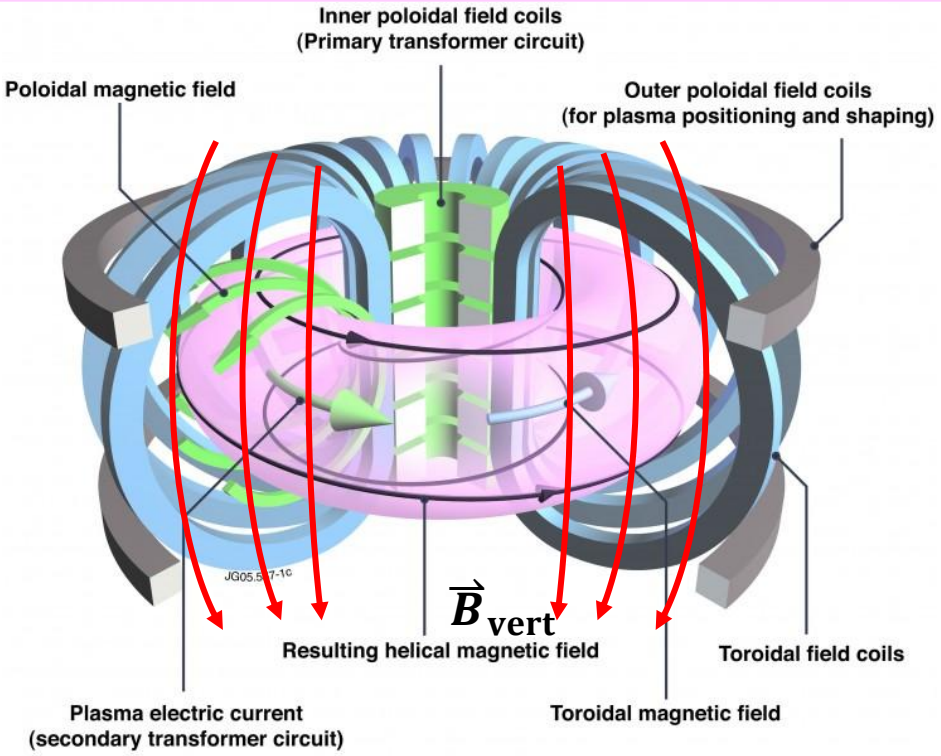

- **Toroidal field coils (in poloidal direction) – generate toroidal field for confinement.**
- **Poloidal field coils – generate vertical field for plasma positioning and shaping.**
- **Central solenoid – for breakdown and generating plasma current (in toroidal direction) and thus generating poloidal field for confinement.**

https://www.euro-fusion.org/2011/09/tokamak-principle-2/

Fluxes and currents

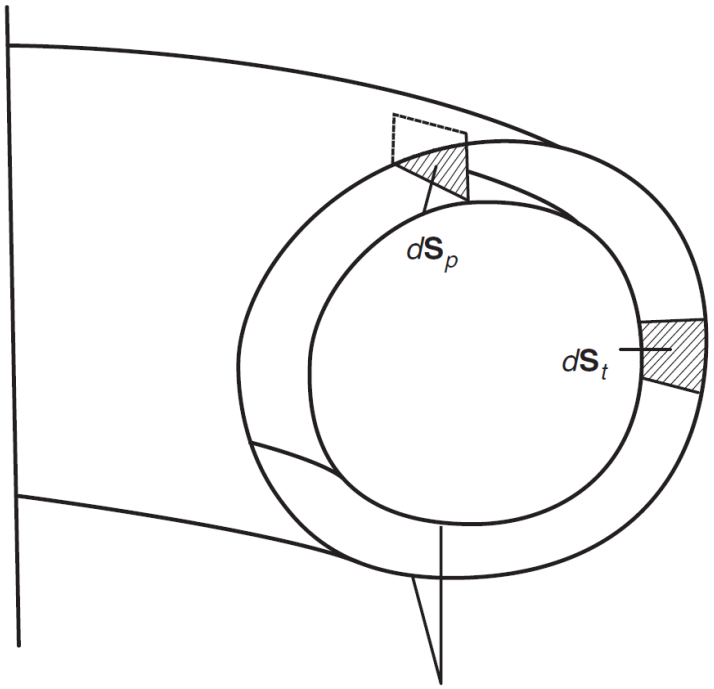

Two neighboring flux surfaces

- **Poloidal flux:** $\psi_{\mathrm{p}} = \int \vec{B} \cdot d\vec{S}_{\mathrm{p}}$

  $\psi_{\mathrm{p}} = \psi_{\mathrm{p}}(p)$

- **Toroidal flux:** $\psi_{\mathrm{t}} = \int \vec{B} \cdot d\vec{S}_{\mathrm{t}}$

- **Poloidal current:** $I_{\mathrm{p}} = \int \vec{j} \cdot d\vec{S}_{\mathrm{p}}$

- **Toroidal current:** $I_{\mathrm{t}} = \int \vec{j} \cdot d\vec{S}_{\mathrm{t}}$

Normalized plasma pressure, β

$$\beta = \frac{\text{plasma pressure}}{\text{magnetic pressure}} = \frac{2\mu_o\langle p\rangle}{B^2}$$

- **Plasma pressure:** $\langle p\rangle = \frac{1}{V_p}\int p\,d\vec{r}$
- **Magnetic pressure:** $P_B = \frac{B^2}{2\mu_o}$

$$B^2 = {B_t}^2 + {B_p}^2 = {B_o}^2 + \left(\frac{\mu_o I_p}{2\pi a}\right)^2 \frac{2}{1+\kappa^2}$$

$${B_t}^2 = {B_o}^2 \qquad B_o = B\ @R = R_o$$

$${B_p}^2 = \left(\frac{\mu_o I_p}{2\pi a}\right)^2 = \left(\frac{\mu_o I_p}{C_p}\right)^2$$

$$C_p \approx 2\pi a\sqrt{\frac{1+\kappa^2}{2}}$$

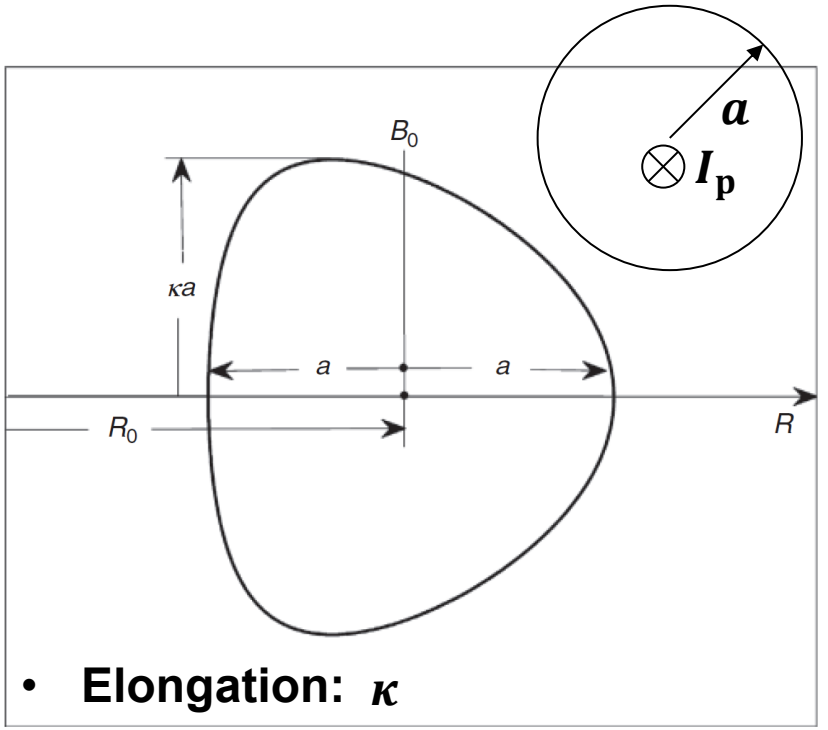

- **Elongation:** κ

$$\beta_t = \frac{2\mu_o\langle p\rangle}{{B_o}^2} \qquad \beta_p = \frac{4\pi^2 a^2(1+\kappa^2)p}{\mu_o {I_p}^2}$$

$$\frac{1}{\beta} = \frac{1}{\beta_t} + \frac{1}{\beta_p}$$

Different poloidal shapes

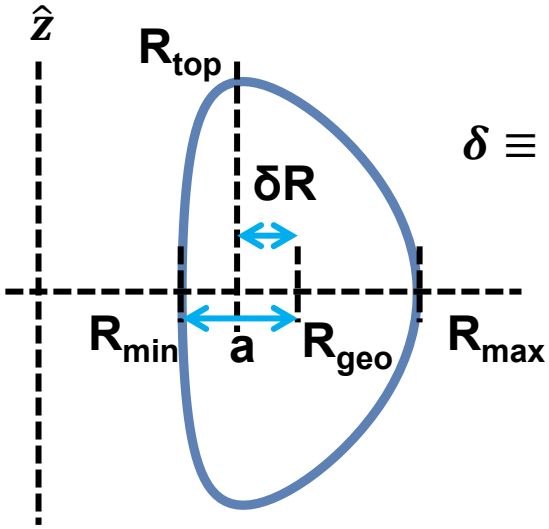

$$\delta \equiv \frac{\delta R}{a}$$

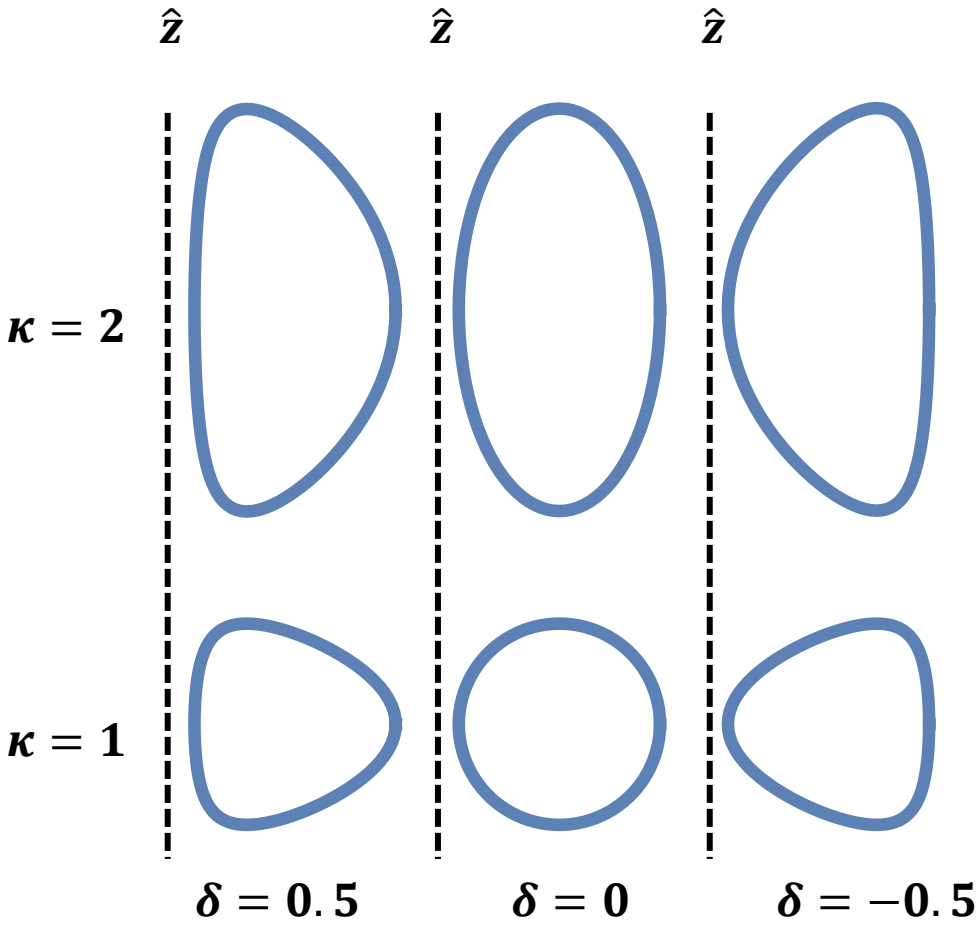

$$r = R + a\mathrm{Cos}\left(\theta + \delta \mathrm{Sin}(\theta)\right)$$

$$z = a\kappa \mathrm{Sin}(\theta)$$

- Aspect ratio: $\frac{R}{a}$
- Elongation: κ
- Triangularity: δ

Safety factor

- **Kink Safety Factor:**

$$q^*(r) = \frac{aB_o}{R_o B_p} = \frac{2\pi a^2 \kappa B_o}{\mu_o R_o I_o}$$

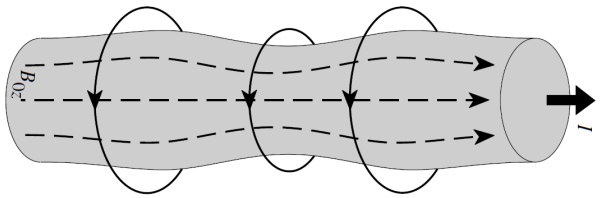

$$q(r) = \frac{rB_z(r)}{R_o B_\theta(r)}$$

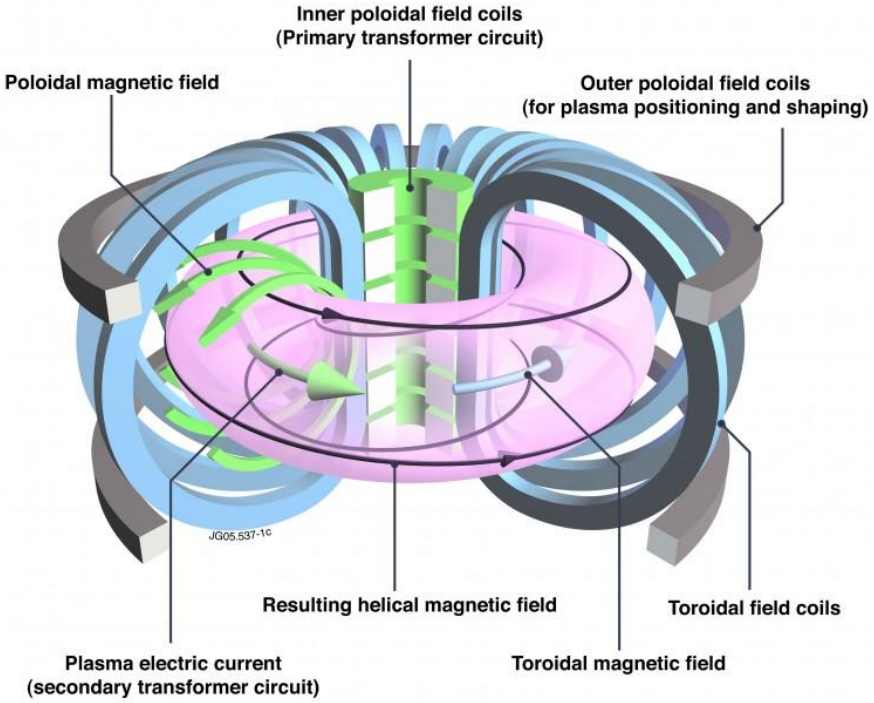

Kink instability in action in a 3 by 25-cm pyrex tube at Aldermaston

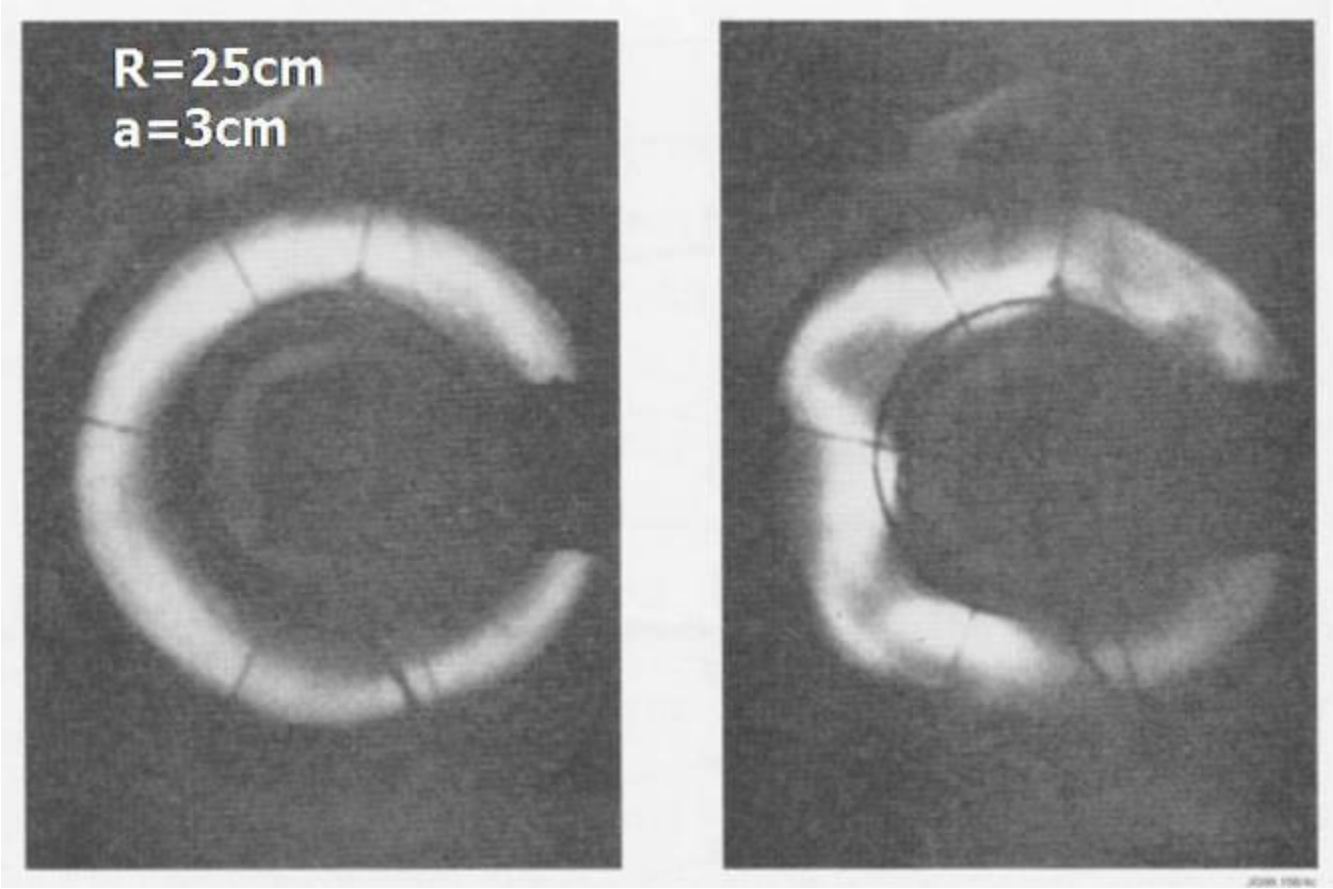

https://en.wikipedia.org/wiki/Kink_instability
R A Bingham et al 2026 Plasma Phys. Control. Fusion 68 030201

Safety factor

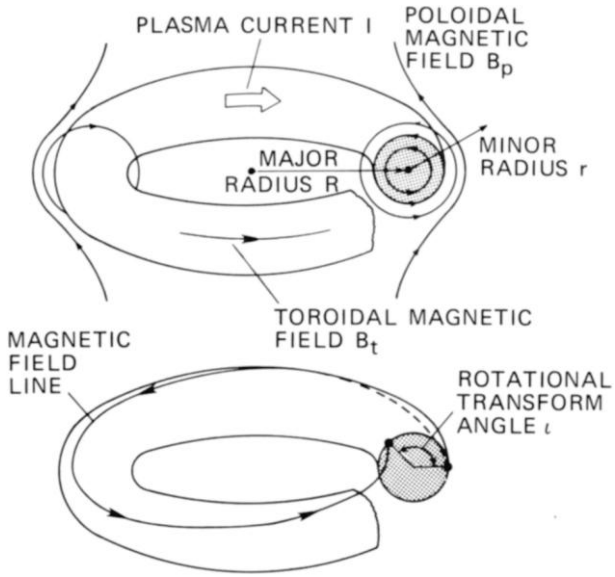

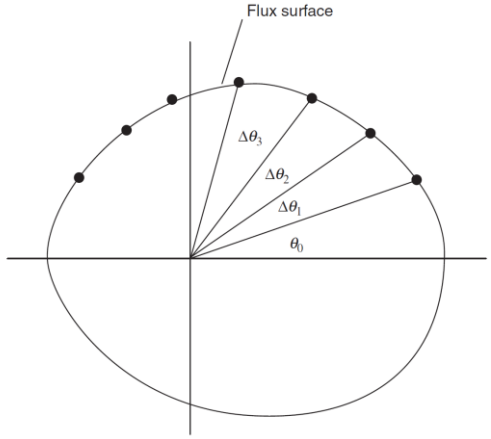

- **Shear:**

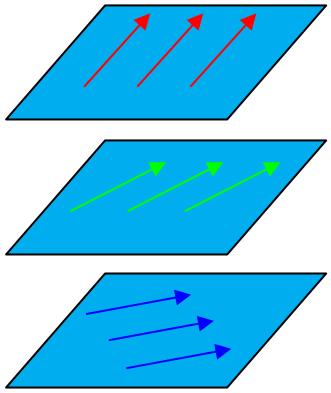

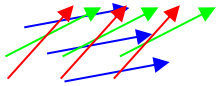

- **Rotational transform:** $\boldsymbol{\iota \equiv \lim_{N\to\infty} \frac{1}{N} \sum_{1}^{N} \Delta\theta_n}$
- **MHD safety factor:** $\boldsymbol{q(V) \equiv \frac{2\pi}{\iota(V)} = \frac{d\psi_t/dV}{d\psi_p/dV}}$ $\boldsymbol{\psi_t = \psi_t(V)}$ $\boldsymbol{\psi_p = \psi_p(V)}$
- **Shear:** $\boldsymbol{s(V) \equiv 2\frac{V}{q}\frac{dq}{dV}}$ $\boldsymbol{\iota(V) \equiv 2\pi\left(\frac{d\psi_p/dV}{d\psi_t/dV}\right)}$

C. C. Baker, *et al*, Nuclear Technology/Fusion, 1, 5 (1981)

Global magnetic shear

- Shear

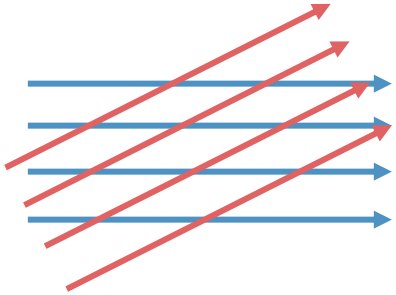

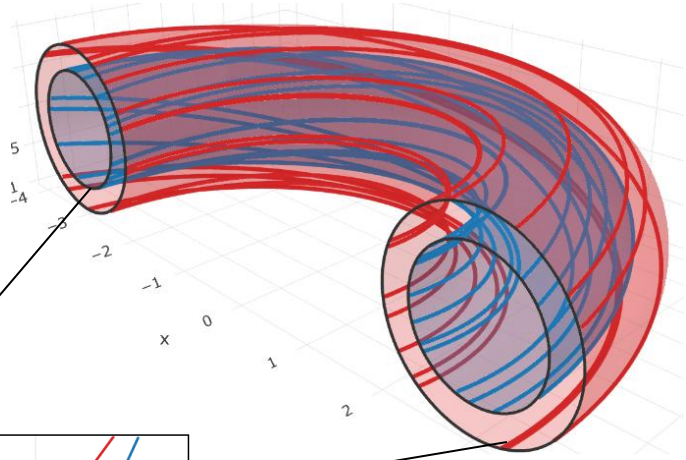

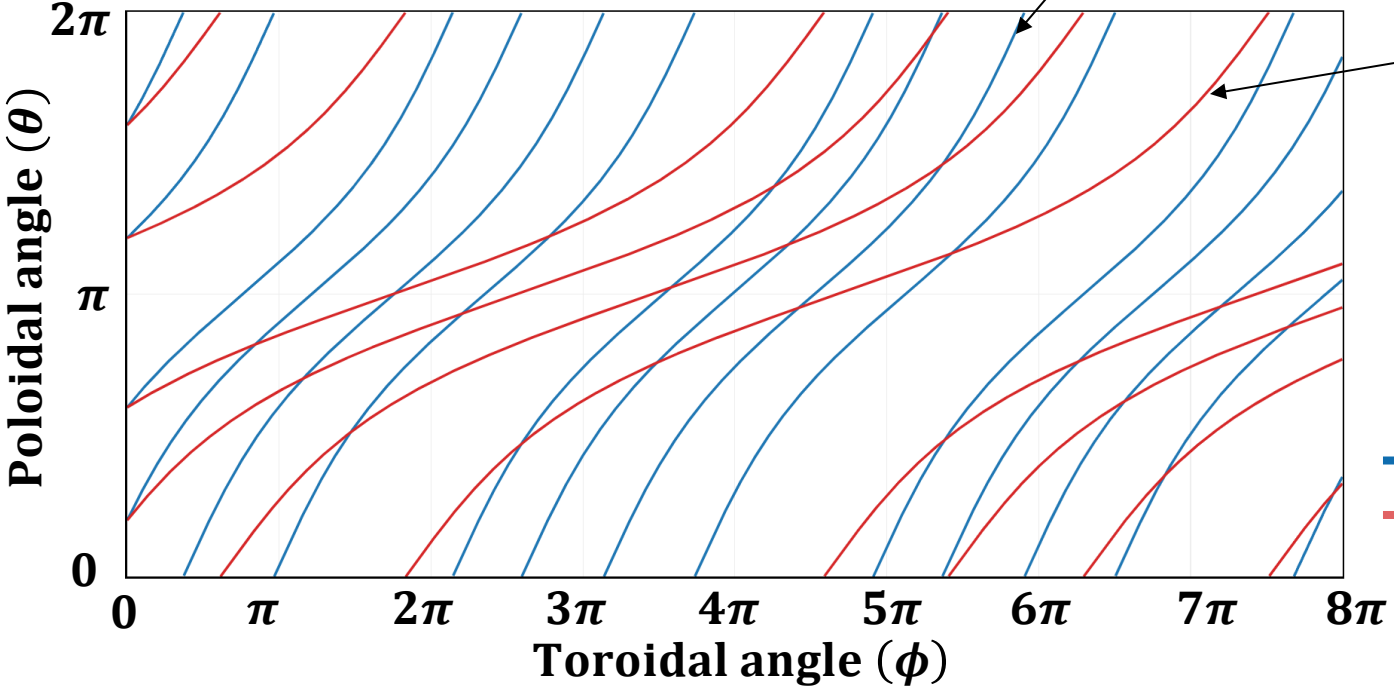

Volume of the constant flux

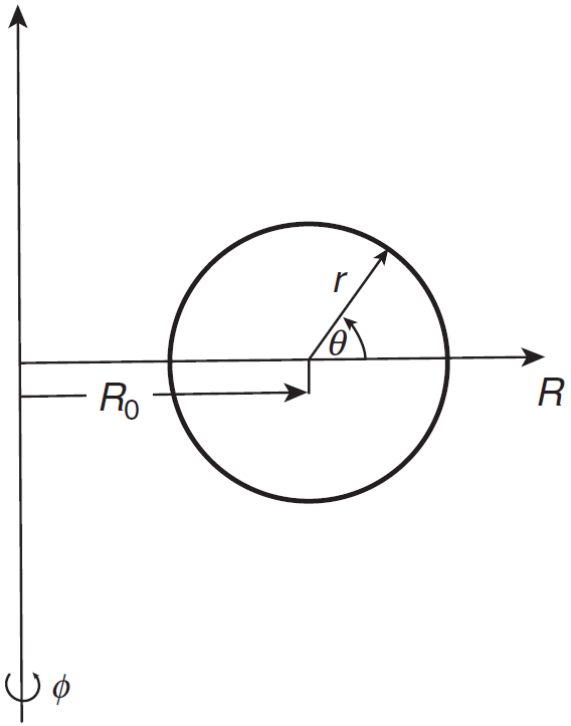

$$R = R_o + r\cos\theta$$

$$Z = r\sin\theta$$

$$\psi = \psi(r, \theta)$$

$$r = \hat{r}(\theta, \psi)$$

$$V(\psi) = \int_0^{2\pi} \int_0^{2\pi} \int_0^{\hat{r}} R r dr d\theta d\phi$$

$$V(\psi) = \pi R_o \int_0^{2\pi} d\theta \hat{r} \left[1 + \frac{2}{3}\left(\frac{\hat{r}}{R_o}\right) cos\theta\right]$$

A cylindrical plasma column is stable when the safety factor is greater than unity

- **Sausage instability (m=0)**

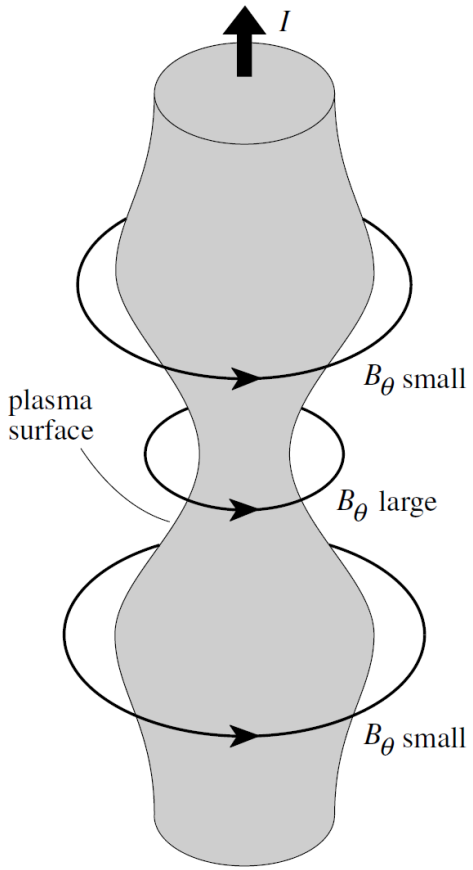

- **Kink instability**

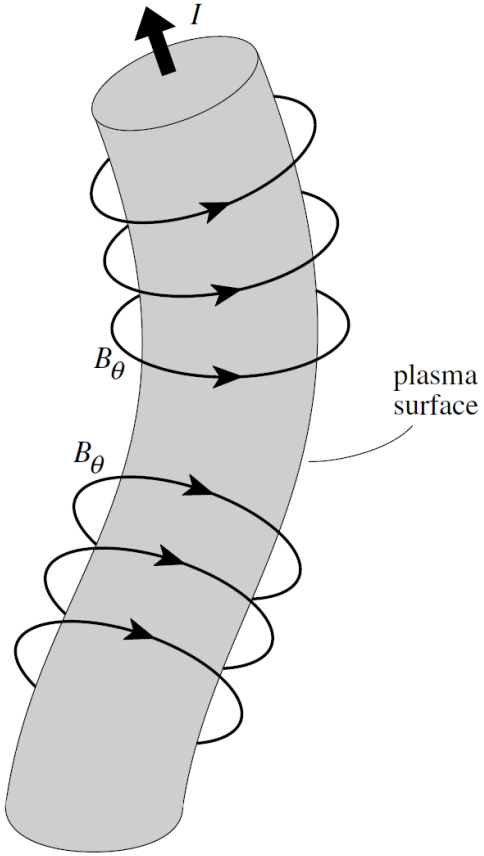

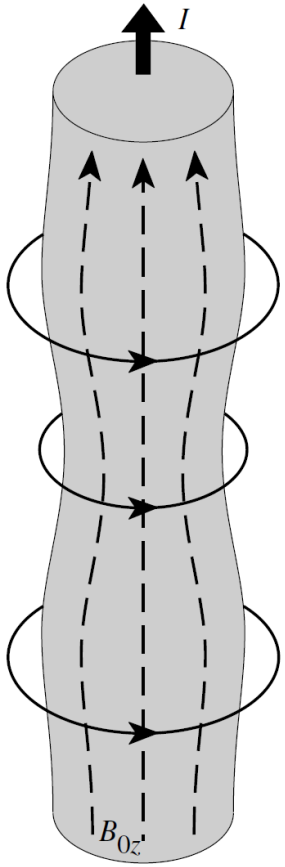

- **MHD Safety factor:** $q(r) = \dfrac{rB_z(r)}{R_o B_\theta(r)}$ **Kruskal–Shafranov limit**

Magnetic well

$$\widehat{W} = 2\frac{V}{\langle B^2 \rangle}\frac{d}{dV}\left\langle \frac{B^2}{2} \right\rangle$$

$$= 2\frac{V}{\langle B^2 \rangle}\frac{d}{dV}\left\langle \mu_o p + \frac{B^2}{2} \right\rangle$$

- **A magnetic well is a quantity that measures plasma stability against short perpendicular wavelength modes driven by the plasma pressure gradient.**

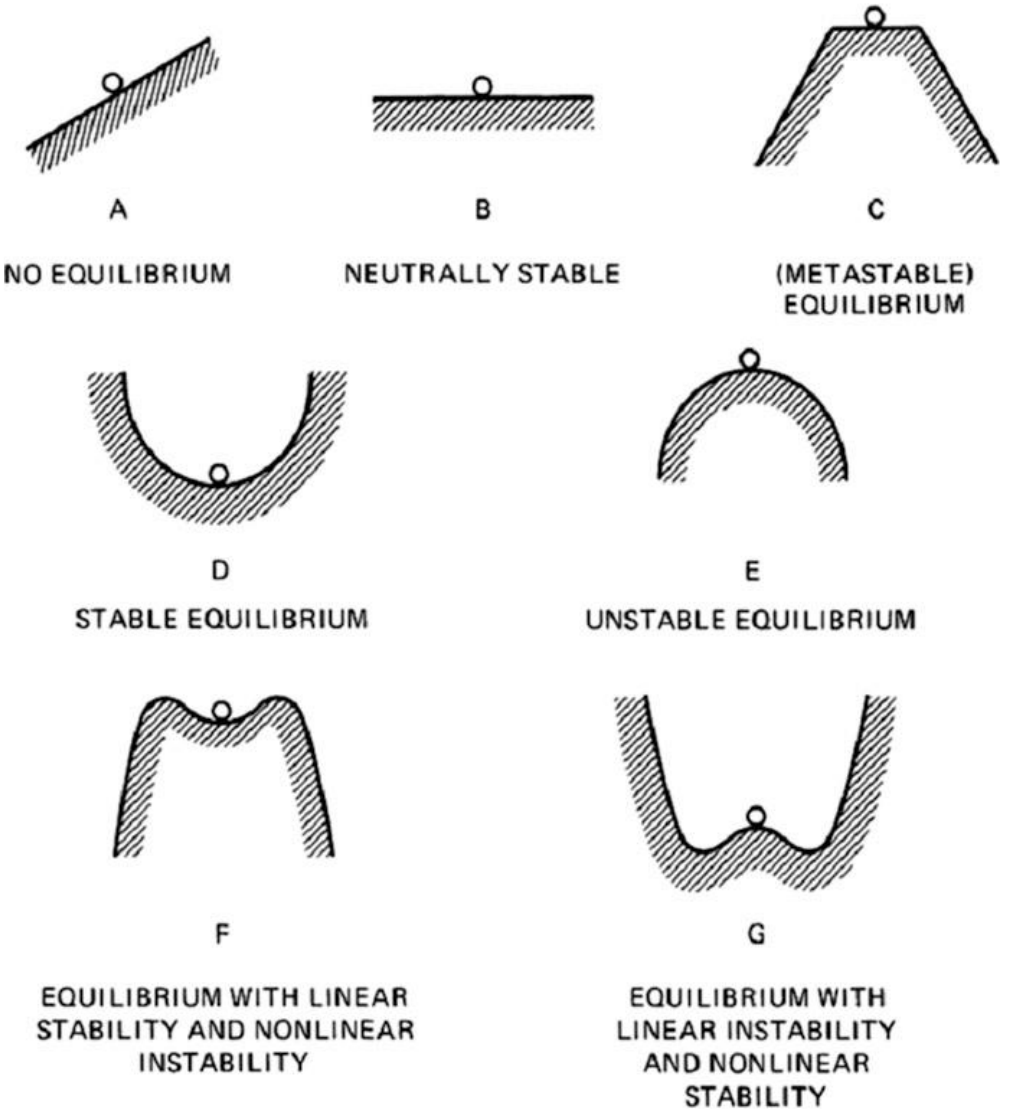

Variational formulation for checking stabilization

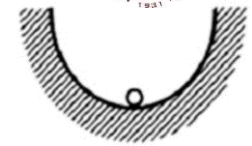

D

STABLE EQUILIBRIUM

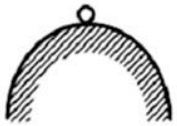

E

UNSTABLE EQUILIBRIUM

- **Equilibrium state:** $\vec{j}_o \times \vec{B}_o = \nabla p_o$
- **Momentum eq:** $\rho_m \left[\frac{\partial \vec{v}}{\partial t} + (\vec{v}\cdot\nabla)\vec{v}\right] = \vec{j}\times\vec{B} - \nabla\cdot\overleftrightarrow{P}$

$$\rho_m = \rho_o + \tilde{\rho}_1 \qquad p = p_o + \tilde{p}_1 \qquad \vec{v} = \vec{v}_o + \tilde{\vec{v}}_1 = \tilde{\vec{v}}_1 \equiv \frac{\partial \vec{\xi}}{\partial t}$$

$$\vec{j} = \vec{j}_o + \tilde{\vec{j}}_1 \qquad \vec{B} = \vec{B}_o + \tilde{\vec{B}}_1 \equiv \vec{B}_o + \vec{Q}$$

$$\rho_m \frac{\partial^2 \vec{\xi}}{\partial t^2} = \vec{F}(\vec{\xi}) \qquad \vec{F}(\vec{\xi}) = \vec{j}_o \times \vec{Q} + \vec{j}_1 \times \vec{B}_o - \nabla\tilde{p}_1$$

$$\vec{F}(\vec{\xi}) = \frac{1}{\mu_o}(\nabla\times\vec{B}_o)\times\vec{Q} + \frac{1}{\mu_o}(\nabla\times\vec{Q})\times\vec{B}_o + \nabla(\vec{\xi}\cdot\nabla p + \gamma p \nabla\cdot\vec{\xi})$$

- **The change in potential energy associated with the perturbation:**

$$\delta W = -\frac{1}{2}\int \vec{\xi}^{\,*}\cdot\vec{F}(\vec{\xi})\,d\vec{r}$$

- **Stable requirement:** $\delta W \geq 0$

$$\delta W_F = \frac{1}{2}\int d\vec{r}\left[\frac{|\vec{Q}_\perp|^2}{\mu_o} + \frac{B^2}{\mu_o}\left|\nabla\cdot\vec{\xi}_\perp + 2\vec{\xi}_\perp\cdot\vec{\kappa}\right|^2 + \gamma p\left|\nabla\cdot\vec{\xi}\right|^2 - 2(\vec{\xi}_\perp\cdot\nabla p)\left(\vec{\kappa}\cdot\vec{\xi}_\perp^{\,*}\right) - J_{||}\left(\vec{\xi}_\perp^{\,*}\times\vec{b}\right)\cdot\vec{Q}_\perp\right]$$

Variational formulation for checking stabilization

- **The change in potential energy associated with the perturbation:**

$$\delta W = -\frac{1}{2}\int \vec{\xi}^{\,*}\cdot\vec{F}\left(\vec{\xi}\right)d\,\vec{r}$$

- **Stable requirement:** $\delta W \geq 0$

$$\delta W_F = \frac{1}{2}\int d\,\vec{r}\left[\frac{\left|\vec{Q}_\perp\right|^2}{\mu_o}+\frac{B^2}{\mu_o}\left|\nabla\cdot\vec{\xi}_\perp+2\,\vec{\xi}_\perp\cdot\vec{\kappa}\right|^2+\gamma p\left|\nabla\cdot\vec{\xi}\right|^2\right.$$
$$\left.-2\left(\vec{\xi}_\perp\cdot\nabla p\right)\left(\vec{\kappa}\cdot\vec{\xi}_\perp^{\,*}\right)-J_{||}\left(\vec{\xi}_\perp^{\,*}\times\vec{b}\right)\cdot\vec{Q}_\perp\right]$$

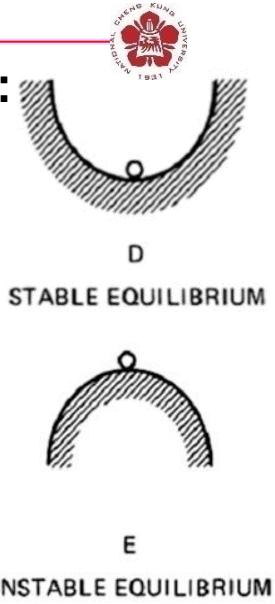

- **Stabilization terms:**

$\frac{\left|\vec{Q}_\perp\right|^2}{\mu_o}$: **For bending magnetic field lines, (shear Alfvén wave).**

$\frac{B^2}{\mu_o}\left(\left|\nabla\cdot\vec{\xi}_\perp+2\,\vec{\xi}_\perp\cdot\vec{\kappa}\right|\right)^2$: **For compressing the magnetic field, (compressional Alfvén wave).**

$\gamma p\left|\nabla\cdot\vec{\xi}\right|^2$: **For compressing the plasma, (sound wave).**

- **Destabilization terms:** $-2\left(\vec{\xi}_\perp\cdot\nabla p\right)\left(\vec{\kappa}\cdot\vec{\xi}_\perp^{\,*}\right)-J_{||}\left(\vec{\xi}_\perp^{\,*}\times\vec{b}\right)\cdot\vec{Q}_\perp$

Alfvén waves

- **Shear Alfvén wave:**

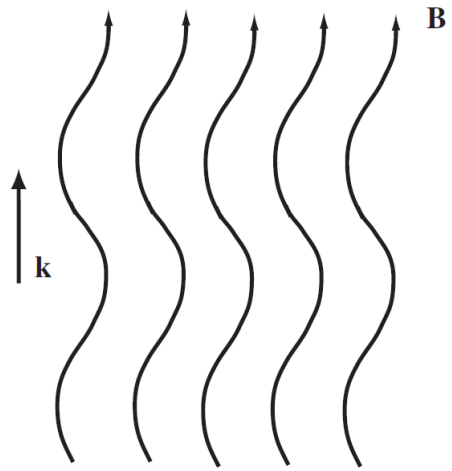

- **Longitudinal sound wave (the slow magnetosonic wave)**

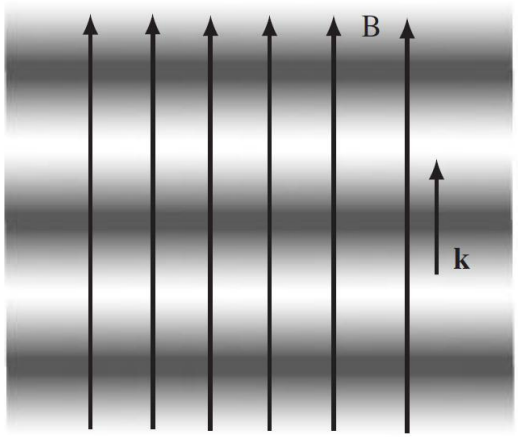

- **The fast magnetosonic wave (Compressional Alfvén wave):**

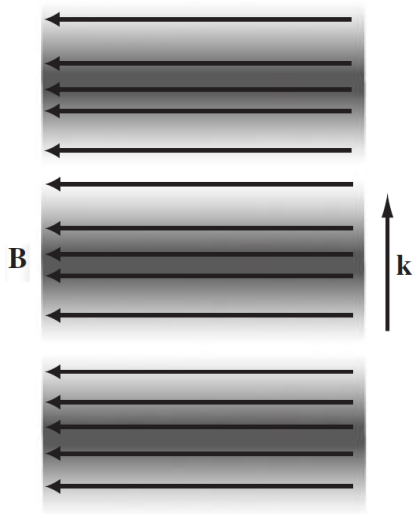

Alfvén waves

- **Shear Alfvén wave:**

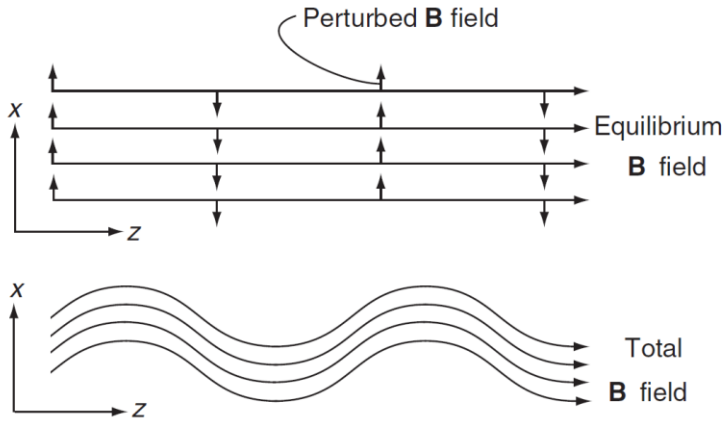

- **The fast magnetosonic wave (Compressional Alfvén wave):**

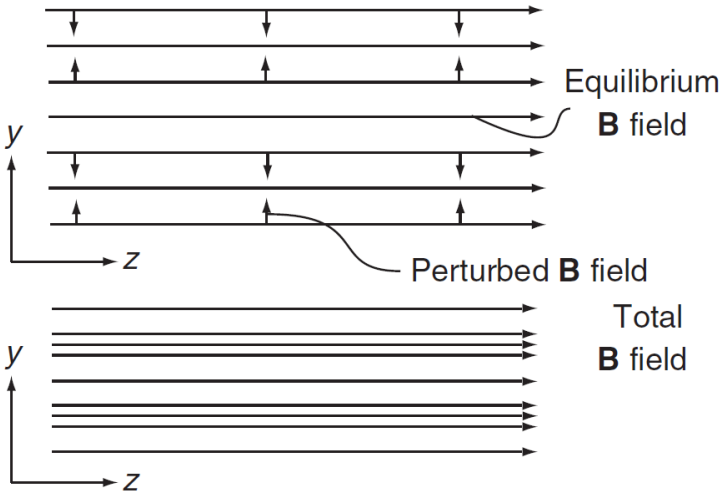

- **The slow magnetosonic wave (Shear + Compressional Alfvén wave):**

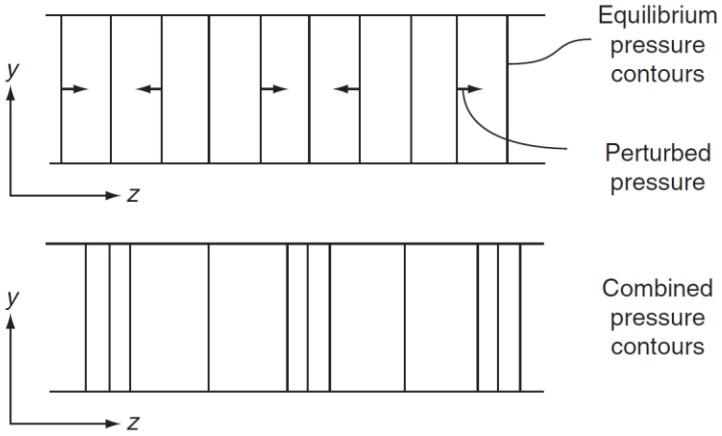

Classification of MHD instabilities

- **Locations:**
  - **Internal/Fixed boundary modes: mode structure does not require any motion of the plasma-vacuum interface away from its equilibrium position.**
  - **External/Free-boundary modes: the plasma-vacuum interface moves from its equilibrium position during an unstable MHD perturbation.**
- **Dominant destabilizing term**
  - **Pressure-driven modes: the dominant destabilizing term is the one proportional to ∇p.**
  - **Current-driven modes: the dominant destabilizing term is the one proportional to $J_{||}$.**

$$\delta W_F = \frac{1}{2}\int d\vec{r}\left[\frac{\left|\vec{Q}_\perp\right|^2}{\mu_o} + \frac{B^2}{\mu_o}\left|\nabla\cdot\vec{\xi}_\perp + 2\,\vec{\xi}_\perp\cdot\vec{\kappa}\right|^2 + \gamma p\left|\nabla\cdot\vec{\xi}\right|^2 \right.$$
$$\left. -2\left(\vec{\xi}_\perp\cdot\nabla p\right)\left(\vec{\kappa}\cdot\vec{\xi}_\perp^{\,*}\right) - J_{||}\left(\vec{\xi}_\perp^{\,*}\times\vec{b}\right)\cdot\vec{Q}_\perp\right]$$

Classification of MHD instabilities

- **Locations:**
  - **Internal/Fixed boundary modes: mode structure does not require any motion of the plasma-vacuum interface away from its equilibrium position.**
  - **External/Free-boundary modes: the plasma-vacuum interface moves from its equilibrium position during an unstable MHD perturbation.**
- **Dominant destabilizing term**
  - **Current-driven modes, e.g., kink instability, sausage instability.**
  - **Pressure-driven modes, e.g., interchange mode, ballooning mode.**

External mode vs internal mode

- **Predicted behaviors of the plasma in ITER**

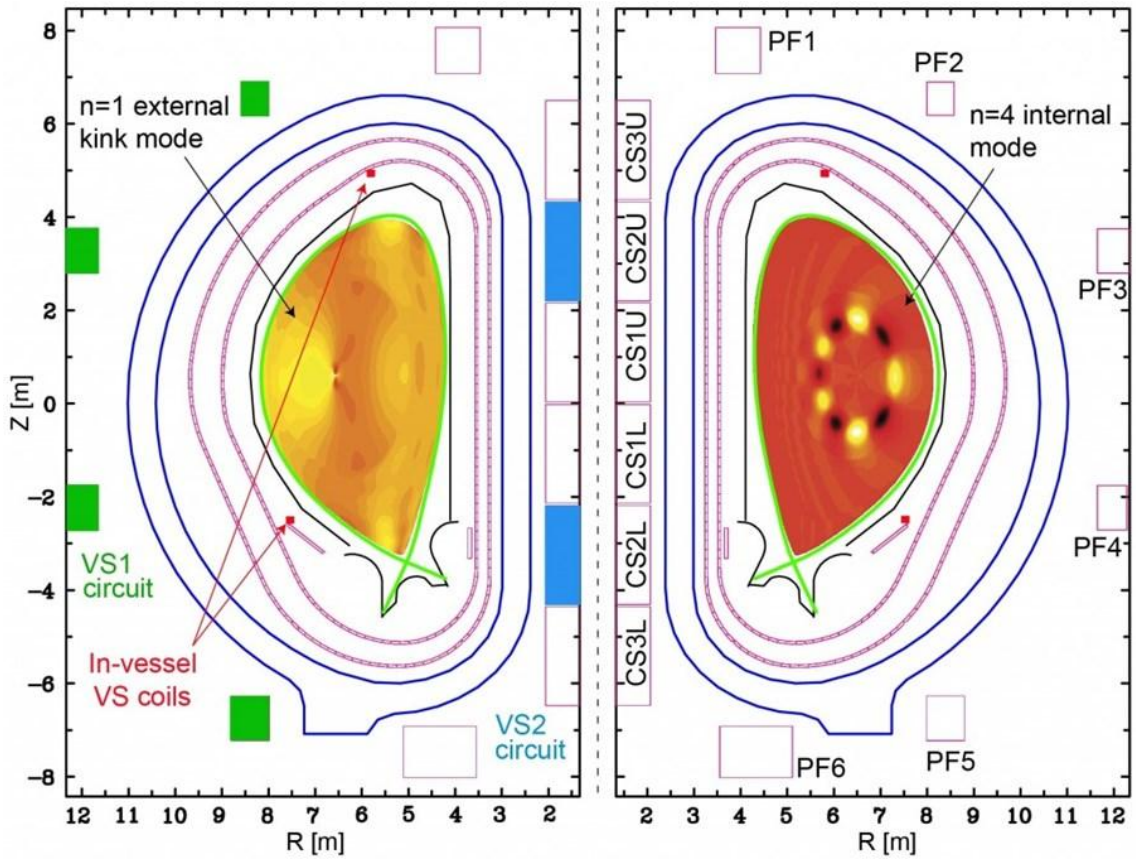

https://www.iter.org/newsline/-/3401

External vs internal kink instability

- **External kink instability**

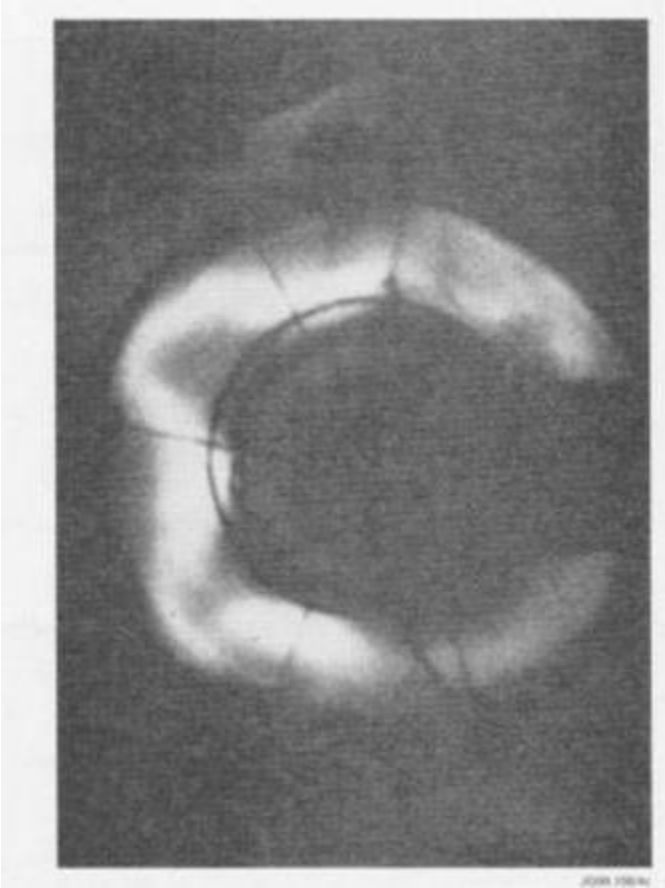

- **Internal kink instability**

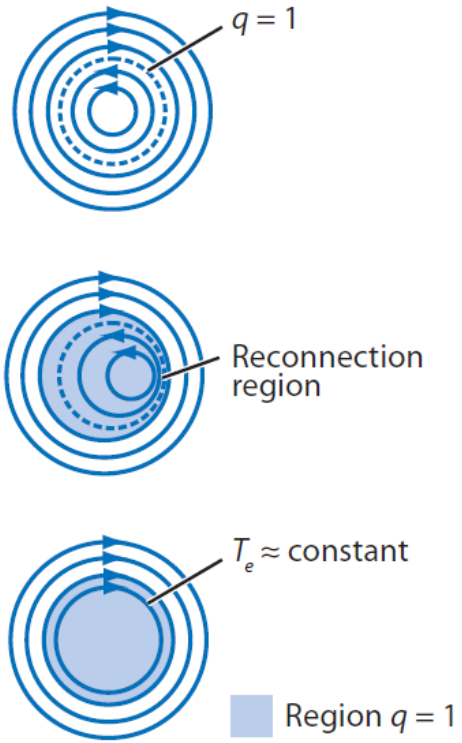

https://en.wikipedia.org/wiki/Kink_instability
R A Bingham et al 2026 Plasma Phys. Control. Fusion 68 030201
E. G. Zweibel and M. Yamada, Annu. Rev. Astron. Astrophys., 47, 291 (2009)

Current-driven instability

- **Sausage instability (m=0)**

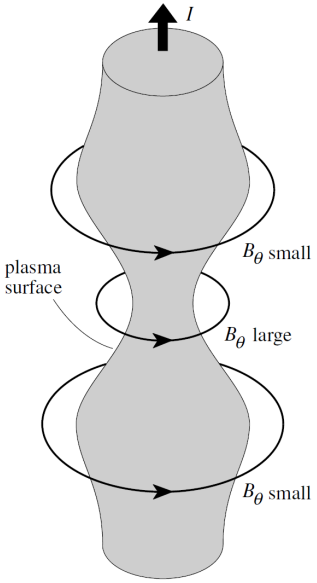

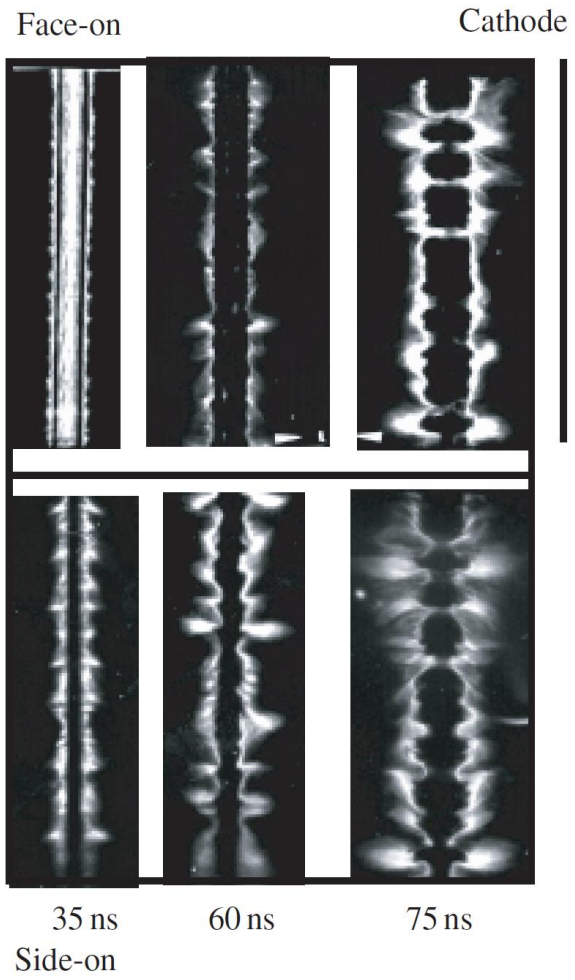

- **Kink instability (m=1)**

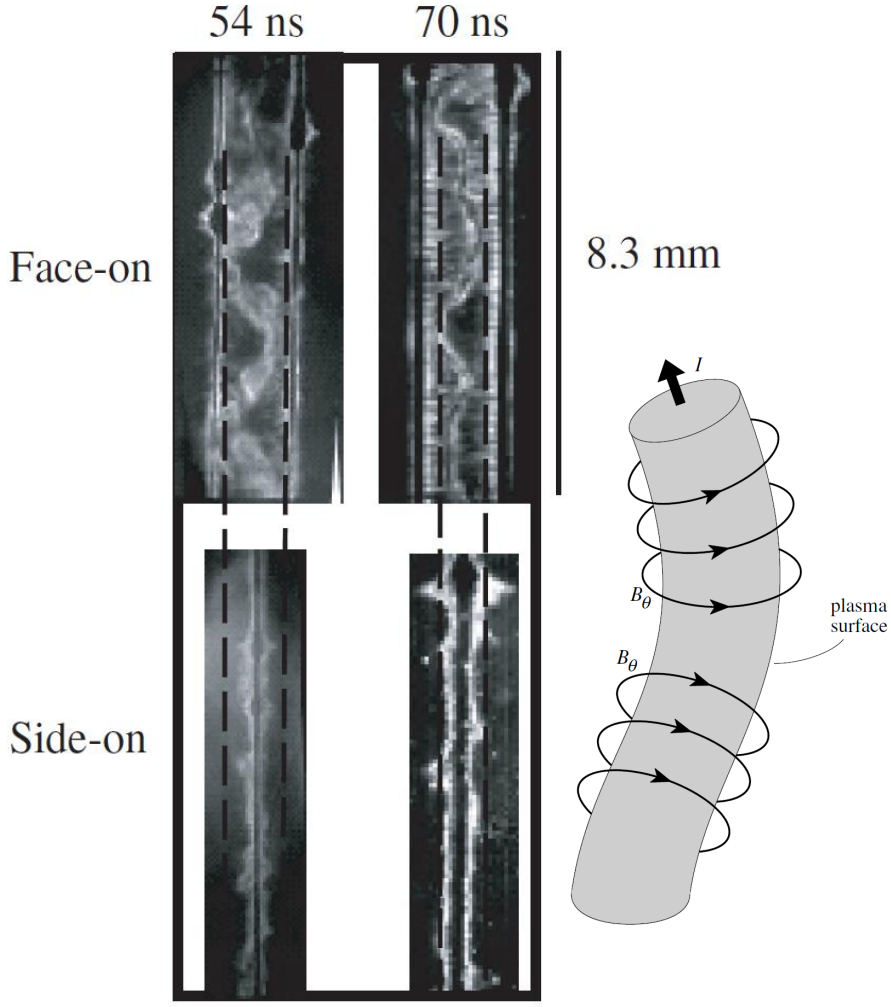

F. N. Beg, et. Al., Plasma Phys. Control. Fusion **46**, 1 (2004)

Kink instabilities in the lab

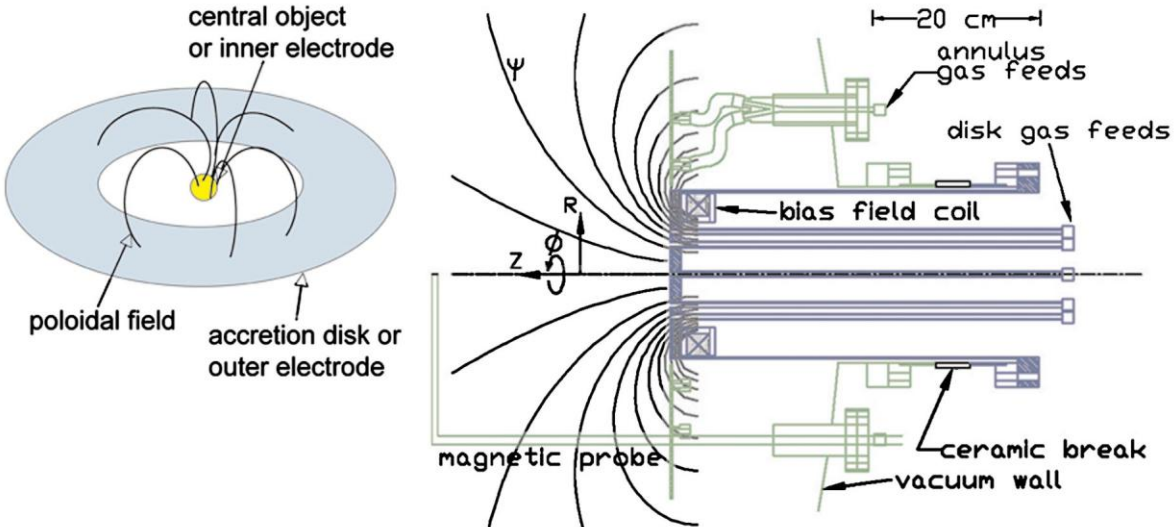

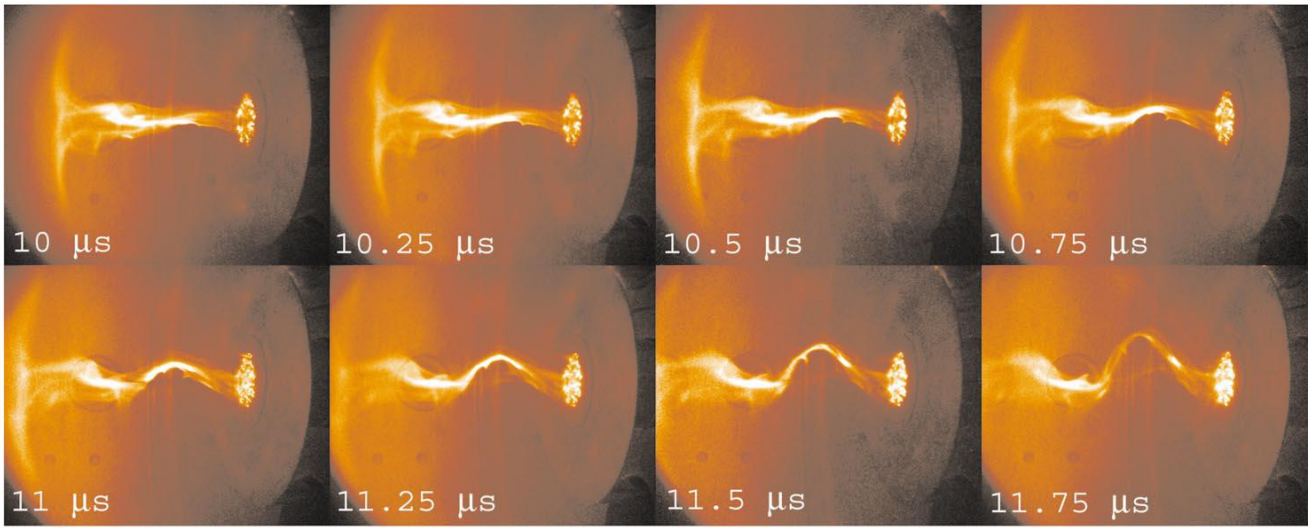

S. C. Hsu, P. M. Bellan, Phys. Plasma **12**, 032103 (2005)

Kink instabilities in space

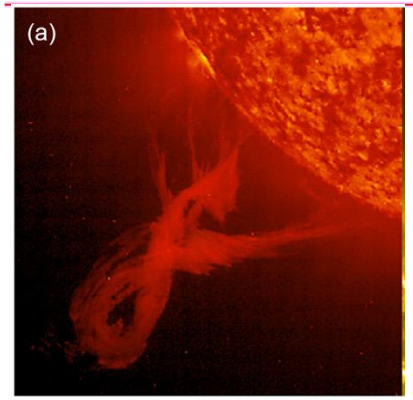

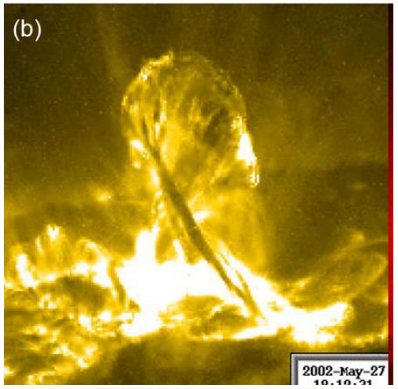

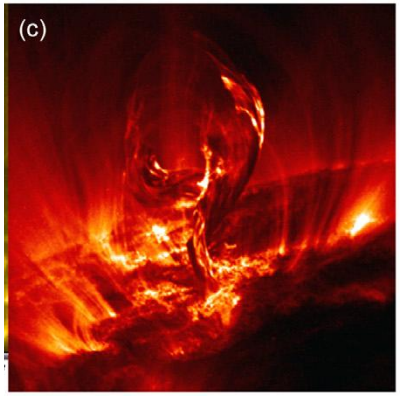

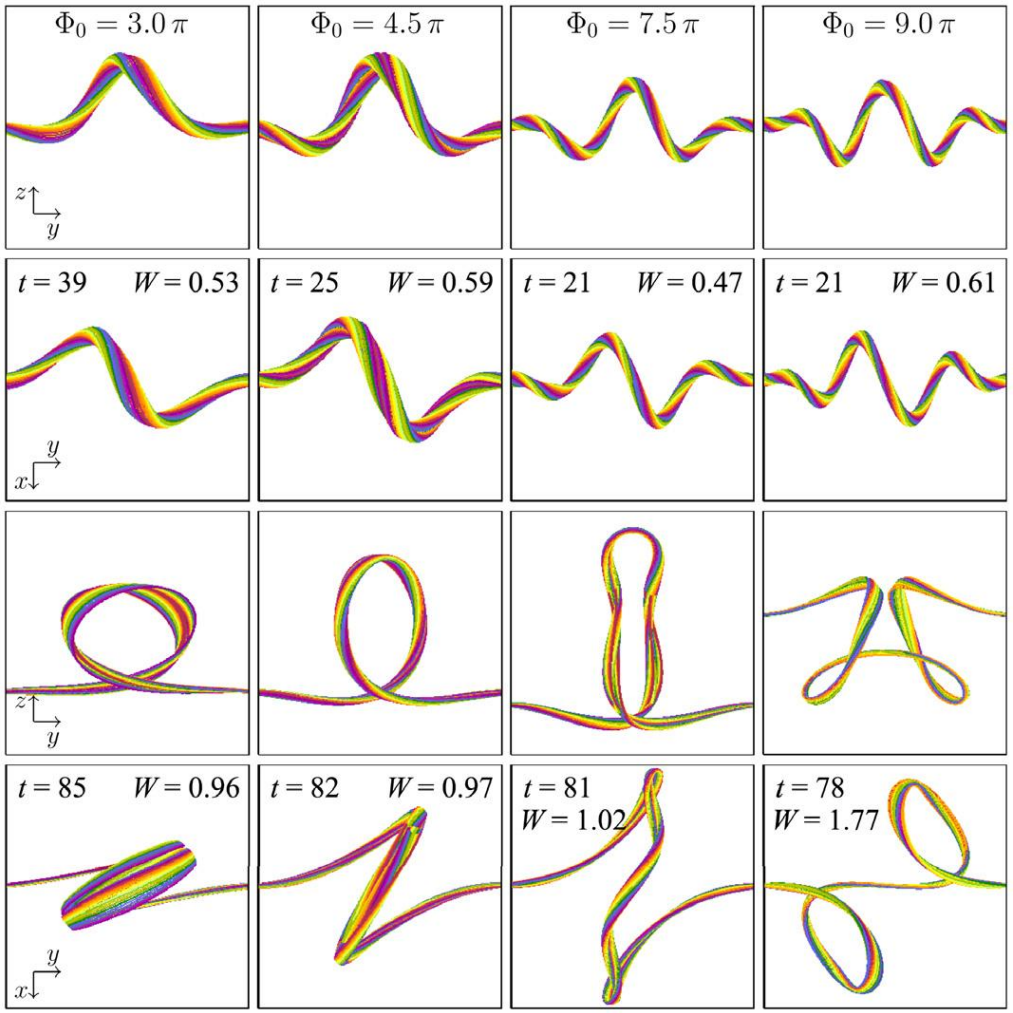

T Török *et al*, Plasma Phys. Control. Fusion **56**, 064012 (2014)

Kink instability in Tokamak

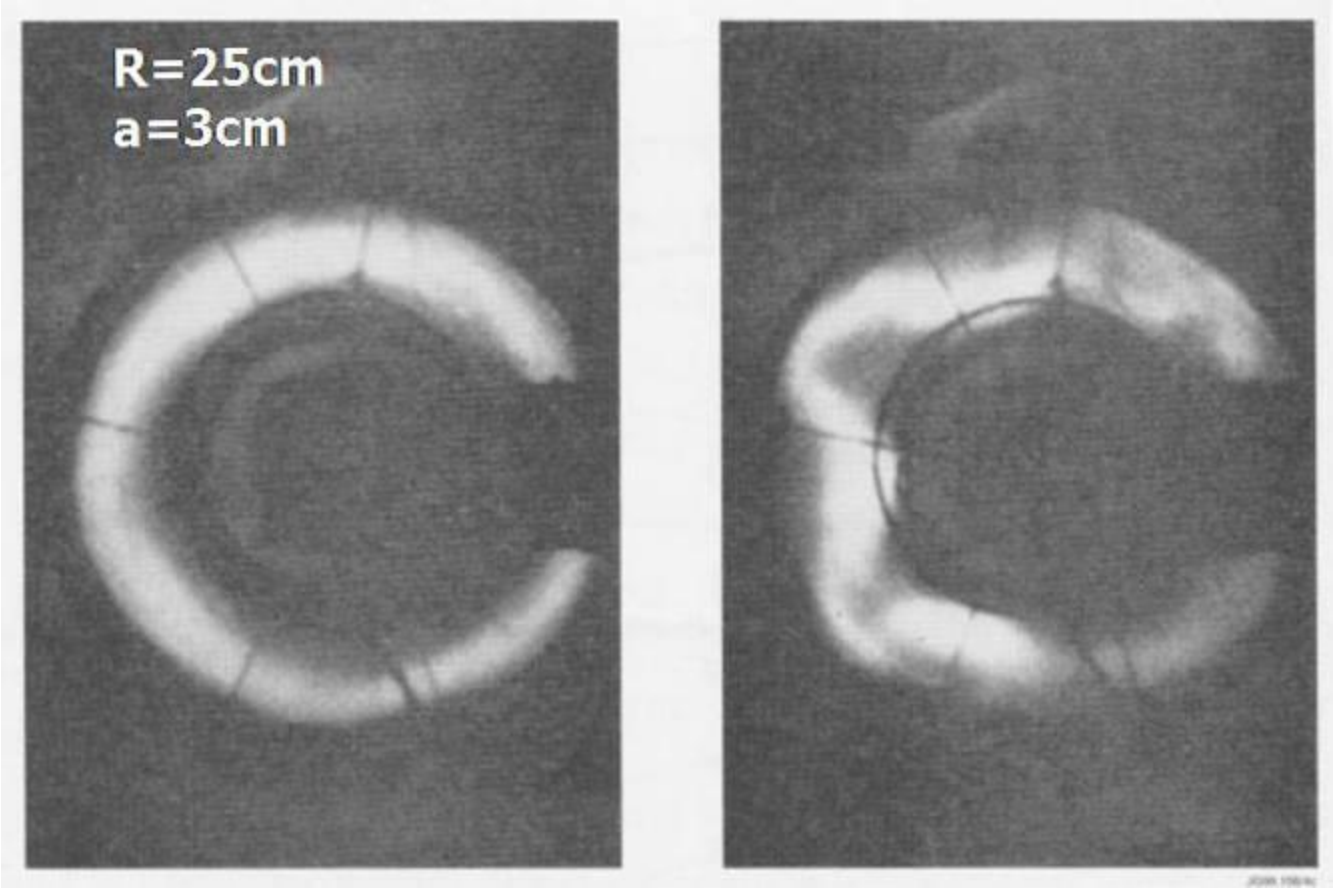

https://en.wikipedia.org/wiki/Kink_instability

Pressure driven instability – interchange perturbations

- **Unstable: bad curvature** $\vec{R}_c \cdot \nabla p < 0$
- **stable: good curvature** $\vec{R}_c \cdot \nabla p > 0$

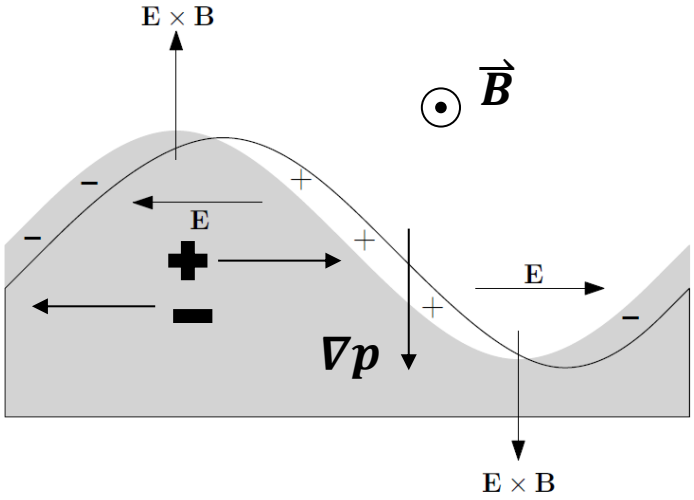

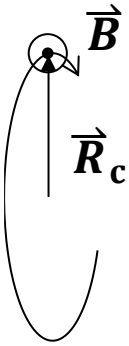

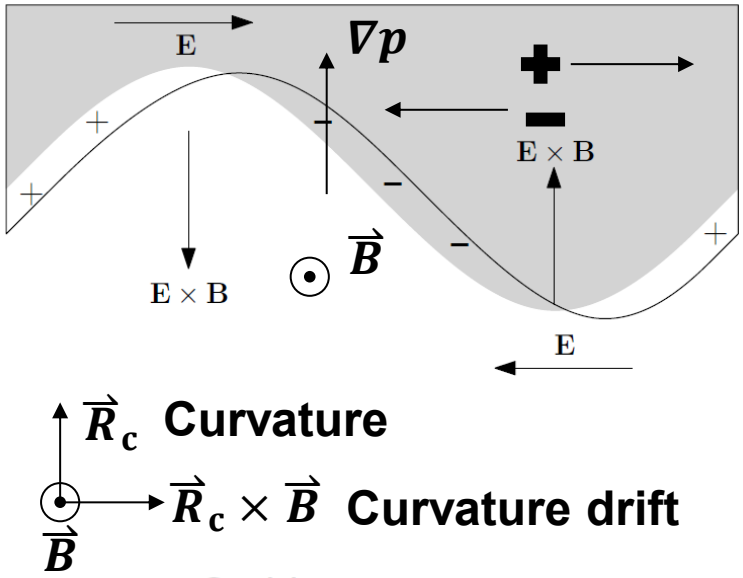

Unstable plasma–vacuum interface

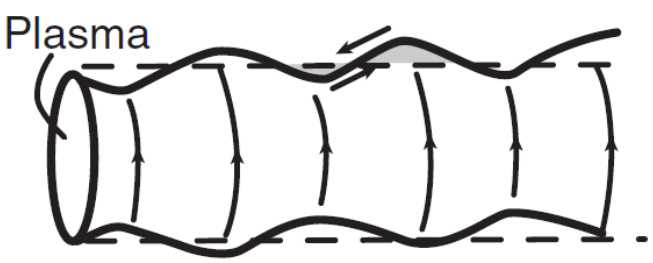

Stable plasma–vacuum interface

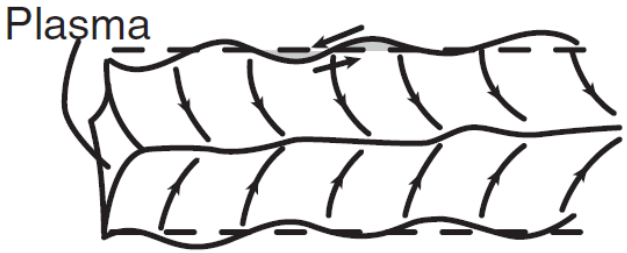

Ben Dudson, Lecture note of Magnetic Confinement Fusion 2014

Rayleigh-Taylor instability

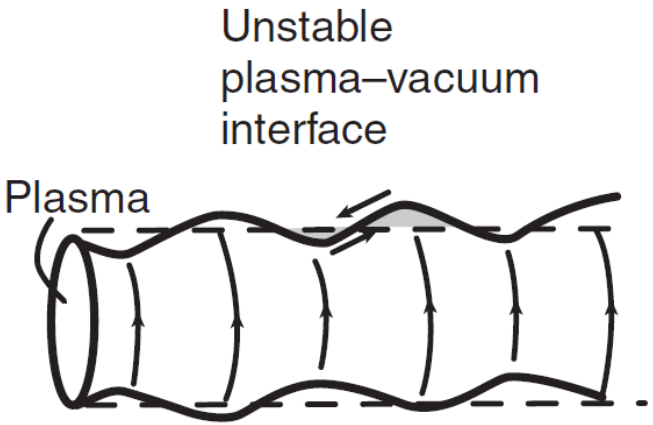

- **Rayleigh-Taylor instability**

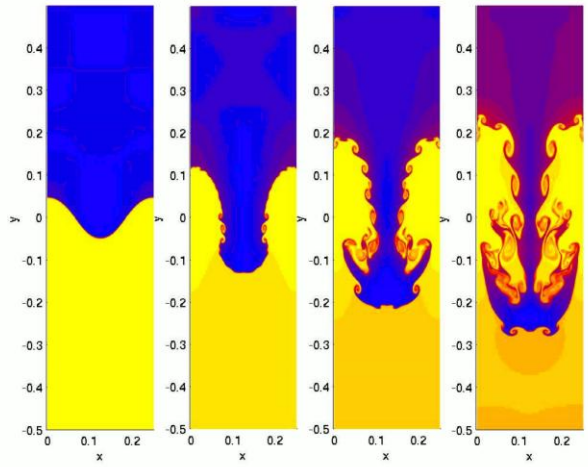

gravity

- **Kelvin-Helmholtz instability**

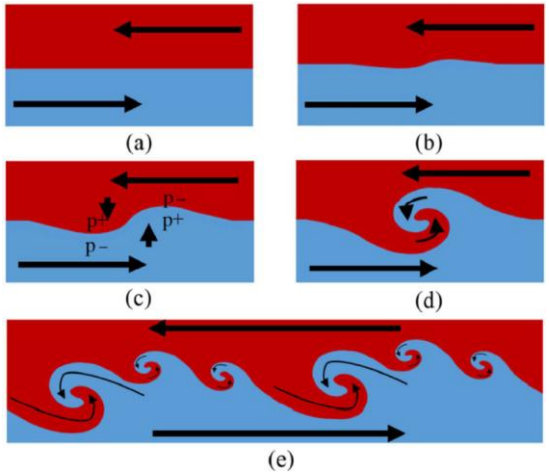

https://en.wikipedia.org/wiki/Rayleigh%E2%80%93Taylor_instability
https://en.wikipedia.org/wiki/Kelvin%E2%80%93Helmholtz_instability
Xie Lei et al, Energy Report **7**, 2262 (2021)

Pressure driven instability – interchange perturbations

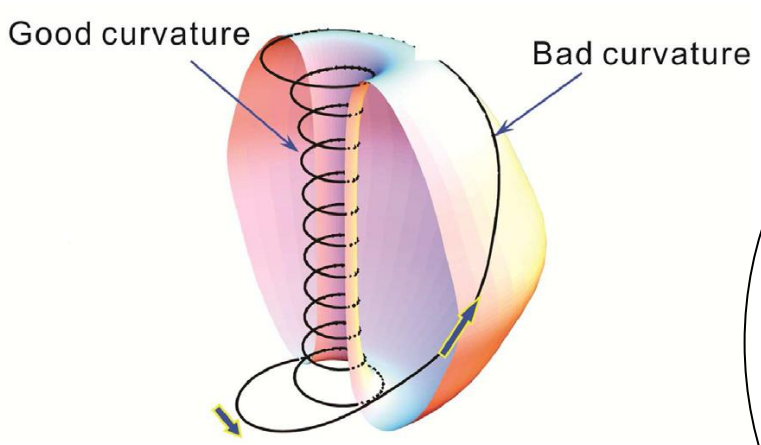

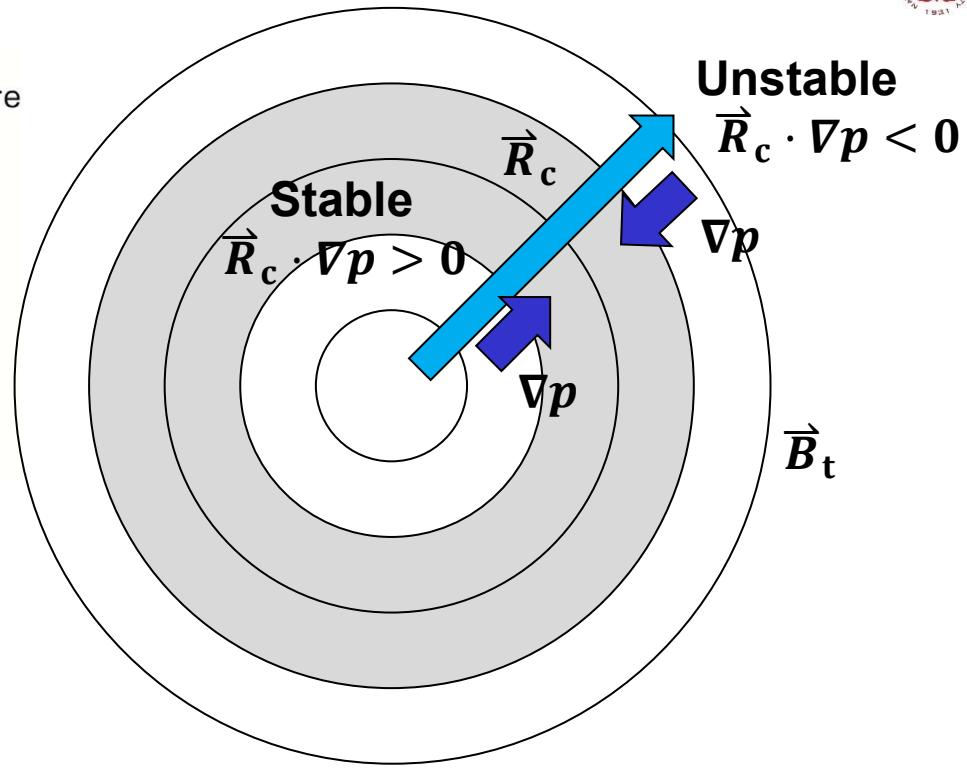

- **Suydam criterion for cylindrical plasmas:** $\mu_o \frac{2r^2}{{B_\theta}^2} \frac{1}{s^2} \vec{R}_c \cdot \nabla p > -\frac{1}{4}$ **Shear:** $s = \frac{r}{q}\frac{dq}{dr}$

- **Mercier criterion for tokamak:** $D = -\mu_o \frac{2r}{B^2} \frac{1}{s^2} \frac{dp}{dr}\left(1 - q^2\right) < \frac{1}{4}$

Ballooning mode – show wavelength mode

$$\delta W_F = \frac{1}{2}\int d\vec{r}\left[\frac{\left|\vec{Q}_\perp\right|^2}{\mu_o} + \frac{B^2}{\mu_o}\left|\nabla\cdot\vec{\xi}_\perp + 2\,\vec{\xi}_\perp\cdot\vec{\kappa}\right|^2 + \gamma p\left|\nabla\cdot\vec{\xi}\right|^2 \right.$$
$$\left. -2\left(\vec{\xi}_\perp\cdot\nabla p\right)\left(\vec{\kappa}\cdot\vec{\xi}_\perp{}^*\right) - J_{||}\left(\vec{\xi}_\perp{}^*\times\vec{b}\right)\cdot\vec{Q}_\perp\right]$$

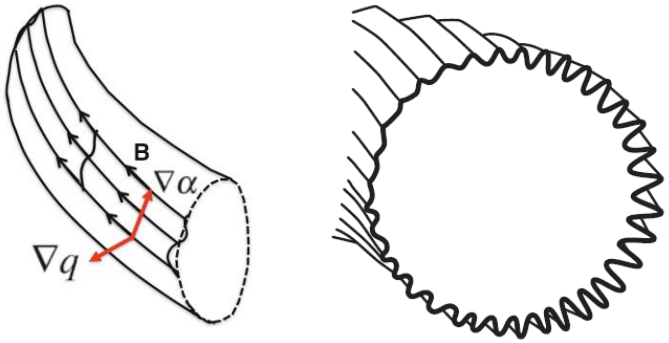

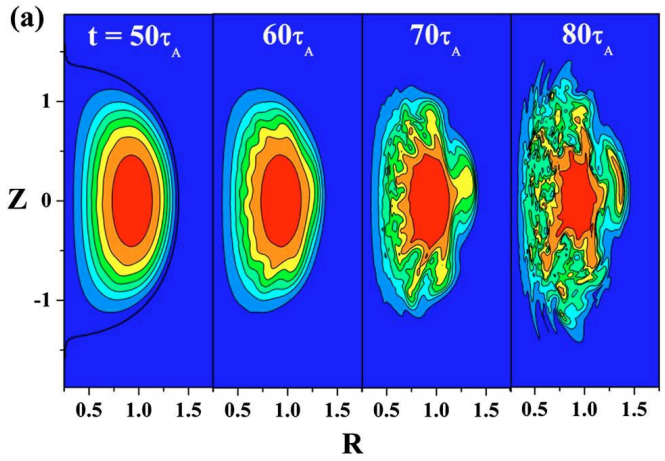

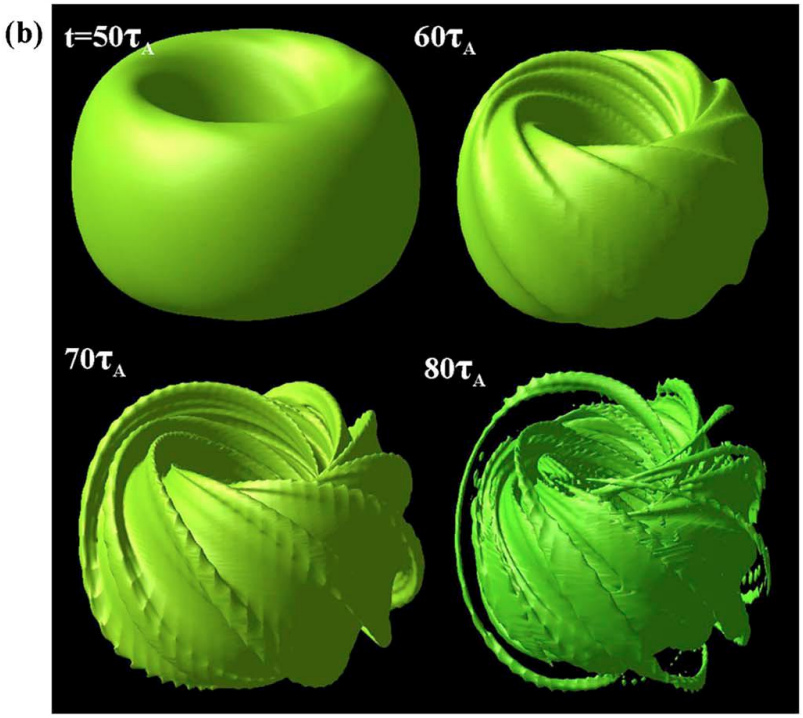

R. Khan et al, Phys. Plasmas **14**, 062302 (2007)

Ballooning mode – show wavelength mode

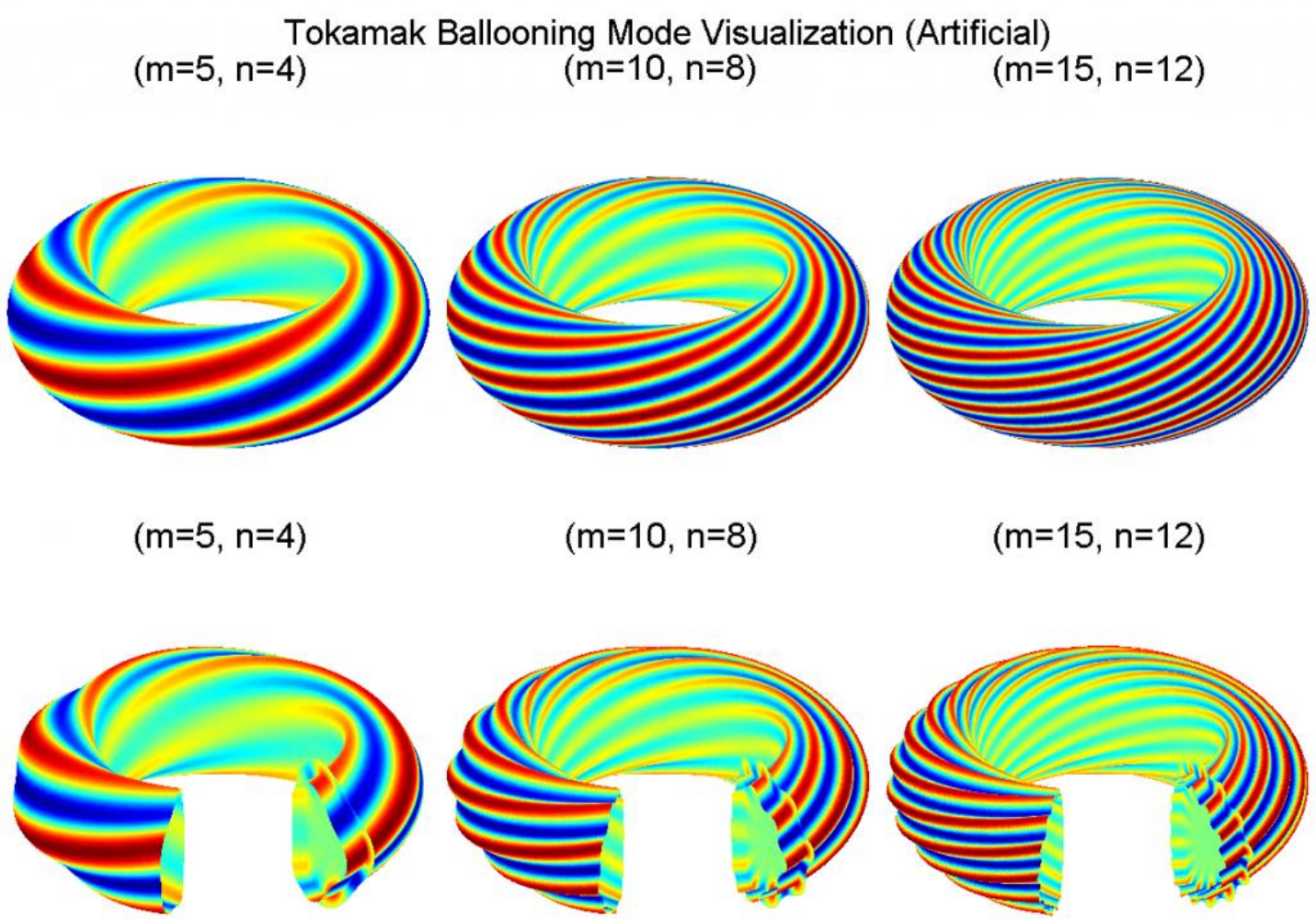

https://blog.sciencenet.cn/home.php?mod=space&uid=222053&do=album&picid=308476#pic_block

The Spherical tokamak

- **Aspect ratio R_o/a ~ 1.6**

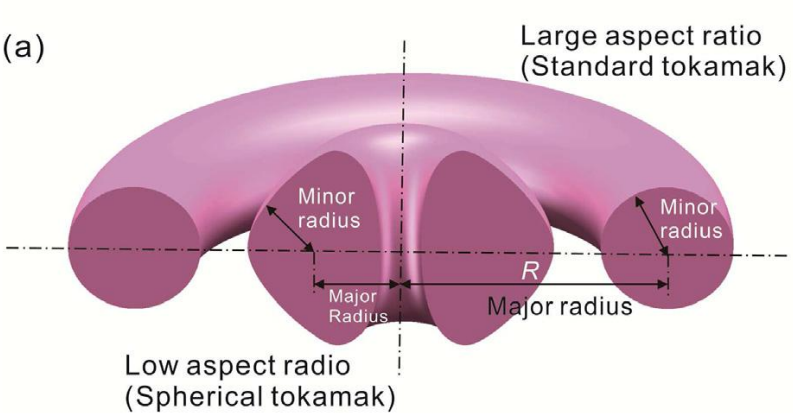

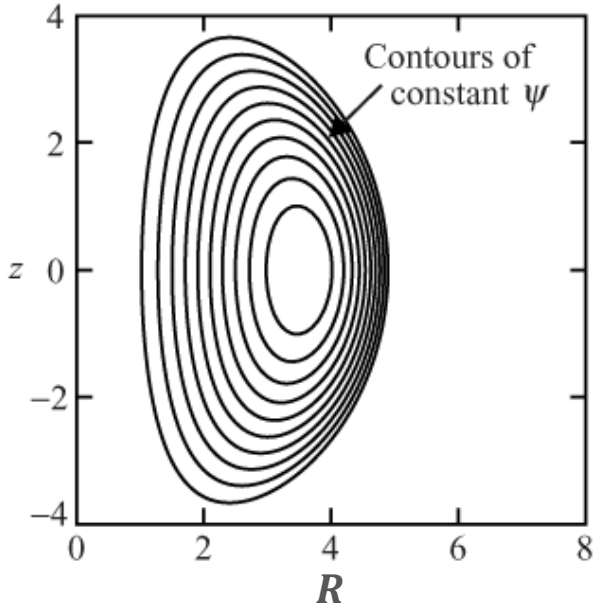

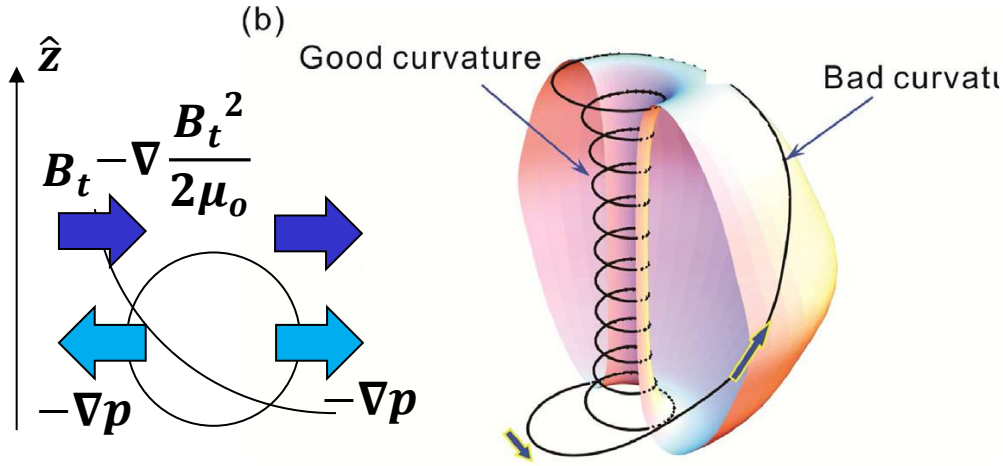

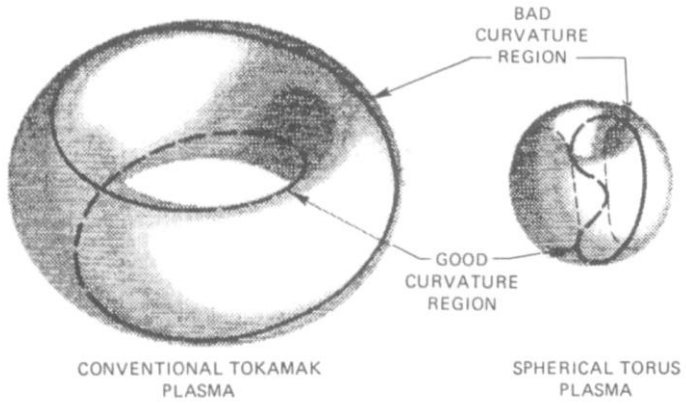

Zhe Gao, Matter and Radia. Extrem., **1**, 153 (2016)
Y-k. M.Peng and D. J. Strickler, Nucl. Fusion **26**, 769 (1986)

The Spherical tokamak

- **Aspect ratio $R_o/a \sim 1.6$**
- **Advantages:**
  - **Higher β_t limit.**
  - **A compact design almost spherical in appearance.**
- **Challenges:**
  - **Minimum space is given in the center of the torus to accommodate the toroidal field coils.**
  - **With a very compact design the technology associated with the construction and maintenance of the device may be more difficult than for a "normal" tokamak.**
  - **Large currents will have to be driven noninductively, a costly and physically difficult requirement.**

Limiter protects the vacuum chamber from plasma bombardment and defines the edge of the plasma

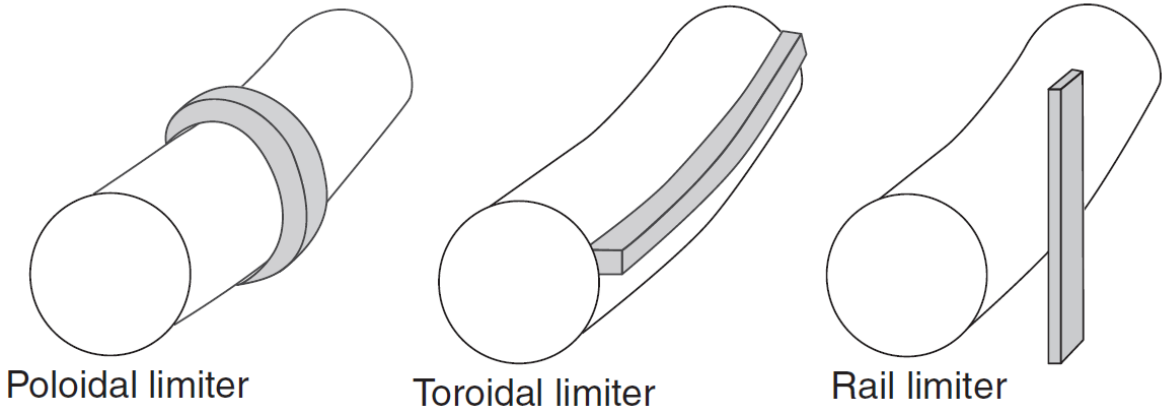

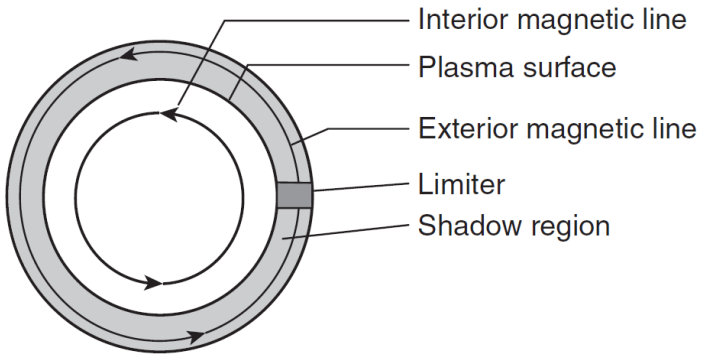

- **Vertical field is correct.**

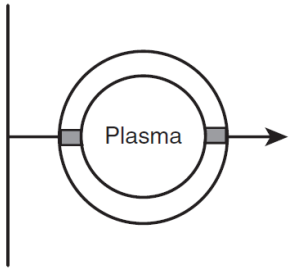

- **Vertical field is too small.**

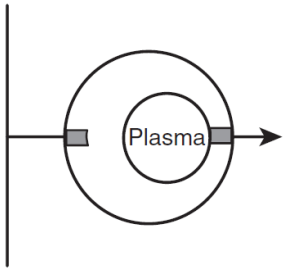

- **Vertical field is too large.**

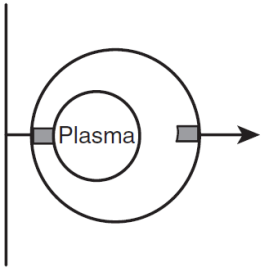

Limiter protects the vacuum chamber from plasma bombardment and defines the edge of the plasma

- A mechanical limiter is a robust piece of material, often made of tungsten, molybdenum, or graphite placed inside the vacuum chamber.
- Some of the particles of the limiter surface may escape. Neutral particles can penetrate some distance into the plasma before being ionized.
- The high-z impurities can lead to significant additional energy loss in the plasma through radiation.
- In ignition experiments and fusion reactors, the bombardment is more intense and extends over longer periods of time. In addition, if the impurity level is too high, it may not be possible to achieve a high enough temperature to ignite.

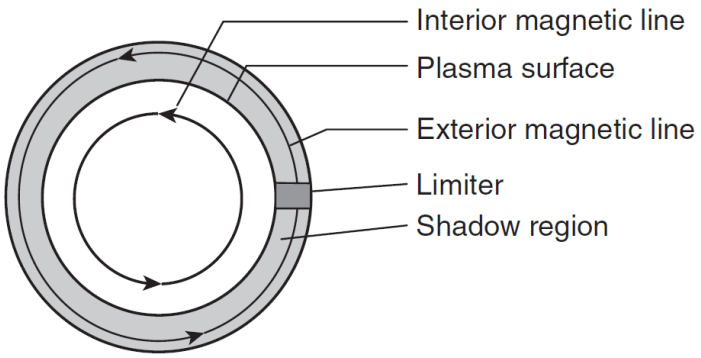

The magnetic divertor – guide a narrower layer of magnetic lines away from the edge of the plasma

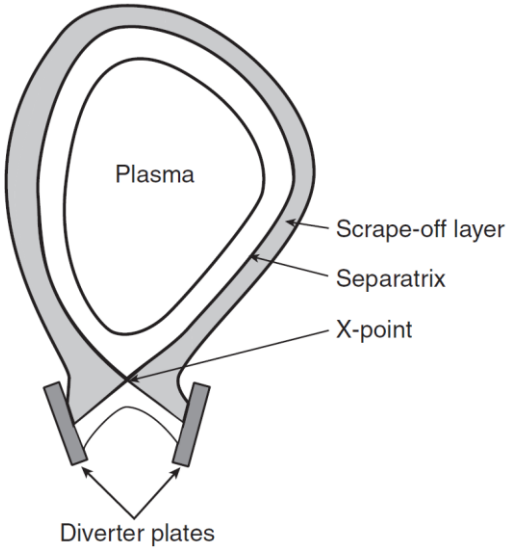

- **Single-null poloidal-field divertors for tokamak**

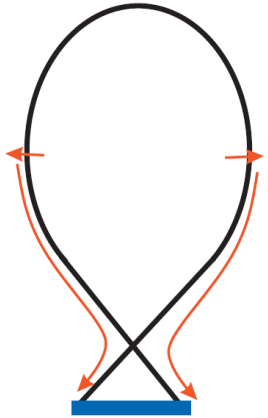

- **Double-null poloidal-field divertors for tokamak**

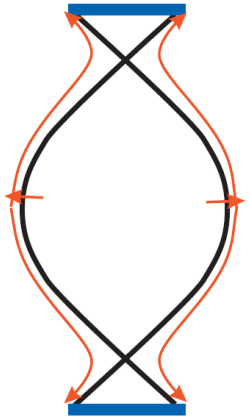

- **Island divertor for stellerators**

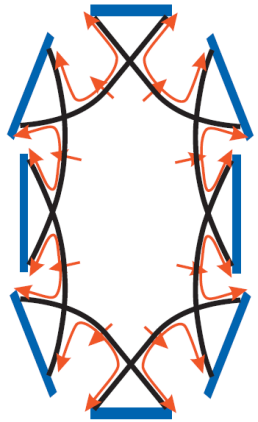

- **Standard**

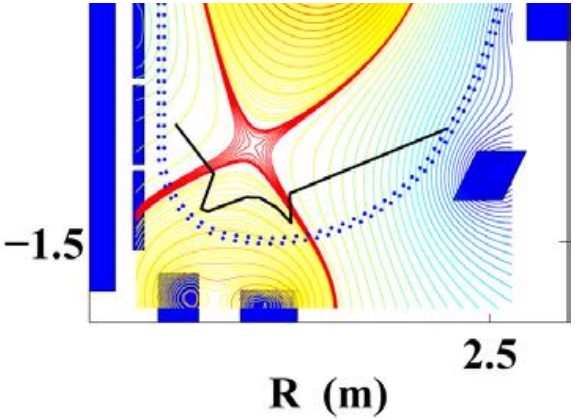

- **Snowflake**

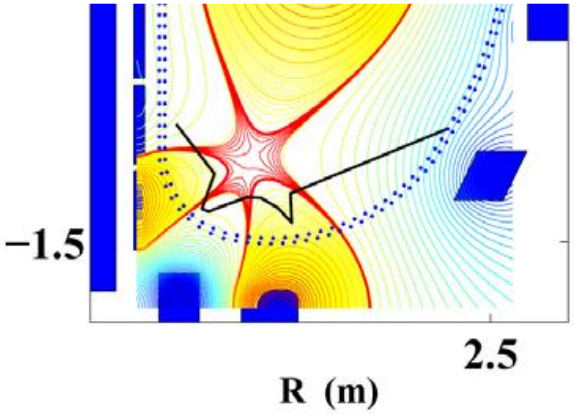

Y. Feng, Nucl. Fusion, **46**, 807 (2006)
L Xue *et al*, Plasma Phys. Control. Fusion **58**, 055005 (2016)

Pros and cons of a divertor

- **Advantages:**
  - **The collector plate is remote from the plasma. There is space available to spread out the magnetic lines.**
  - **A lower intensity of particles and energy bombard the collector plate leading to a longer replacement time.**
  - **It is more difficult for impurities to migrate into the plasma.**
  - **There are longer distance distances to travel and if a neutral particle becomes ionized before or during the time it crosses the divertor layer on its way toward the plasma, its parallel motion then carries it back to the collector plate.**
  - **The larger divertor chamber provides more access to pump out impurities.**
  - **The plasma edge is not in direct contact with a solid material such as a limiter.**
- **Disadvantages: larger and more complex system and more expensive.**

Course Outline

- **Magnetic confinement fusion (MCF)**
  - **Gyro motion, MHD**
  - **1D equilibrium (z pinch, theta pinch)**
  - **Drift: ExB drift, grad B drift, and curvature B drift**
  - **Tokamak, Stellarator (toroidal field, poloidal field)**
  - **Magnetic flux surface**
  - **2D axisymmetric equilibrium of a torus plasma: Grad-Shafranov equation.**
  - **Stability (Kink instability, sausage instability, Safety factor Q)**
  - **Central-solenoid (CS) start-up (discharge) and current drive**
  - **CS-free current drive: electron cyclotron current drive, bootstrap current.**
  - **Auxiliary Heating: ECRH, Ohmic heating, Neutral beam injection.**

Collisions play an important role in ionization process

- At the microscopic level, breakdown requires the presence of sufficiently energy charge particles that have acquired enough energy from the applied electric field between two energy-dissipating collisions to ionize the material and to create more charge particles.

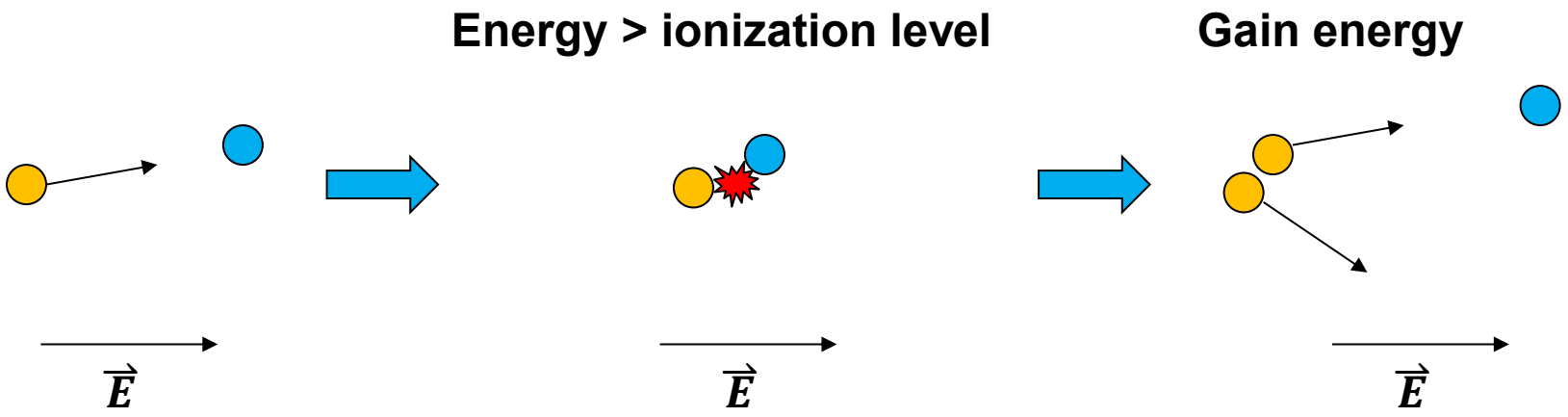

In most cases, electrons dominate the breakdown process since its mobility is much larger than that of ions

$$E_k = \frac{1}{2}mv^2 \qquad v = \sqrt{\frac{2E_k}{m}} \qquad E_k \sim kT$$

Collision time: $$t = \frac{s}{\sqrt{\frac{2E_k}{m}}} \sim \frac{n^{-1/3}}{\sqrt{T}}\sqrt{m} \qquad n = \frac{\#/}{V} \sim \frac{\#//}{S^3} \qquad s \sim n^{-1/3}$$

$$\frac{m_i}{m_e} \sim 2000 \times \text{Atomic mass} \qquad \frac{t_i}{t_e} \sim 45 \times \sqrt{A}$$

Mean free path is important in ionization process

- For an electron to acquire enough energy between collisions, its <u>mean free path</u> in the material must be sufficiently long.

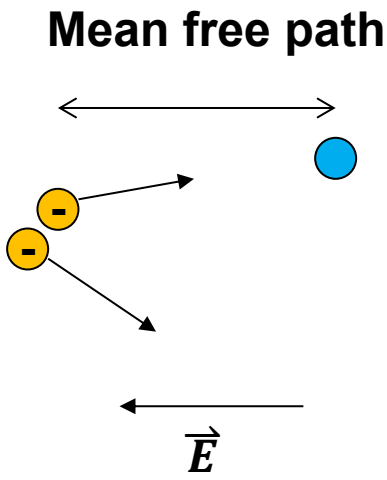

$$E_k = e \times E \times \lambda = eV$$

Electron impact ionization is the most important process in a breakdown of gases

- **Electron impact ionization:** $A + e^- \rightarrow A^+ + e^- + e^-$
  - **The most important process in the breakdown of gases but is not sufficient alone to result in the breakdown.**

$$eE\lambda_{e,i} \geq eV_i$$

V_i: ionization potential

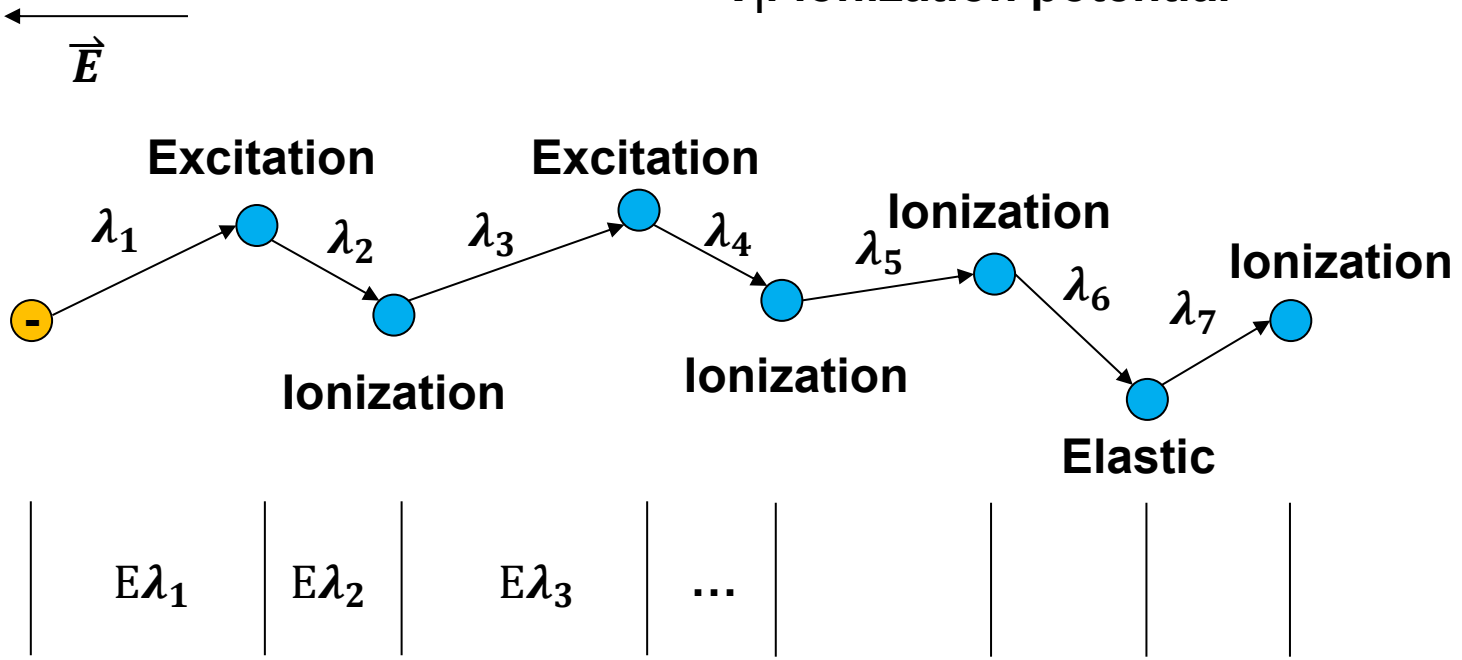

Collision cross-sections of elastic, ionizing collisions between e^- and H_2 and coulomb collisions

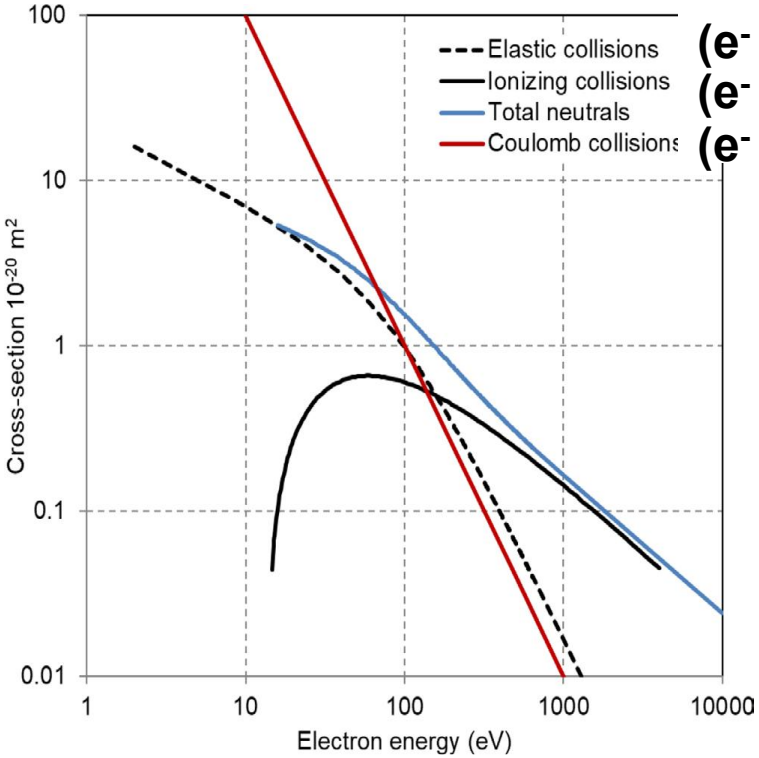

(e^- vs H_2)

($e^- + H_2 \rightarrow 2e^- + H^+ + H$)

(e^- vs H^+)

$$\sigma_{\text{elastic,m}^2} = \frac{1.75 \times 10^{-16}}{\left(W_{\text{e,eV}}{}^{1.5} + 750\right)\sqrt{W_{\text{e,eV}}}}$$

$$\sigma_{\text{ionizing,m}^2} \sim 3 \times 10^{-20}\left(ln\epsilon - 0.69 + \frac{0.66}{\epsilon}\right)\epsilon^{-1}$$

$$\epsilon = \frac{W_e}{E_{ion}} \quad E_{ion} \sim 15 \text{ eV for } H_2$$

$$\sigma_{\text{coulomb}} = \frac{e^4}{4\pi\epsilon_0{}^2 m_e{}^2 v_e{}^2}\ln\Lambda$$

$$= \frac{e^4}{16\pi\epsilon_0{}^2 W_e{}^2}\ln\Lambda \sim 10^{-16} W_e{}^{-2}$$

$$\text{for } \ln\Lambda \sim 13 - 15$$

$$\nu = n v_E \sigma$$

$$\lambda = \frac{1}{n\sigma}$$

P. C. de Vries and Y. Gribov, Nucl. Fusion, **59**, 096043 (2019)

Townsend avalanche process for Tokamak breakdown

- The first Townsend coefficient α: the number of ionizing collisions made on the average by an electron as it travels 1 m along the electric field:

$$\alpha \sim \frac{1}{\lambda_i} = \frac{\nu_{ei}}{\bar{v}_e} = \frac{n_0 \langle \sigma v_e \rangle_{ne}}{\bar{v}_e} = \frac{p}{T} \frac{\langle \sigma v \rangle_{ne}}{\bar{v}_e} \equiv Ap \qquad A \equiv \frac{1}{T} \frac{\langle \sigma v \rangle_{ne}}{\bar{v}_e}$$

- Number of primary electrons with energy higher than the ionization potential:

$$dn_e = -n_e \frac{dx_i}{\lambda_i} \quad \Rightarrow \quad \frac{n_e(x_i)}{n_{e0}} = \exp\left(-\frac{x_i}{\lambda_i}\right)$$

$$\alpha \equiv \frac{\#/\text{ ionization collisions}}{\text{per electron}} \times (\#/\text{electron with E} > \text{ionization potential})$$

$$= \frac{1}{\lambda_i} \frac{n_e(x_i)}{n_{e0}} = \frac{1}{\lambda_i} \exp\left(-\frac{x_i}{\lambda_i}\right)$$

$$\alpha = Ap \exp(-Apx_i)$$

A = 3.83 $m^{-1}Pa^{-1}$ = 1060 $m^{-1}Torr^{-1}$

B = 96.6 $Vm^{-1}Pa^{-1}$ = 35000 $m^{-1}Torr^{-1}$

$$\alpha = Ap\exp\left(-\frac{AV^*}{E/p}\right) \equiv Ap\exp\left(-\frac{B}{E/p}\right) \qquad x_i \approx \frac{V^*}{E} \text{ where } V^* > V_i$$

- The parameters *A* and *B* must be experimentally determined.

Paschen-like curve for minimum breakdown voltage

$$\alpha \sim \frac{1}{\lambda_i} = Ap \quad \alpha = Ap\exp\left(-\frac{B}{E/p}\right)$$

A = 3.83 m^{-1}Pa^{-1} = 1060 m^{-1}Torr^{-1}

B = 96.6 Vm^{-1}Pa^{-1} = 35000 m^{-1}Torr^{-1}

- **For p=1 mPa, $\lambda_i \sim 262$ m , for ITER, $2\pi r_o \sim 38$ m $\quad \frac{\lambda_i}{2\pi r_o} \sim 7$**

- **For breakdown to happen:**

$$\alpha L > 1 \quad \alpha L = ApL\exp\left(-\frac{BpL}{V_{BD}}\right) > 1$$

$$\exp\left(-\frac{BpL}{V_{BD}}\right) > \frac{1}{ApL}$$

$$-\frac{BpL}{V_{BD}} > -\ln(ApL)$$

$$V_{BD} > \frac{BpL}{\ln(ApL)} \quad E_{BD} > \frac{Bp}{\ln(ApL)}$$

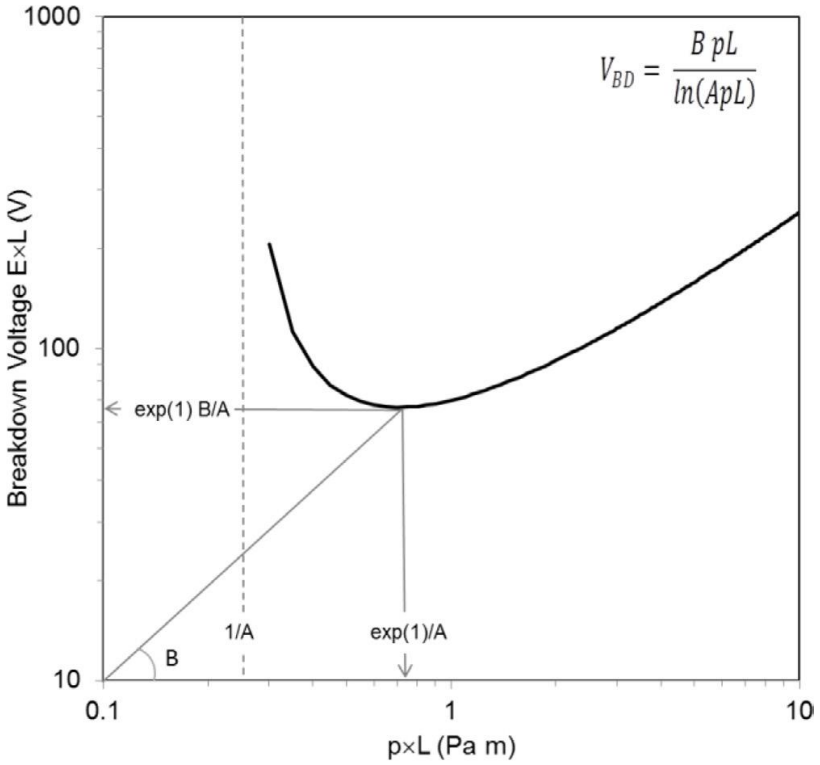

P. C. de Vries and Y. Gribov, Nucl. Fusion, **59**, 096043 (2019)

Perpendicular stray-field (B_z) needs to be as small as possible

- For p=1 mPa, $\lambda_i \sim 262\ \mathrm{m}$, for ITER, $2\pi r_o \sim 38\ \mathrm{m}$ $\dfrac{\lambda_i}{2\pi r_o} \sim 7$

  $\dfrac{B_z}{B_T} \sim 10^{-3}$ $\lambda_i \times \dfrac{B_z}{B_T} = 0.26\ \mathrm{m}$

- For ITER,

  $E \sim E_{\mathrm{loop}} = 0.3\ \mathrm{V/m}$

  $p = 1\ \mathrm{mPa}$ $L_{\mathrm{BD}} = 357\ \mathrm{m}$

- Required loop field:

  $$E_{\mathrm{BD}} > \frac{Bp}{\ln(ApL)}$$

  $$E_{\mathrm{BD}} > \frac{1.25 \times 10^4 P_{\mathrm{Torr}}}{\ln(510 P L_c)}$$

  $$L_c = 0.25 a_{\mathrm{eff}} \left(\frac{B_z}{B_T}\right)$$

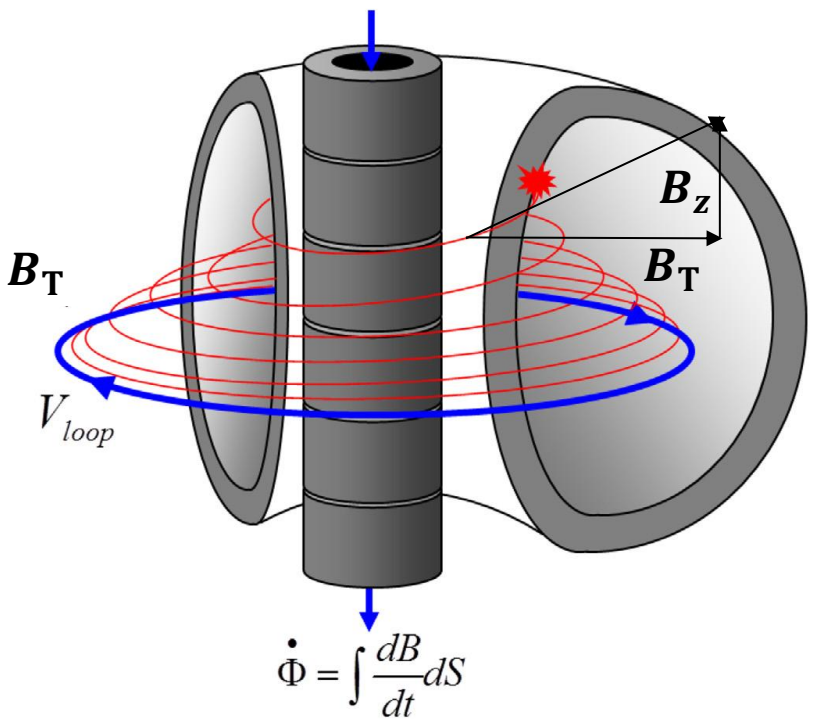

- W/ preionization: $E_T \dfrac{B_T}{B_z} \geq 100\ \mathrm{V/m}$
- Purely Ohmic discharges: $E_T \dfrac{B_T}{B_z} \geq 1000\ \mathrm{V/m}$

P. C. de Vries and Y. Gribov, Nucl. Fusion, **59**, 096043 (2019)
S. J. Doyle et al, Fusion Eng. Des. **171**, 112706 (2021)

Examples or required loop electric fields

$$E_{BD} > \frac{1.25 \times 10^4 P_{Torr}}{\ln(510 P L_c)}$$

$$L_c = 0.25 a_{eff}\left(\frac{B_z}{B_T}\right)$$

- W/ preionization: $E_T \frac{B_T}{B_z} \geq 100\,V/m$
- Purely Ohmic discharges: $E_T \frac{B_T}{B_z} \geq 1000\,V/m$

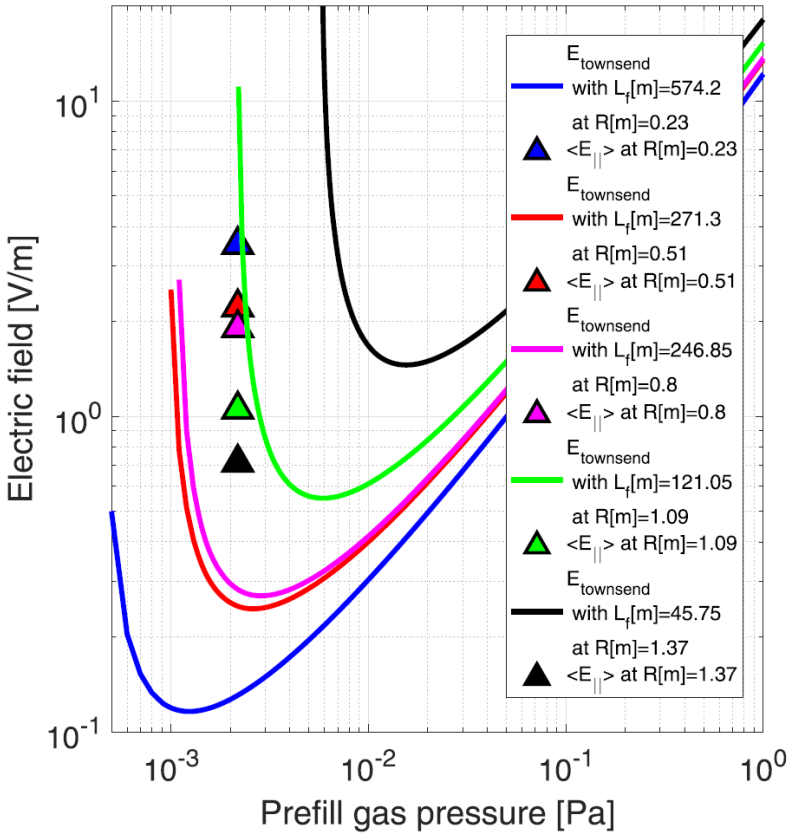

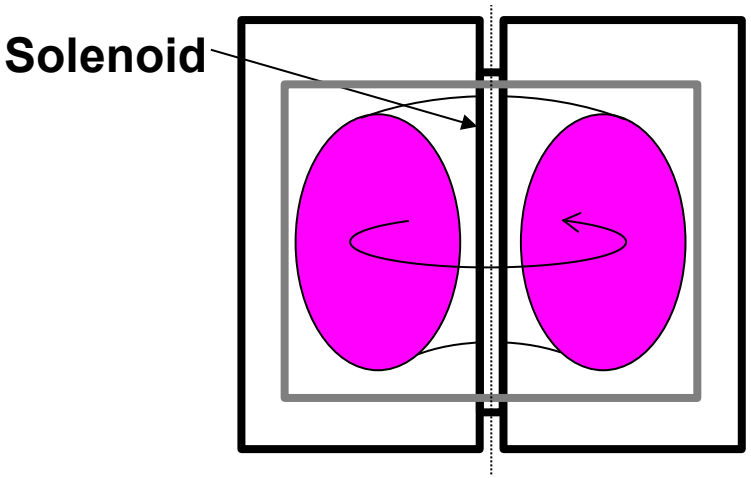

$$V_\phi = -\frac{\partial \phi}{\partial t} \equiv M \frac{\partial I_{CS}}{\partial t}$$

$$E_\phi = -\frac{1}{2\pi r}\frac{\partial \phi}{\partial t}$$

H.-T. Kim, etc., Nucl. Fusion **62**, 126012 (2022)
S. J. Doyle et al, Fusion Eng. Des. **171**, 112706 (2021)

Central solenoid can be used to provide the required loop voltage for breakdown

- **SMART:**

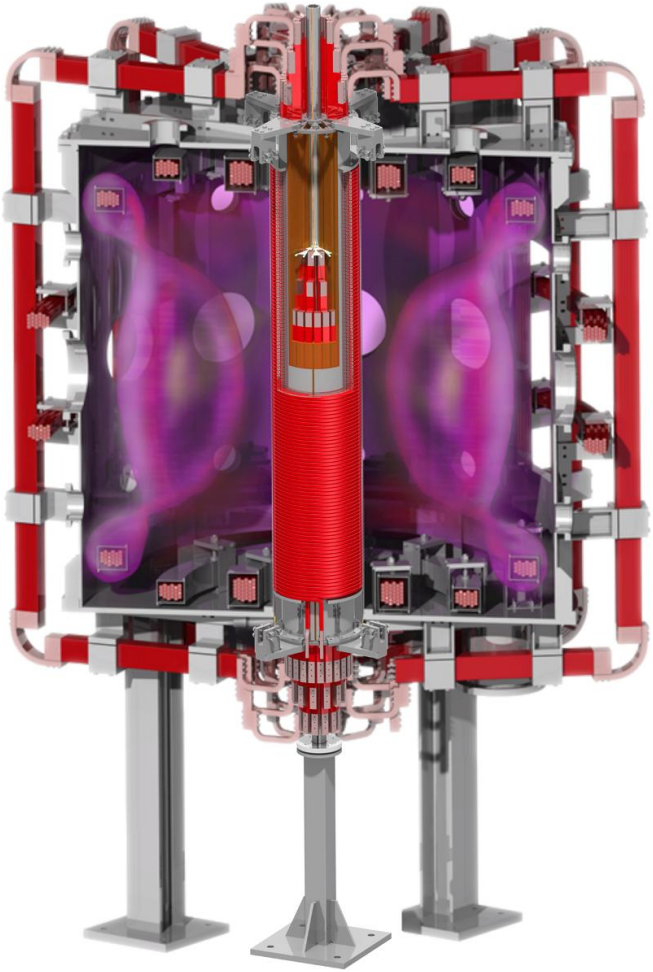

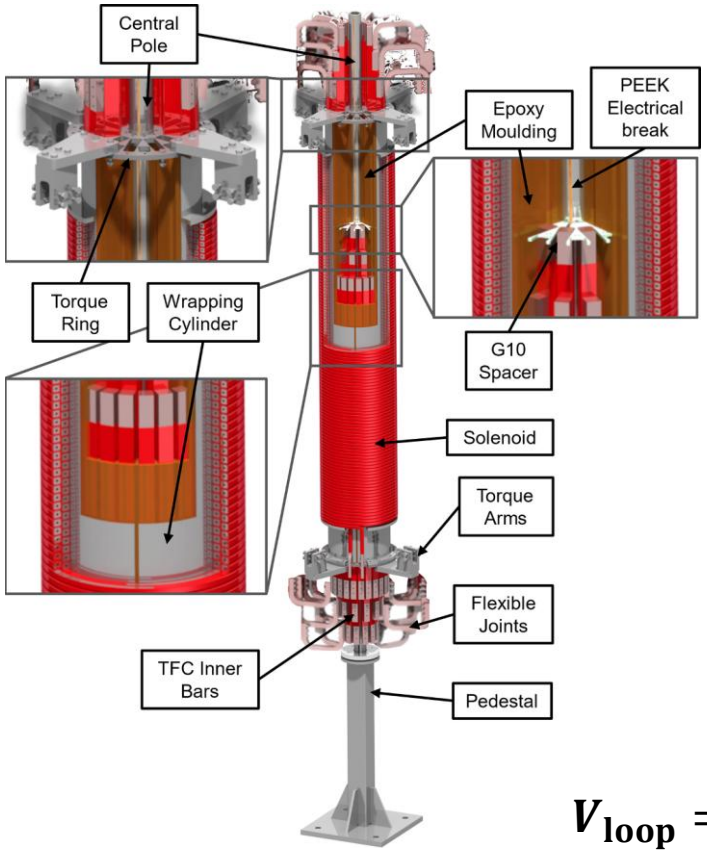

$$V_{\mathbf{loop}} = \frac{A_{\mathbf{sol}} \mu N_{\mathbf{sol}}}{L_{\mathbf{sol}}} \frac{dI_{\mathbf{sol}}}{dt}$$

J. Segado-Fernandez et al, Fusion Eng. Des. **193**, 113832 (2023)

Poloidal coils are used to reduce the stray field during breakdown

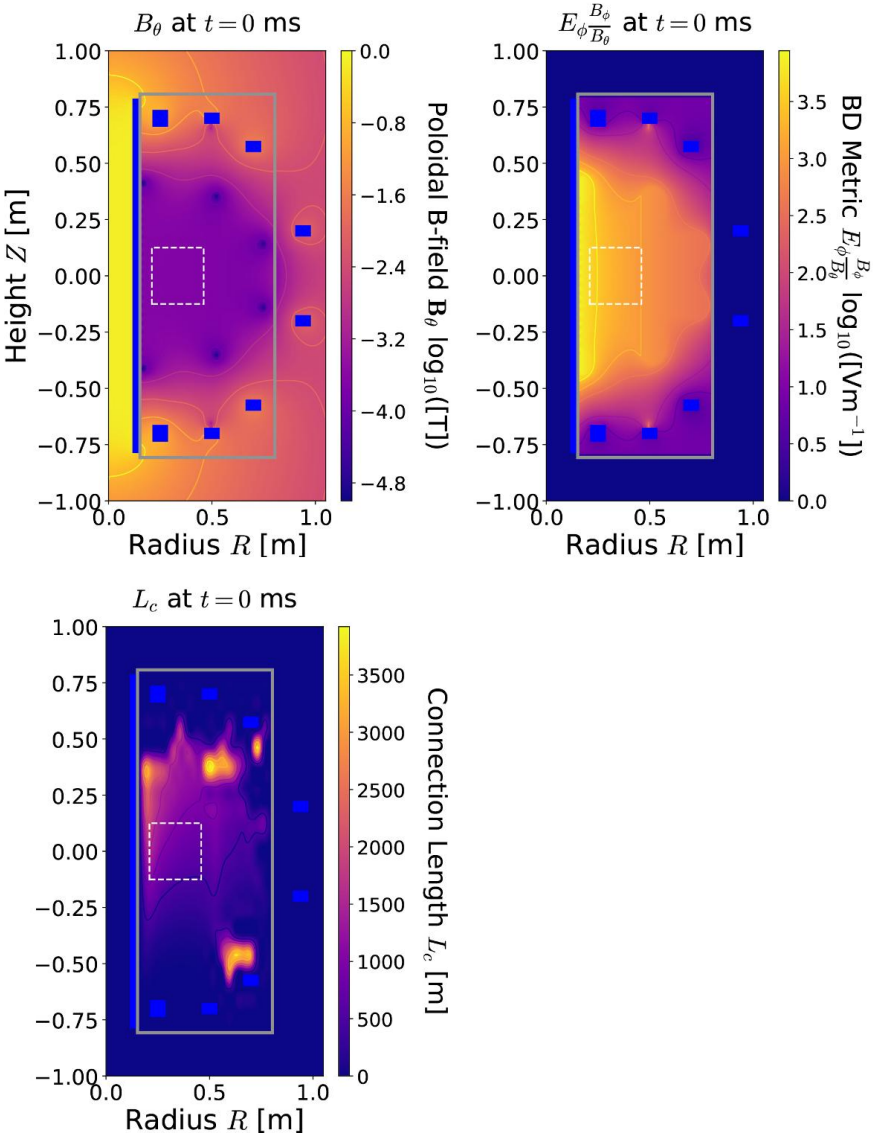

- **Currents of SMART**

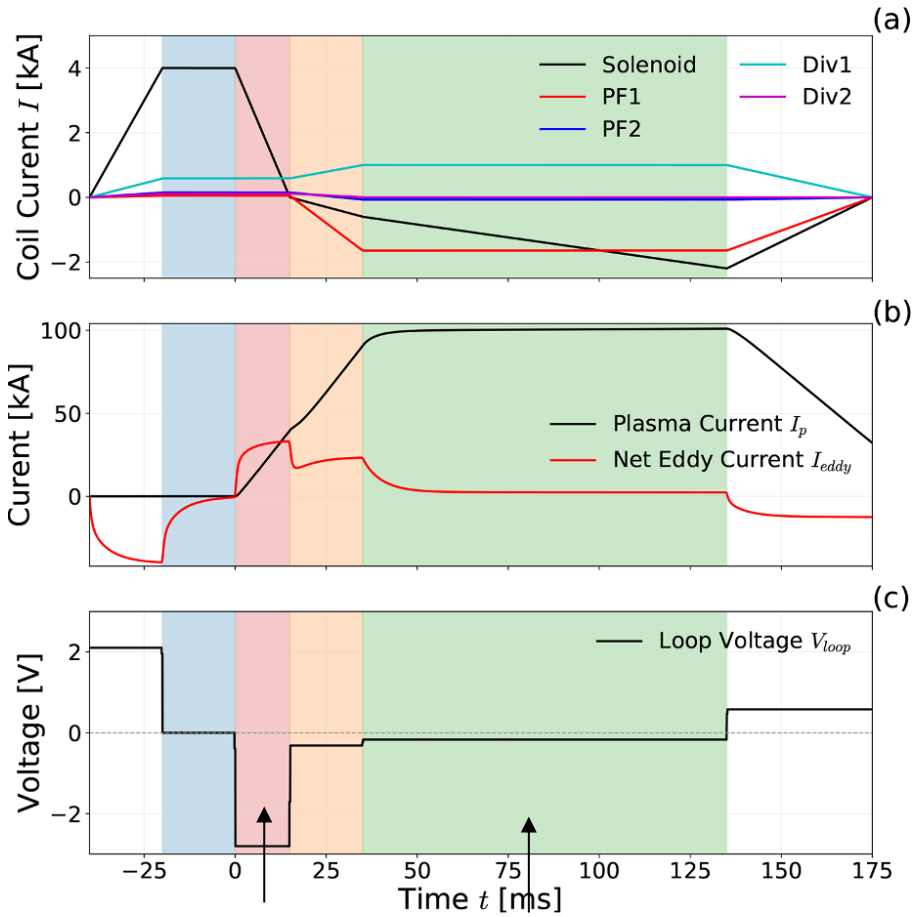

Breakdown **Plasma current is driven**

S. J. Doyle, etc., Fusion Eng. Des. **171**, 112706 (2021)

Momentum exchange may be needed to drive plasma current

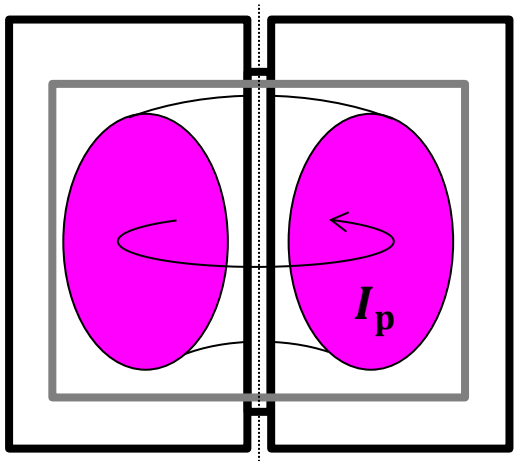

$$\vec{j}_p = \Sigma qn\,\vec{v} = -en_e\,\vec{v}_e + en_i\,\vec{v}_i$$

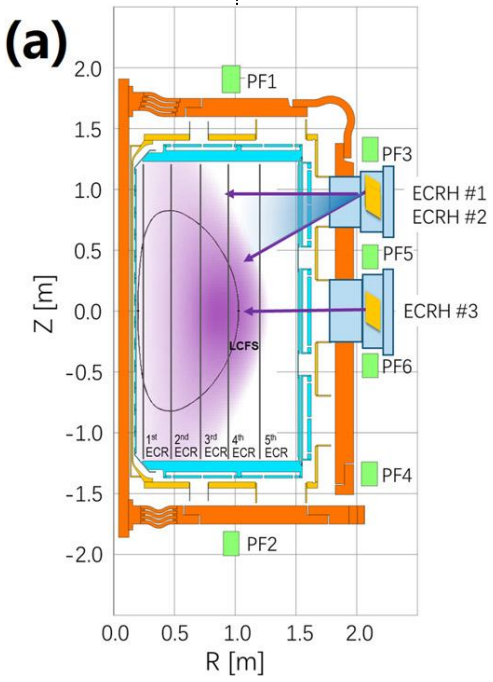

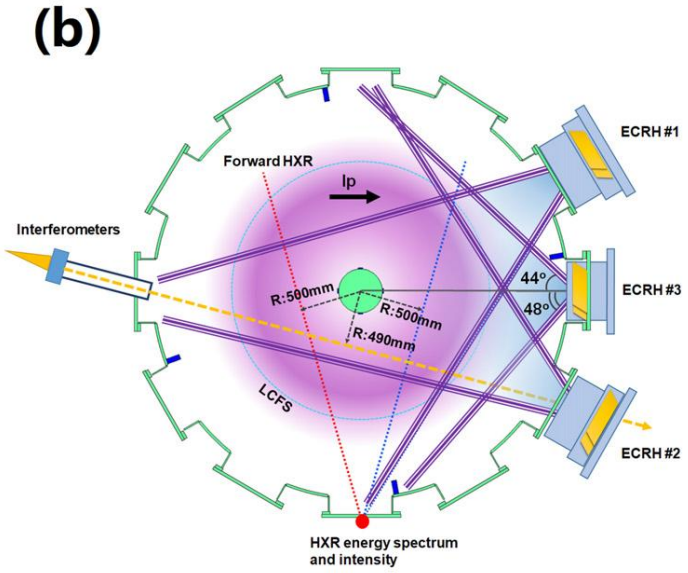

Yuejiang Shi et al, Nucl. Fusion **62**, 086047 (2022)

Solenoid can be used to drive the plasma current

$$L_{\text{tor}}\frac{dI}{dt} + IR = V_{\text{loop}} = M\frac{dI_{\text{sol}}}{dt}$$

$$L_{\text{tor}} = \mu_{\text{o}} r_{\text{o}}\left[\ln\left(\frac{8r_{\text{o}}}{a}\right) - 1.5\right]$$

$$R_{\text{spitzer}} = \eta_{\text{spiter}}\frac{2\pi r_{\text{o}}}{A_{\text{tor}}}$$

$$\eta_{\text{spiter}} = 5.2\times 10^{-3} Z \ln\Lambda\, T_{e,(\text{eV})}^{-3/2}$$

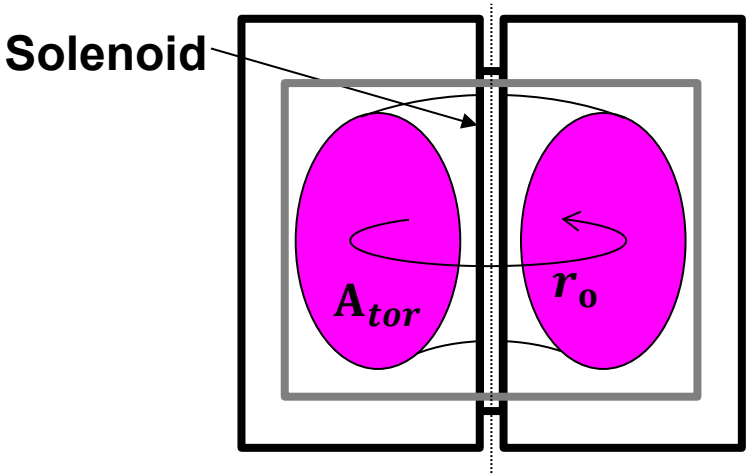

Current is initially driven at the surface and then diffuses into the plasma

- **Simplified Ohm's law:** $\vec{E} + \vec{v} \times \vec{B} = \eta \vec{j}$

- **Assuming a stationary plasma:** $\nabla \times \vec{E} = -\frac{\partial \vec{B}}{\partial t} = \nabla \times (\eta \vec{j})$

- **Assuming a constant η:**

$$-\frac{\partial}{\partial t} \nabla \times \vec{B} = \eta \nabla \times \nabla \times \vec{j} = \eta \left(\nabla (\nabla \cdot \vec{j}) - \nabla^2 \vec{j} \right)$$

$$\frac{\partial \vec{j}}{\partial t} = \frac{\eta}{\mu_o} \nabla^2 \vec{j}$$

- **Assuming non-constant η:**

$$\frac{\partial \vec{j}}{\partial t} = \frac{1}{\mu_o} \nabla^2 (\eta \vec{j}) - \nabla [\nabla \cdot (\mu \vec{j})] \qquad \frac{\partial j_T}{\partial t} = \frac{1}{\mu_o} \nabla^2 (\eta j_T)$$

- **Since $\eta \propto T^{-3/2}$, resistance drops with higher temperature. The typical limited temperature is ~3 keV.**

Eddy current needed to be considered

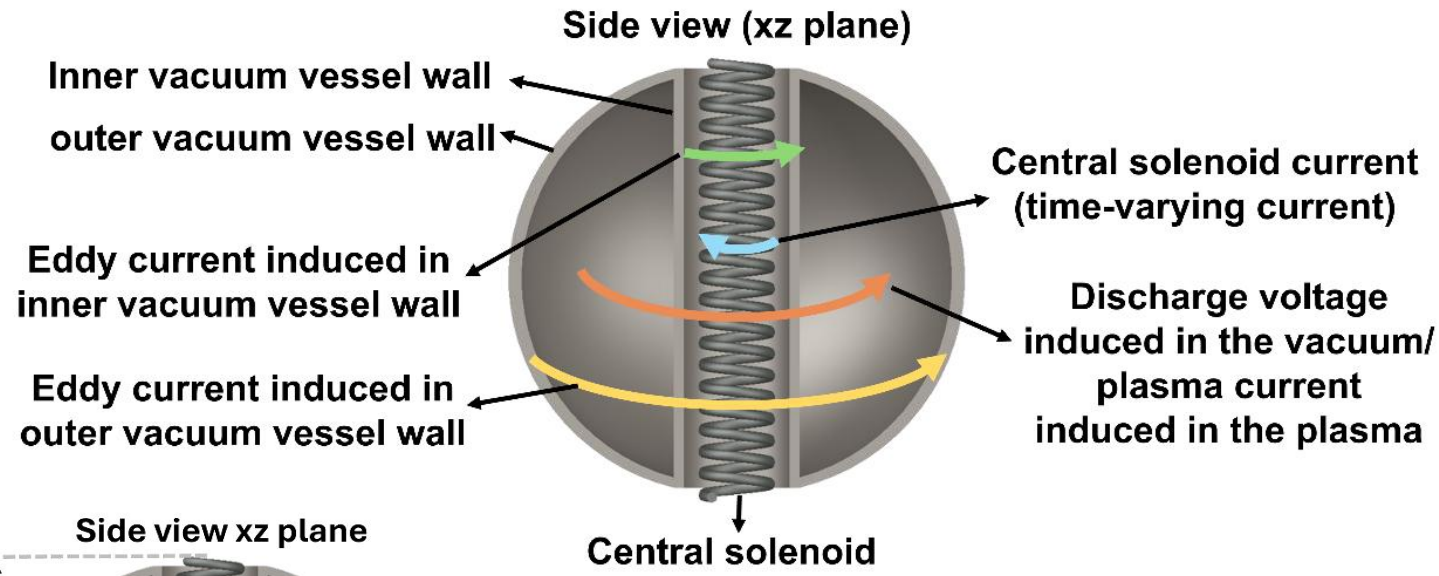

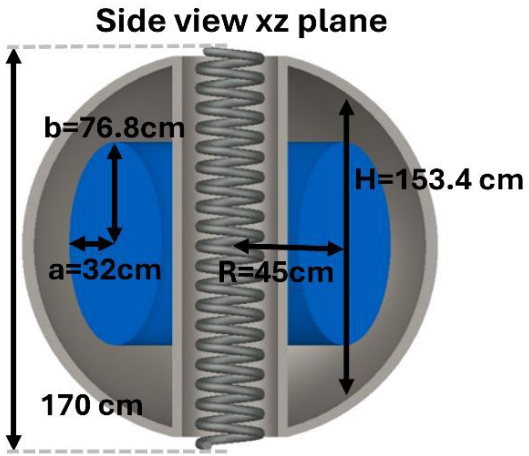

Chamber is broken into ring elements carrying eddy currents

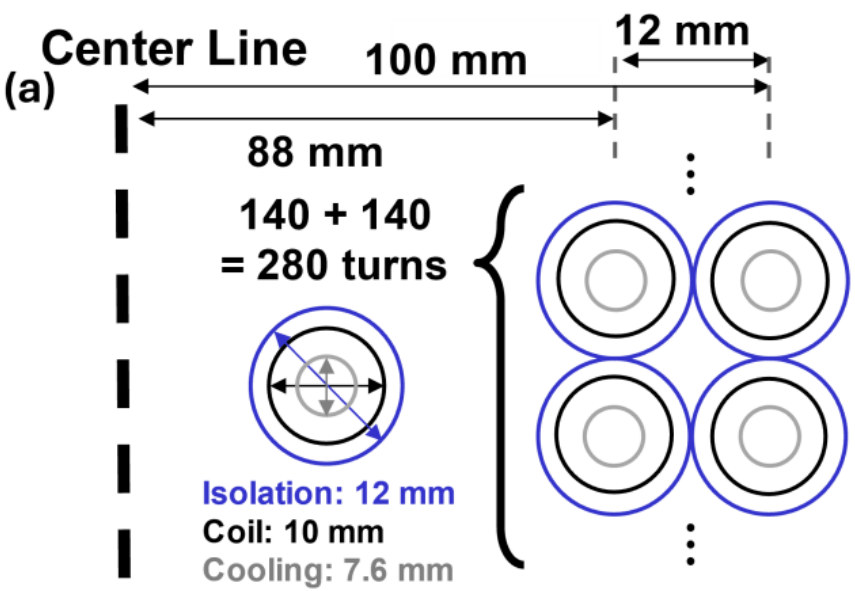

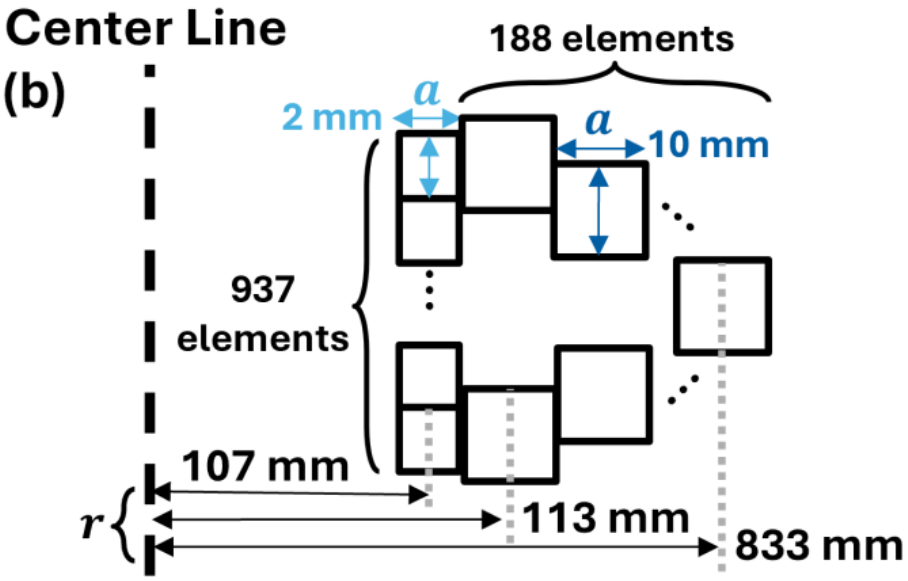

The eddy current in each chamber element is solved numerically

$$\overleftrightarrow{M}\frac{d\vec{I}}{dt}+\overleftrightarrow{R}_{\Omega}\vec{I}=\vec{V} \qquad \overleftrightarrow{M}\frac{\vec{I}'-\vec{I}}{\Delta t}+\overleftrightarrow{R}_{\Omega}\vec{I}=\vec{V}$$

$$\vec{I}'=\left(\overleftrightarrow{1}-\Delta t\overleftrightarrow{M}^{-1}\overleftrightarrow{R}_{\Omega}\right)\vec{I}+\Delta t\overleftrightarrow{M}^{-1}\vec{V}$$

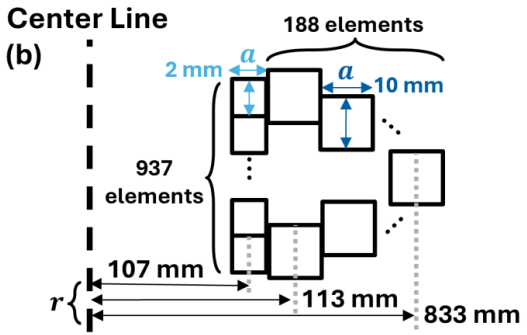

$$\vec{V}=\overleftrightarrow{M}\frac{d\vec{I}}{dt}+\overleftrightarrow{R}\vec{I}$$

$$\Rightarrow\begin{bmatrix}V_{c1}\\V_{c2}\\\vdots\\V_{v1}\\V_{v2}\\\vdots\\V_{p}\end{bmatrix}=\begin{bmatrix}L_{c1} & M_{c1,c2} & M_{c1,c3} & \cdots & M_{c1,v1} & M_{c1,v2} & M_{c1,v3} & \cdots & M_{c1,p}\\ M_{c2,c1} & L_{c2} & M_{c2,c3} & \cdots & M_{c2,v1} & M_{c2,v2} & M_{c2,v3} & \cdots & M_{c2,p}\\ M_{c3,c1} & M_{c3,c2} & L_{c3} & \cdots & M_{c3,v1} & M_{c3,v2} & M_{c3,v3} & \cdots & M_{c3,p}\\ \vdots & \vdots & \vdots & \vdots & \vdots & \vdots & \vdots & \vdots & \vdots\\ M_{v1,c1} & M_{v1,c2} & M_{v1,c3} & \cdots & L_{v1} & M_{v1,v2} & M_{v1,v3} & \cdots & M_{v1,p}\\ M_{v2,c1} & M_{v2,c2} & M_{v2,c3} & \cdots & M_{v2,v1} & L_{v2} & M_{v2,v3} & \cdots & M_{v2,p}\\ M_{v3,c1} & M_{v3,c2} & M_{v3,c3} & \cdots & M_{v3,v1} & M_{v3,v2} & L_{v3} & \cdots & M_{v3,p}\\ \vdots & \vdots & \vdots & \vdots & \vdots & \vdots & \vdots & \vdots & \vdots\\ M_{p,c1} & M_{p,c2} & M_{p,c3} & \cdots & M_{p,v1} & M_{p,v2} & M_{p,v3} & \cdots & L_{p}\end{bmatrix}\begin{bmatrix}I'_{c1}\\I'_{c2}\\\vdots\\I'_{v1}\\I'_{v2}\\\vdots\\I'_{p}\end{bmatrix}$$

$$+\begin{bmatrix}R_{c1} & 0 & \cdots & 0 & 0 & \cdots & 0\\ 0 & R_{c2} & \cdots & 0 & 0 & \cdots & 0\\ \vdots & \vdots & \vdots & \vdots & \vdots & \vdots & \vdots\\ 0 & 0 & \cdots & R_{v1} & 0 & \cdots & 0\\ 0 & 0 & \cdots & 0 & R_{v2} & \cdots & 0\\ \vdots & \vdots & \vdots & \vdots & \vdots & \vdots & \vdots\\ 0 & 0 & \cdots & 0 & 0 & \cdots & R_{p}\end{bmatrix}\begin{bmatrix}I_{c1}\\I_{c2}\\\vdots\\I_{v1}\\I_{v2}\\\vdots\\I_{p}\end{bmatrix}. \qquad (2)$$

Eddy current on the chamber wall is induced when the current of the solenoid changes with time

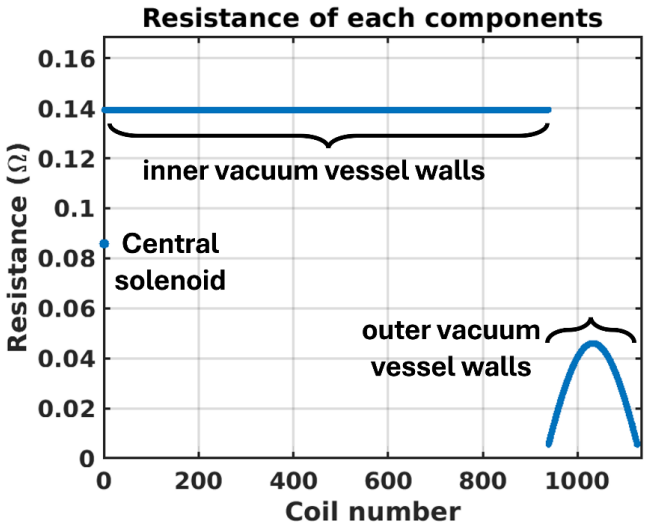

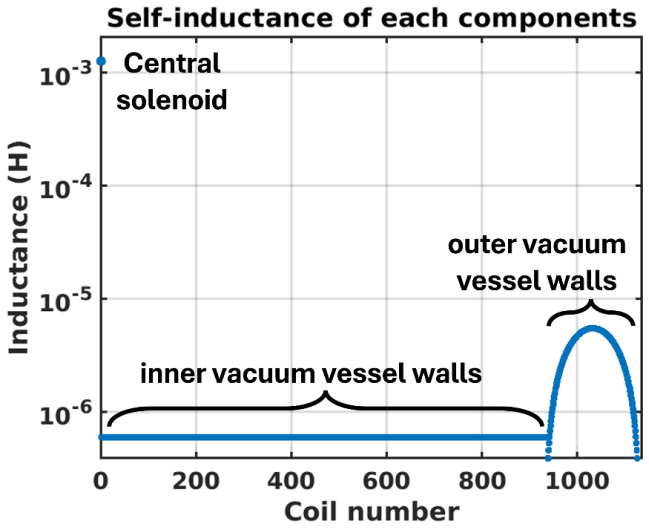

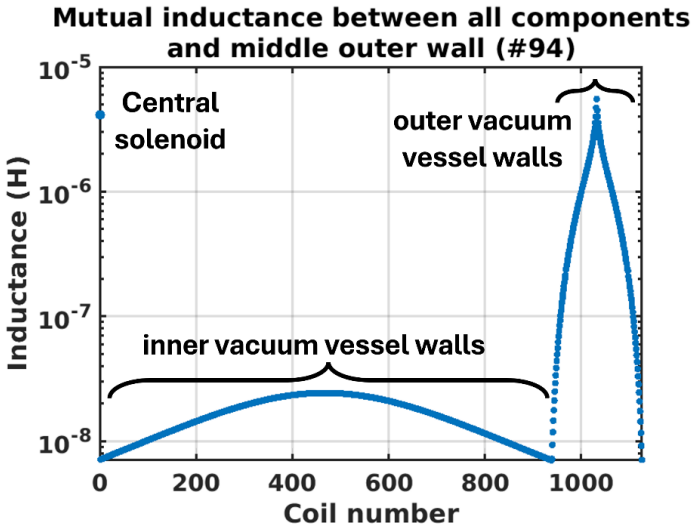

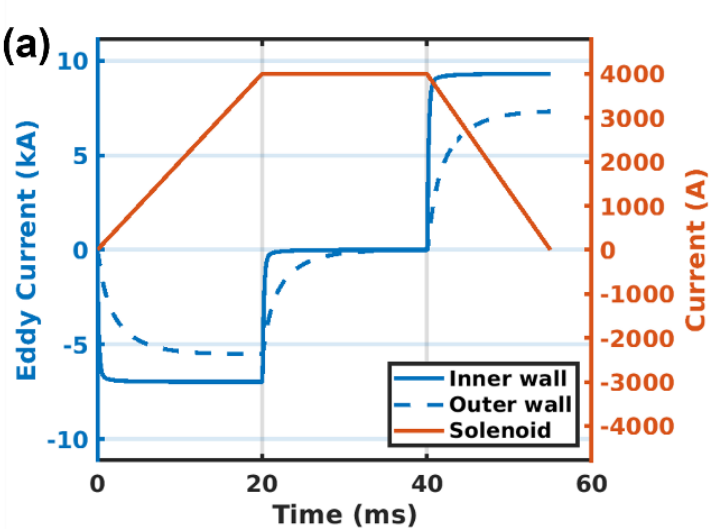

Temperature of 100 eV is the threshold of radiation barrier by impurities

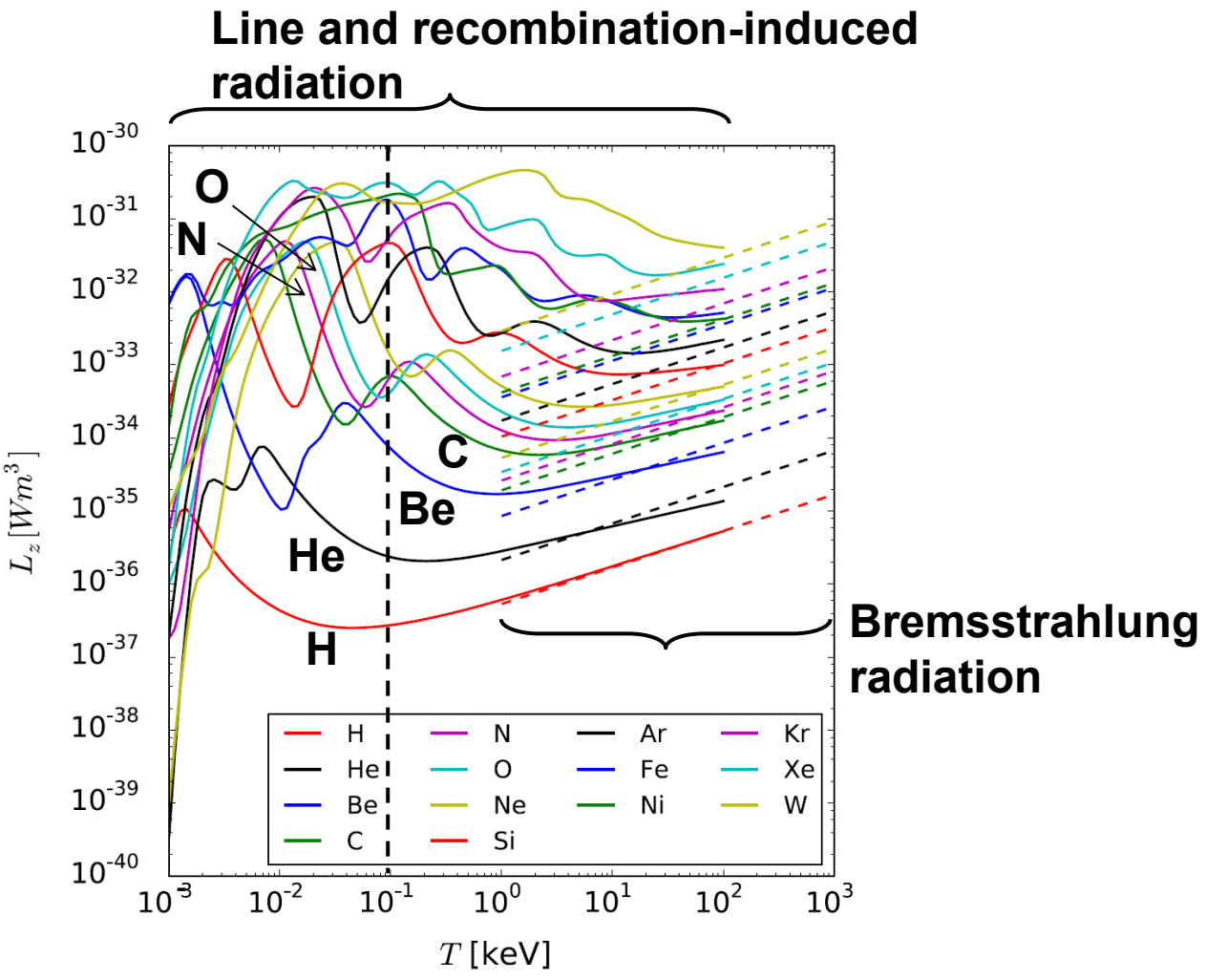

H. Lux, etc., Fusion Eng. Des. **42**, 101 (2015)

Plasma temperature can be estimated using the simple circuit model

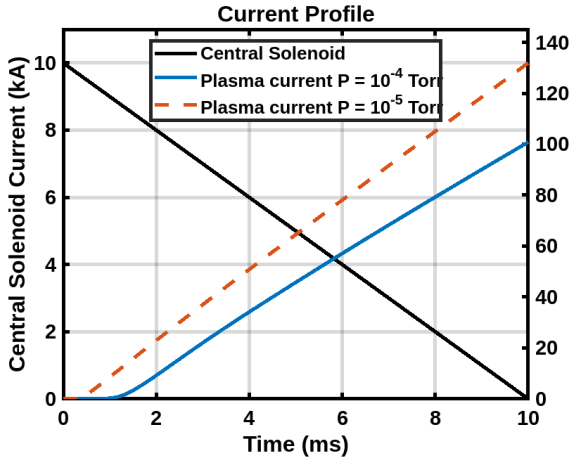

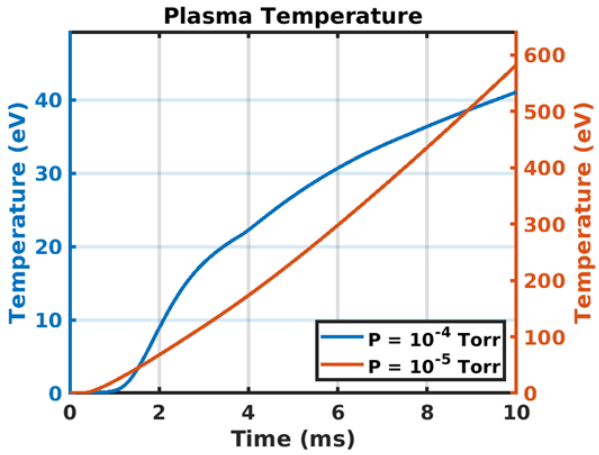

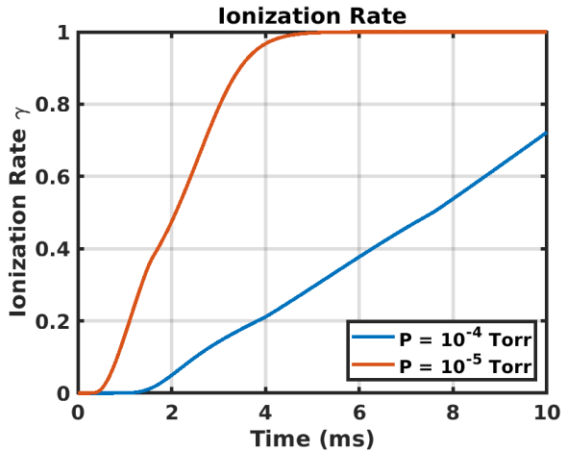

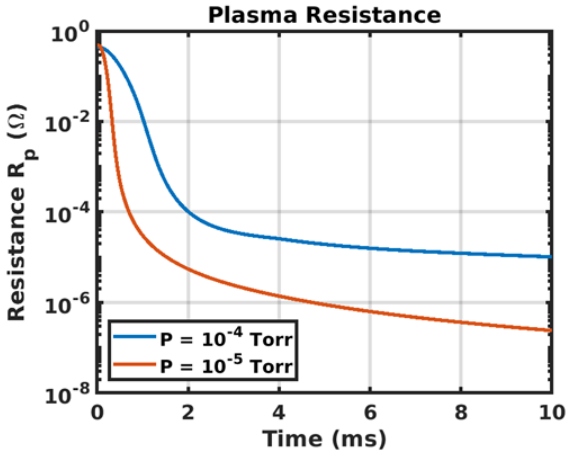

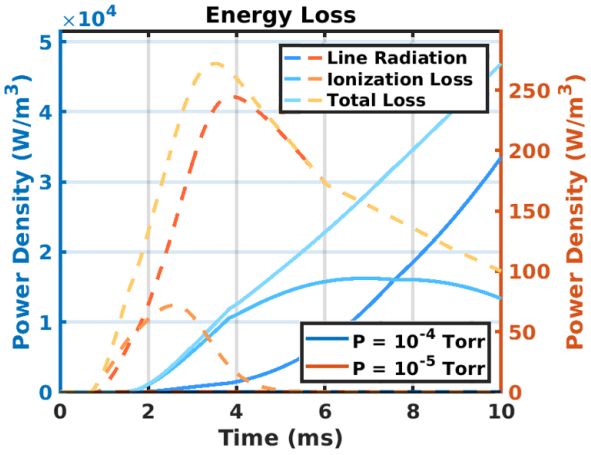

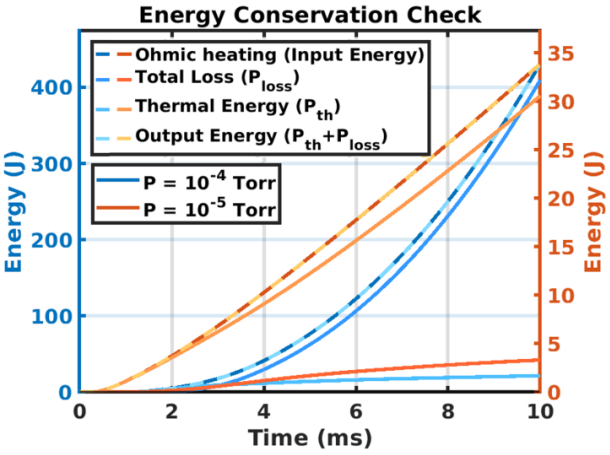

The collisional re-distribution of the ECRH-driven anisotropy in $E_\perp$ causes some parallel momentum to flow from e^- to ions

- **Coulomb collisions are more efficient at lower energies.**

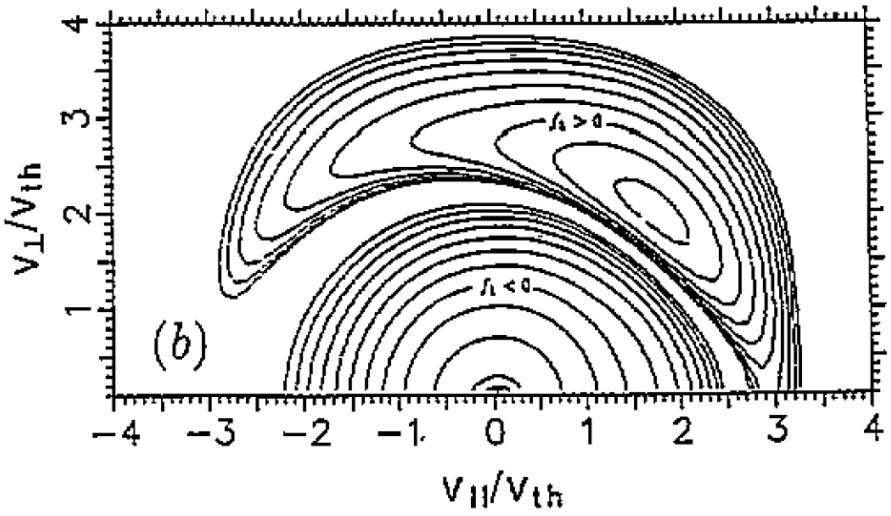

Velocity: $v_2 > v_1$

Collisions: $v_2 < v_1$

- **Electron cyclotron current drive:**

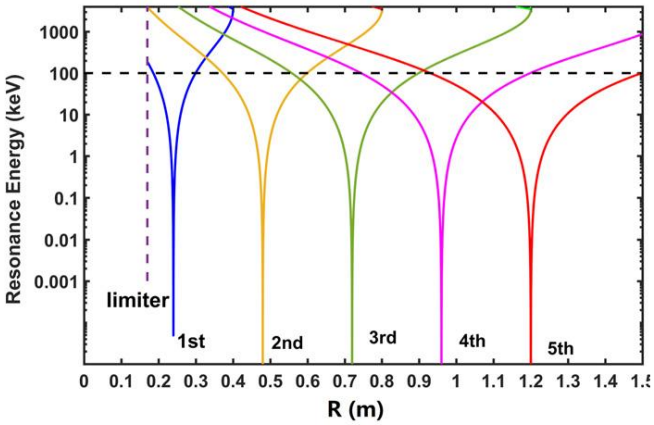

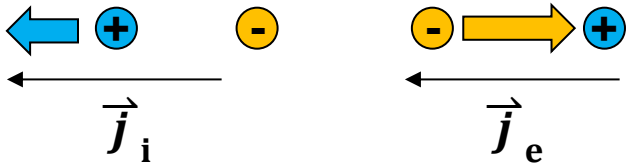

$$\vec{j}_p = -en_e\vec{v}_e + en_i\vec{v}_i$$

$$\vec{P} = n_e m_e \vec{v}_e + n_i m_i \vec{v}_i \approx 0$$

V. Erckmann and U. Gasparion, Plasma Phys. Control. Fusion **36**, 1869 (1994)
Yuejiang Shi et al, Nucl. Fusion **62**, 086047 (2022)

Passing electrons can be trapped if the $v_\perp$ is increased by heating

$$\omega - k_\parallel v_\parallel = \frac{neB}{\gamma m_e}$$

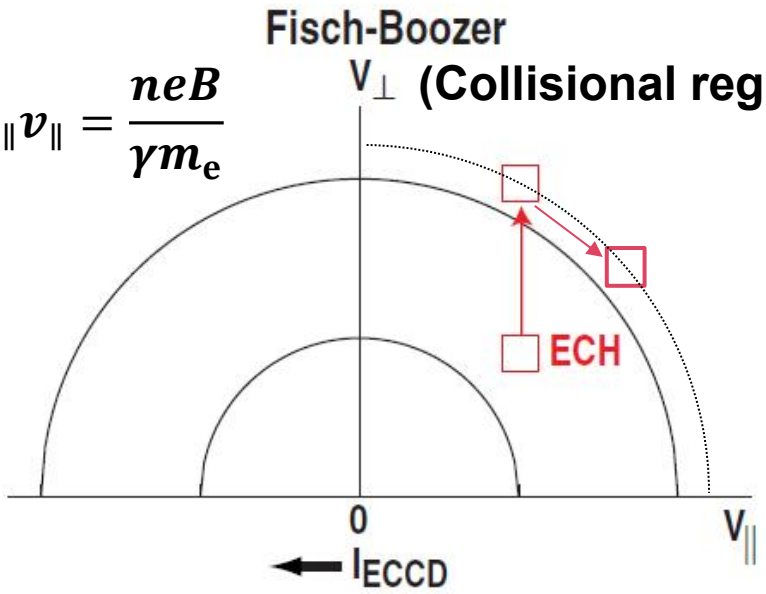

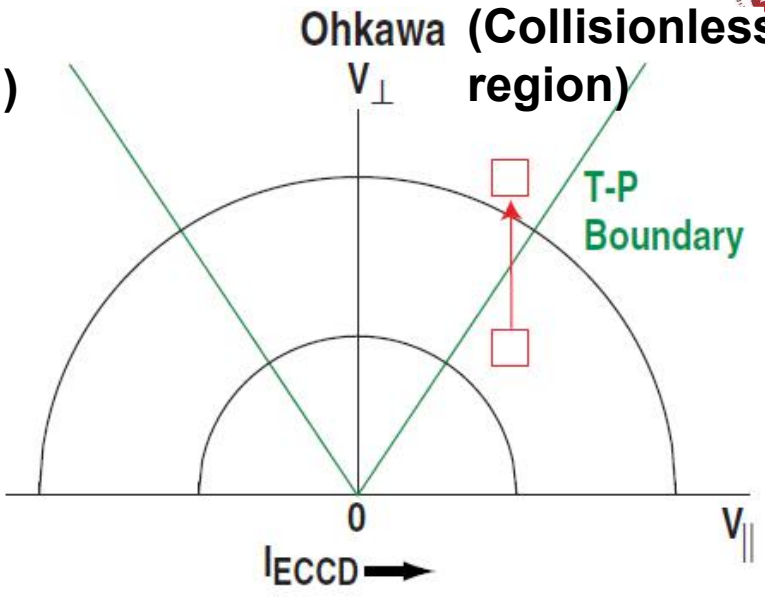

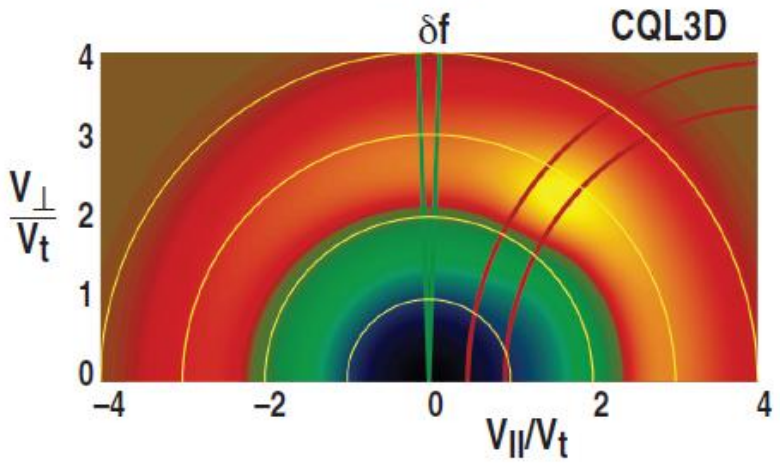

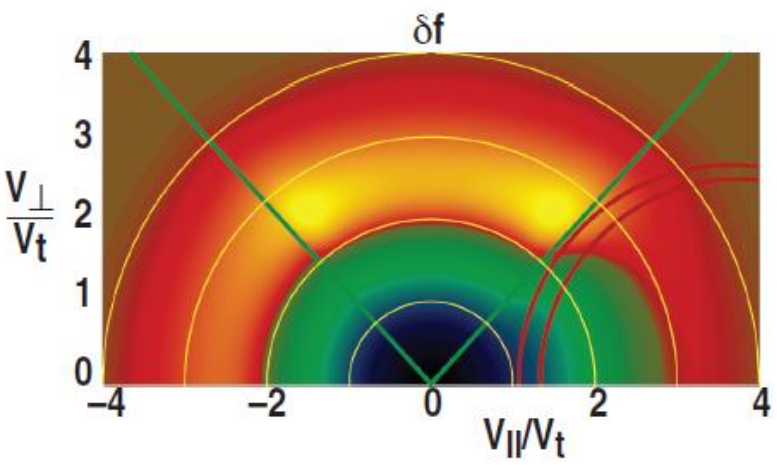

Lecture note "Physics and Applications of Electron Cyclotron Heating and Current Drive" by R. Prater from GA at 6th ITER International School 2012, Institute for Plasma Research, Gandhinagar Ahmedabad, India, December 2-6, 2012

Comparison of Fisch-Boozer Mechanism and Ohkawa Mechanism

Aspect	Fisch–Boozer Mechanism[1]	Ohkawa Mechanism[2]
Physical Process	Asymmetric heating of passing electrons with subsequent collisional momentum transfer	Selective de-trapping of barely trapped electrons into passing orbits (collisionless mechanism)
Requires collisions?	Yes (collisional mechanism)	No (collisionless pitch-angle scattering)
Key Particle Population	Passing electrons	Trapped (or barely trapped) electrons
Wave absorption location	Depends on Doppler-shifted resonance; typically near magnetic axis or mid-radius	Usually near edge where barely trapped particles are abundant

1 N. J. Fisch and A. H. Boozer, Phys. Rev. Lett. 45, 720 (1980).
2 T. Ohkawa, “Steady state operation of tokamaks by rf heating,” General Atomics Report No. GA-A13847 (1976).

Strong absorption occurs when the frequency matches the electron cyclotron frequency

- **Electron cyclotron resonance (ECR) plasma reactor**

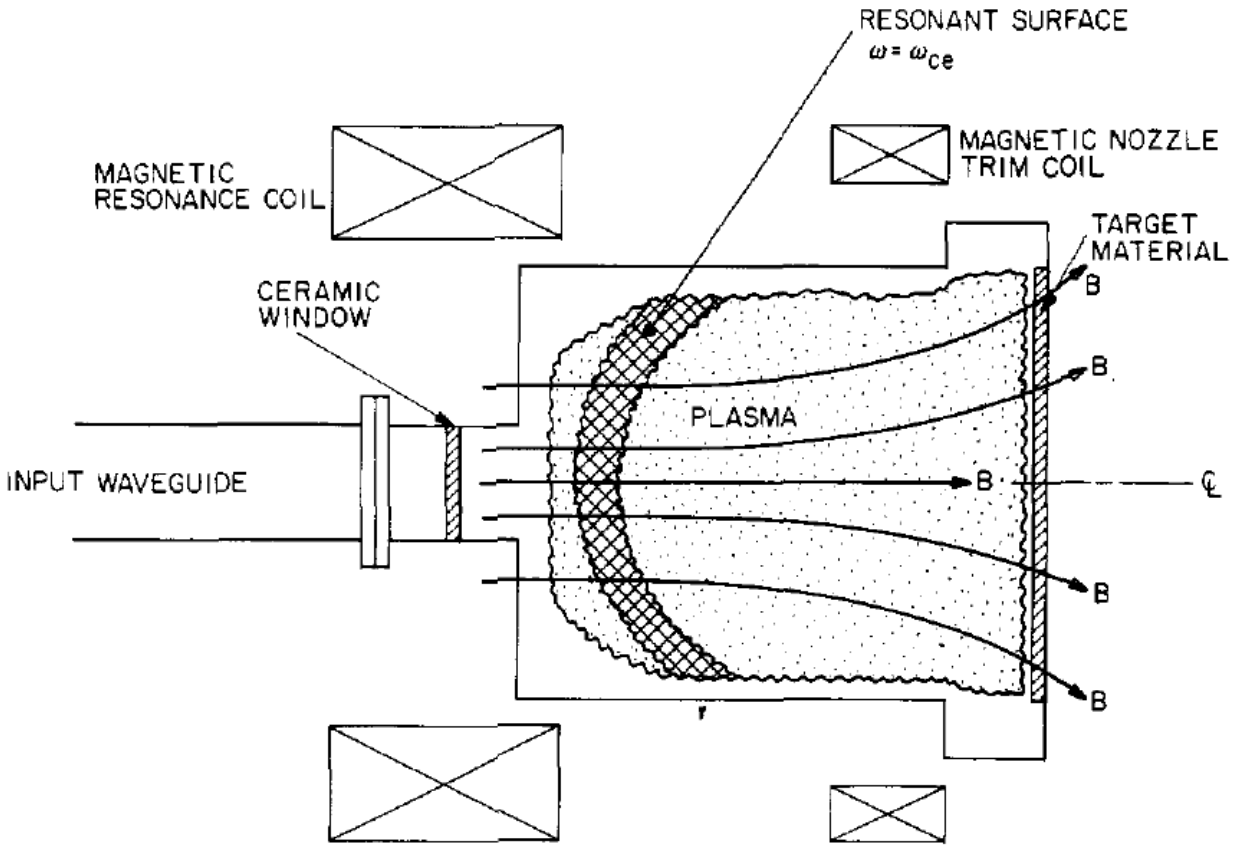

Electron cyclotron frequency depends on magnetic field only

$$m_e \frac{d\vec{v}}{dt} = -\frac{e}{c}\vec{v} \times \vec{B}$$

- Assuming $\vec{B} = B\hat{z}$ and the electron oscillates in x-y plane

$$m_e \dot{v}_x = -\frac{e}{c} B v_y \qquad m_e \dot{v}_z = 0$$

$$m_e \dot{v}_y = \frac{e}{c} B v_x$$

$$\ddot{v}_x = -\frac{eB}{m_e c}\dot{v}_y = -\left(\frac{eB}{m_e c}\right)^2 v_x$$

$$\ddot{v}_y = -\frac{eB}{m_e c}\dot{v}_x = -\left(\frac{eB}{m_e c}\right)^2 v_y$$

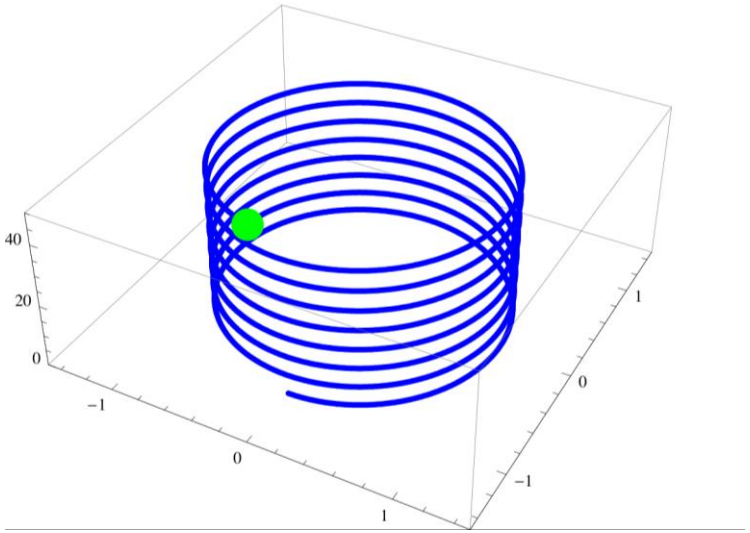

- Therefore

$$\omega_{ce} = \frac{eB}{m_e c}$$

Electrons keep getting accelerated when a electric field rotates in electron's gyrofrequency

$$m_e \frac{d\vec{v}}{dt} = -\frac{e}{c}\vec{v} \times \vec{B} - e\vec{E} \qquad \vec{B} = B_0\hat{z} \qquad \vec{E} = E_0[\hat{x}\cos(\omega t) + \hat{y}\sin(\omega t)]$$

$$m_e\dot{v}_x = -\frac{e}{c}Bv_y + E_0\cos(\omega t) \qquad m_e\dot{v}_y = \frac{e}{c}Bv_x + E_0\sin(\omega t) \qquad m_e\dot{v}_z = 0$$

$$\ddot{v}_x = -\frac{eB}{m_e c}\dot{v}_y - \frac{E_0}{m_e}\omega\sin(\omega t) = -{\omega_{ce}}^2 v_x - \frac{E_0}{m_e}(\omega_{ce} + \omega)\sin(\omega t)$$

$$\ddot{v}_y = -\frac{eB}{m_e c}\dot{v}_x + \frac{E_0}{m_e}\omega\cos(\omega t) = -{\omega_{ce}}^2 v_y + \frac{E_0}{m_e}(\omega_{ce} + \omega)\cos(\omega t)$$

$$\omega_{ce} = \frac{eB}{m_e c}$$

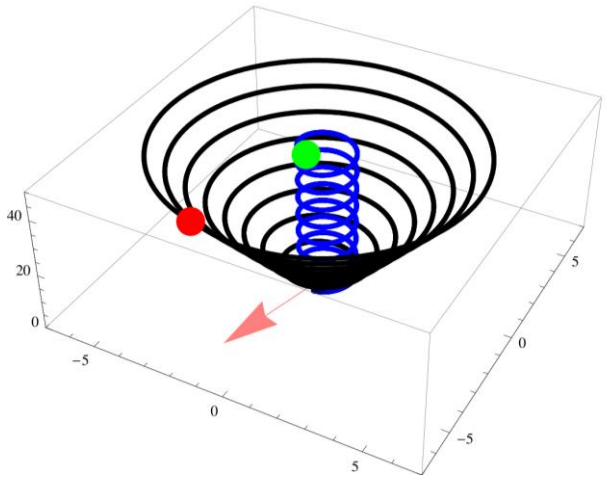

Electric field in a circular polarized electromagnetic wave keeps rotating as the wave propagates

- Right-handed polarization

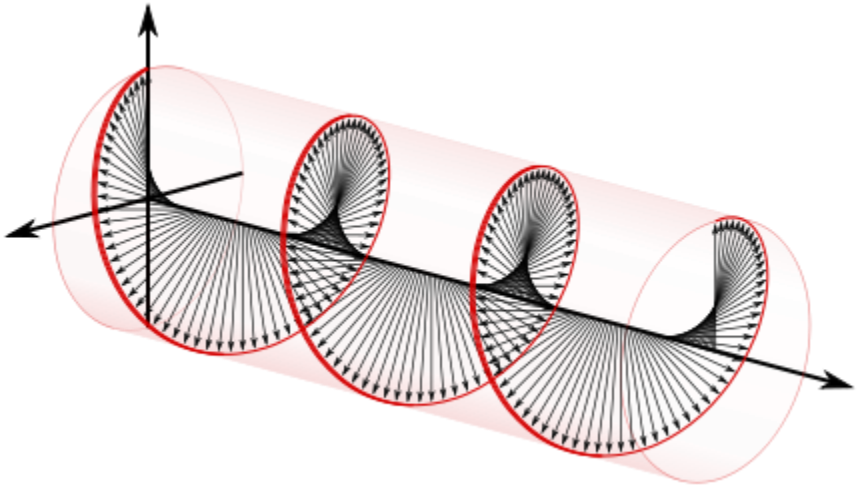

- Left-handed polarization

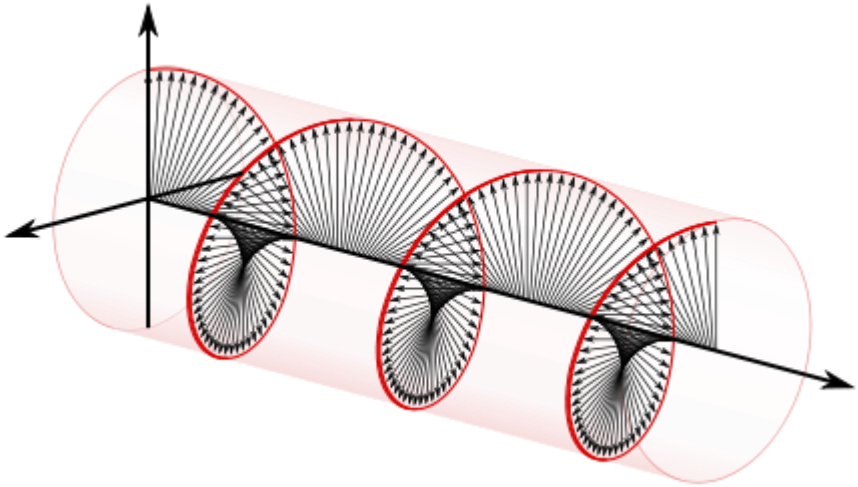

https://en.wikipedia.org/wiki/Circular_polarization

Only right-handed polarization can resonance with electron's gyromotion

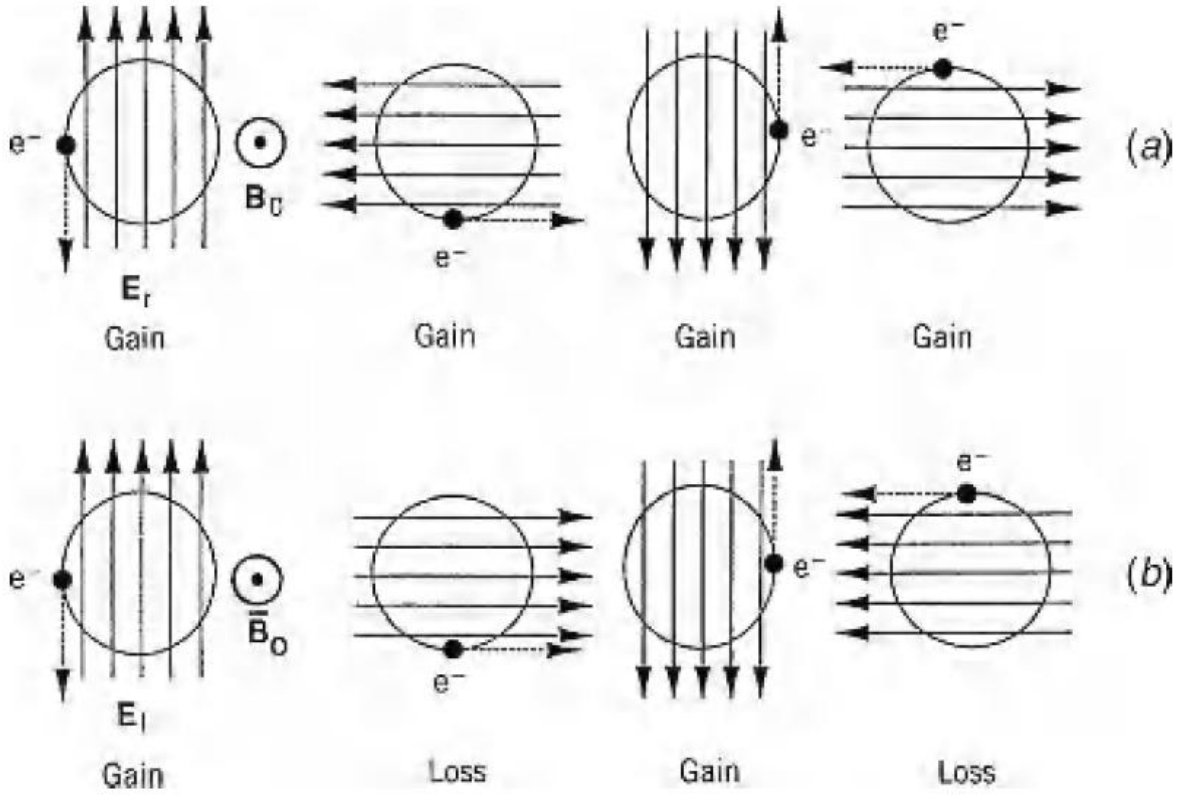

FIGURE 13.5. Basic principle of ECR heating: (*a*) continuous energy gain for right-hand polarization; (*b*) oscillating energy for left-hand polarization (after Lieberman and Gottscho, 1994).

Strong absorption occurs when the frequency matches the electron cyclotron frequency

- **Electron cyclotron resonance (ECR) plasma reactor**

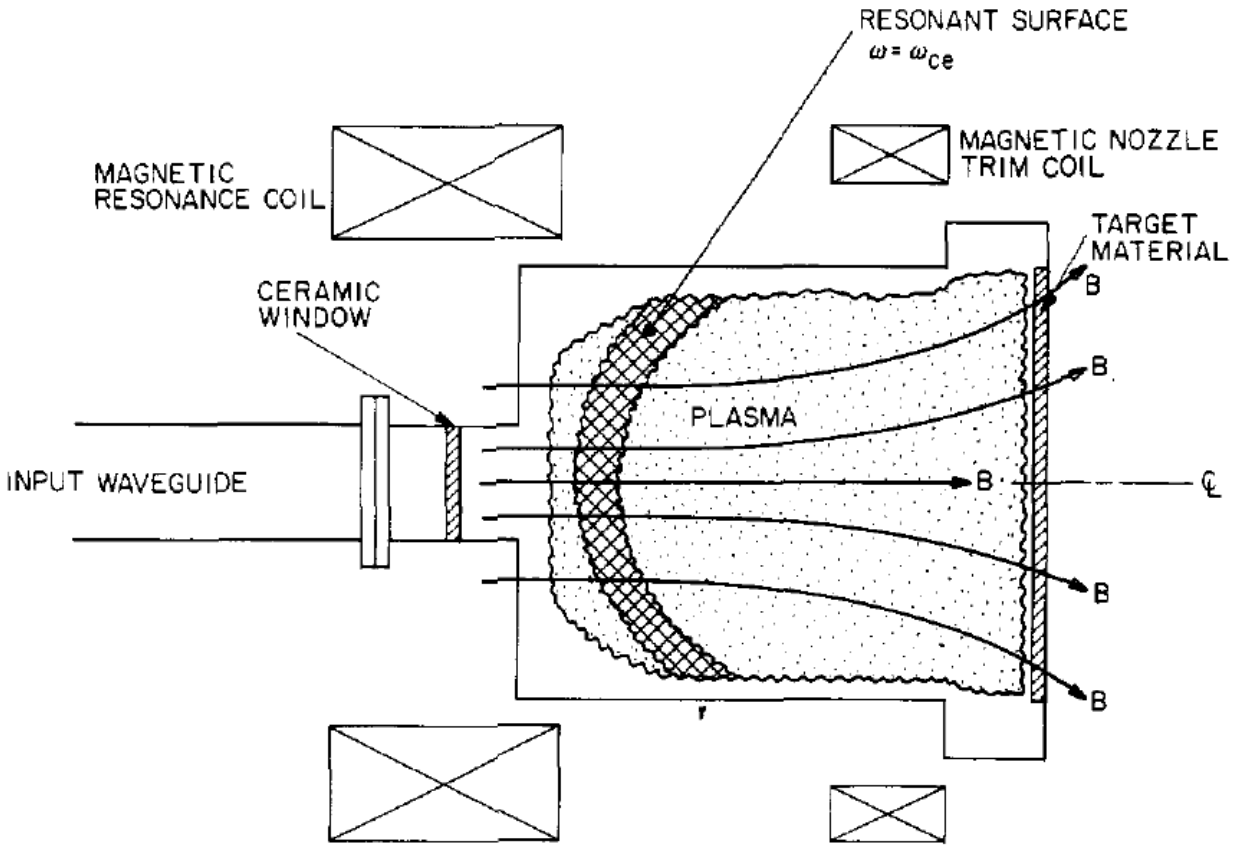

The collisional re-distribution of the ECRH-driven anisotropy in $E_\perp$ causes some parallel momentum to flow from e^- to ions

- **Coulomb collisions are more efficient at lower energies.**

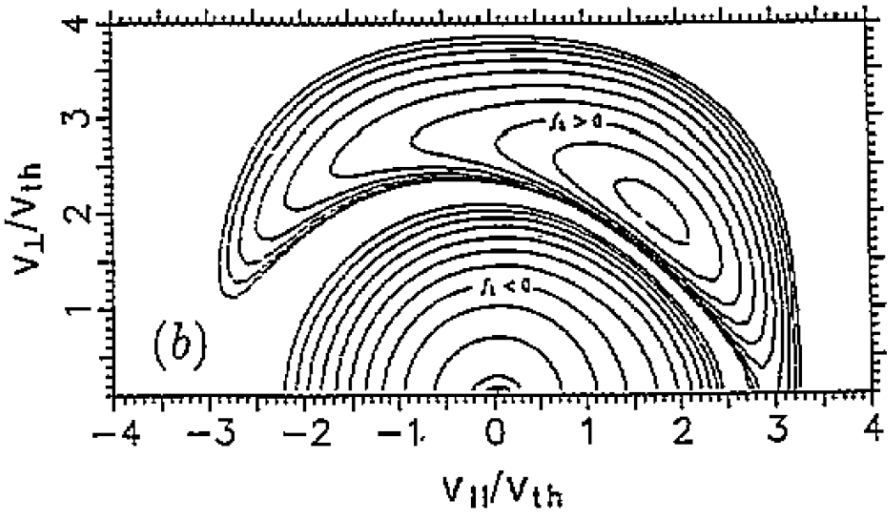

Velocity: $v_2 > v_1$

Collisions: $v_2 < v_1$

- **Electron cyclotron current drive:**

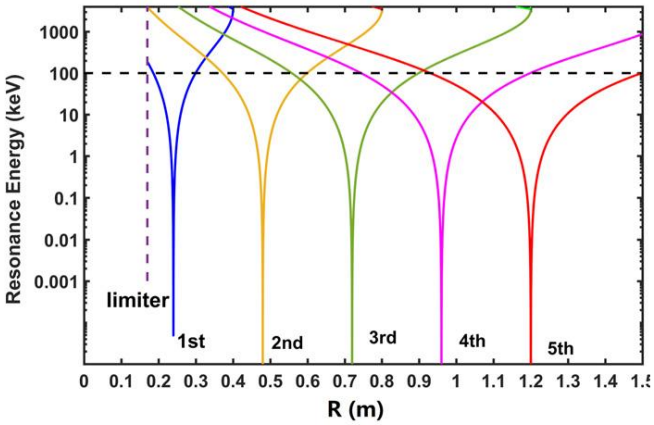

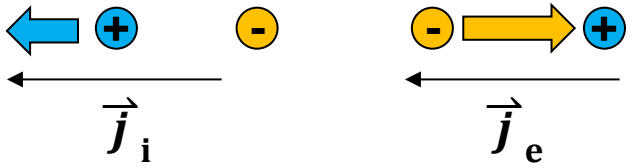

$$\vec{j}_p = -en_e\vec{v}_e + en_i\vec{v}_i$$

$$\vec{P} = n_e m_e \vec{v}_e + n_i m_i \vec{v}_i \approx 0$$

V. Erckmann and U. Gasparion, Plasma Phys. Control. Fusion **36**, 1869 (1994)
Yuejiang Shi et al, Nucl. Fusion **62**, 086047 (2022)

Neutral beam injector is one of the main heat mechanisms in MCF

D. Mazon, etc., NATURE PHYSICS, 12, 14, 2016

https://zh.wikihow.com/%E5%9C%A8%E6%89%8B%E6%8C%87%E4%B8%8A%E8%BD%AC%E7%AF%AE%E7%90%83

Varies way of heating a MCF device

System		Frequency/ energy	Maximum power coupled to plasma	Overall system efficiency	Development/ demonstration required	Remarks
ECRF	Demonstrated in tokamaks	28–157 GHz	2.8 MW, 0.2 s	30–40%	Power sources and windows, off-axis CD	Provides off-axis CD
	ITER needs	150–170 GHz	50 MW, S S			
ICRF	Demonstrated in tokamaks	25–120 MHz	22 MW, 3 s (L-mode); 16.5 MW, 3 s (H-mode)	50–60%	ELM tolerant system	Provides ion heating and smaller ELMs
	ITER needs	40–75 MHz	50 MW, S S			
LHRF	Demonstrated in tokamaks	1.3–8 GHz	2.5 MW, 120 s; 10 MW, 0.5 s	45–55%	Launcher, coupling to H-mode	Provides off-axis CD
	ITER needs	5 GHz	50 MW, S S			
NBI +ve ion	Demonstrated in tokamaks	80–140 keV	40 MW, 2 s; 20 MW, 8 s	35–45%	None	Not applicable
	ITER needs	None	None			
NBI −ve ion	Demonstrated in tokamaks	0.35 MeV	5.2 MW, D^-, 0.8 s (from 2 sources)			
	ITER needs	1 MeV	50 MW, S S	∼37%	System, tests on tokamak, plasma CD	provides rotation

'S S' indicates steady state

Nuclear Fusion, 39, 2495, 1999

Neutral atoms are ionized by collisions in the plasma

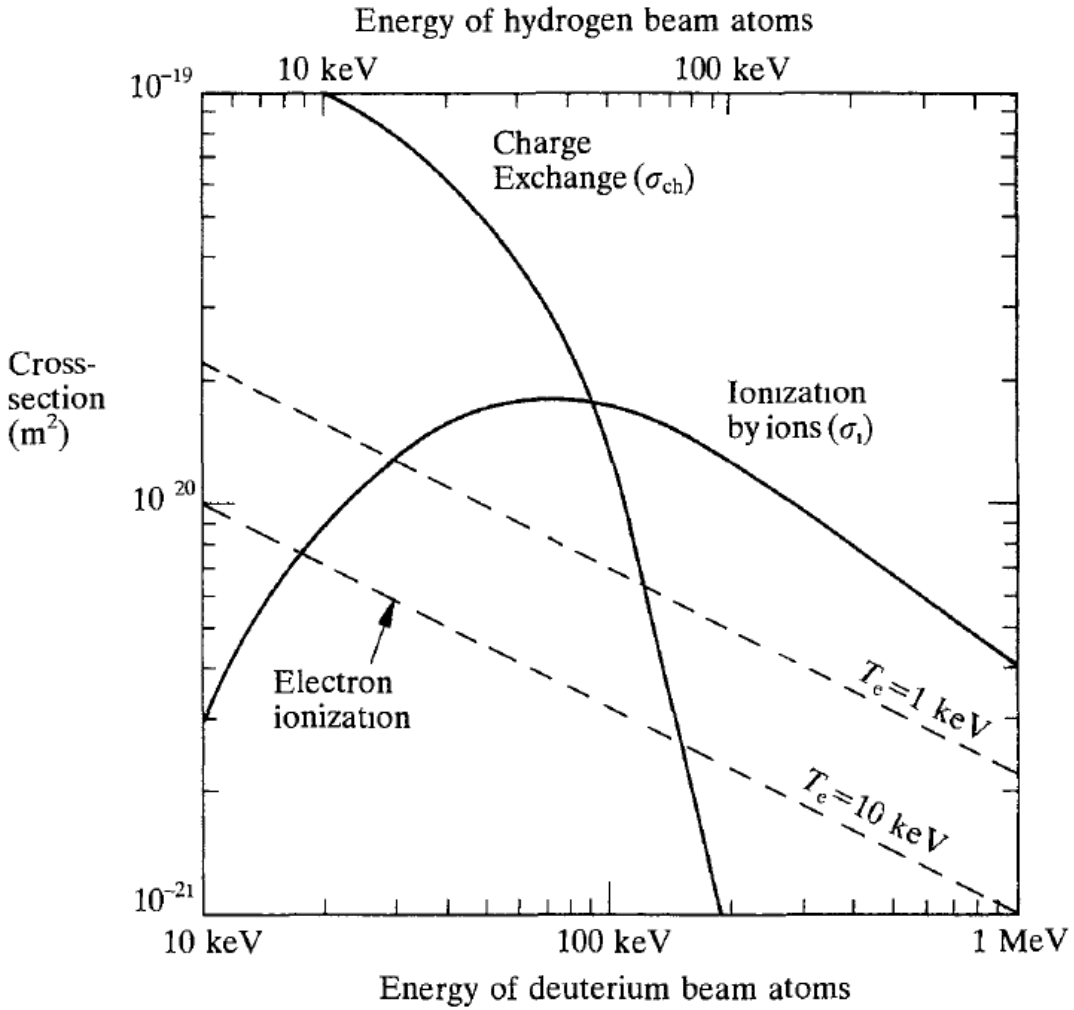

- **Charge exchange:**

  $H_b + H_p^+ \rightarrow H_b^+ + H_p$

- **Ionization by ions**

  $H_b + H_p^+ \rightarrow H_b^+ + H_p^+ + e^-$

- **Ionization by electrons**

  $H_b + e^- \rightarrow H_b^+ + 2e^-$

b: beam
p: plasma

Neutral beam absorption length increases with tangential injection

- **It is more difficult to access through the toroidal field coils with tangential injection.**

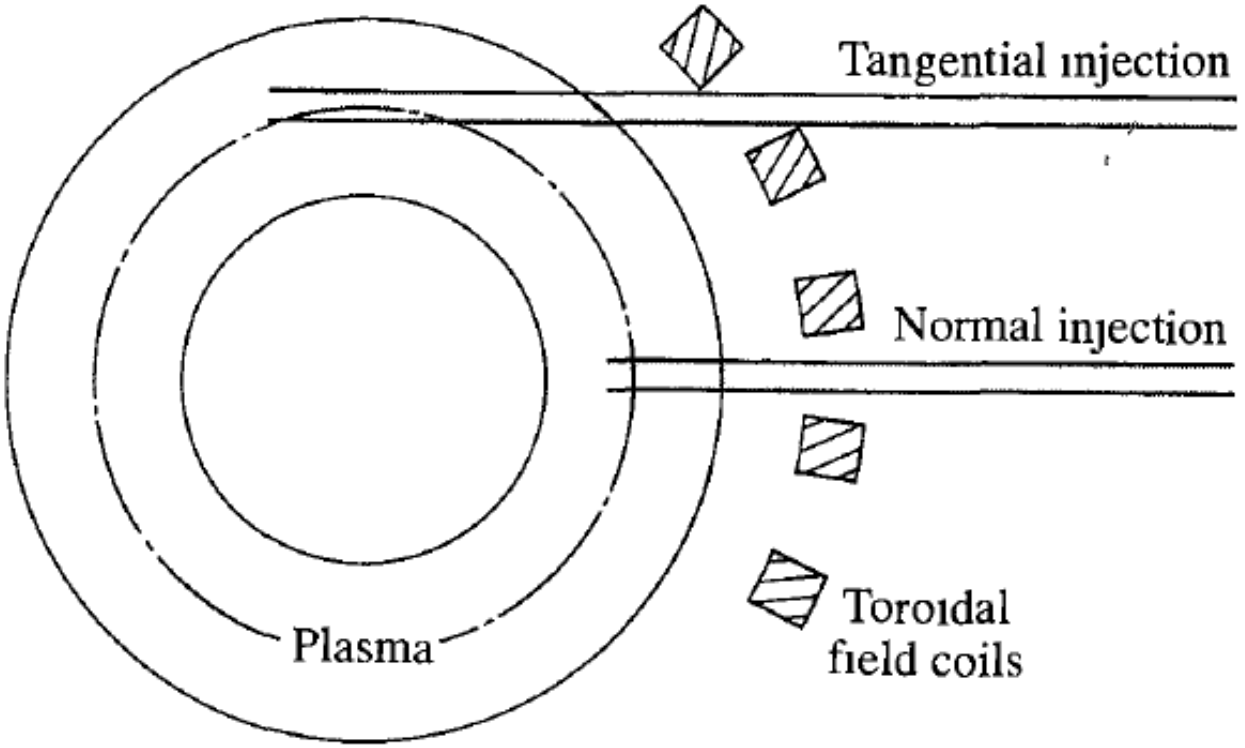

John Wesson, Tokamaks 3rd edition

Neutral particles heat the plasma via coulomb collisions

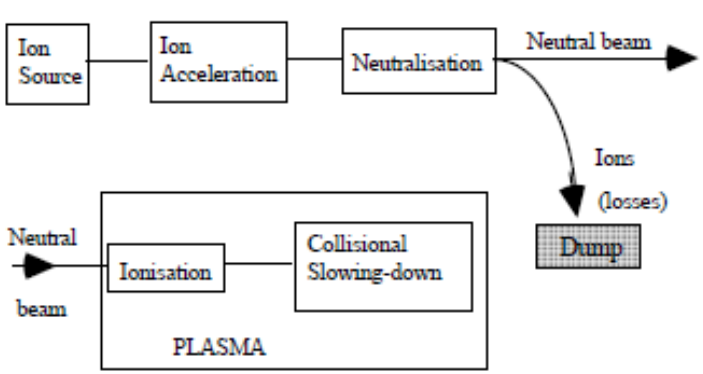

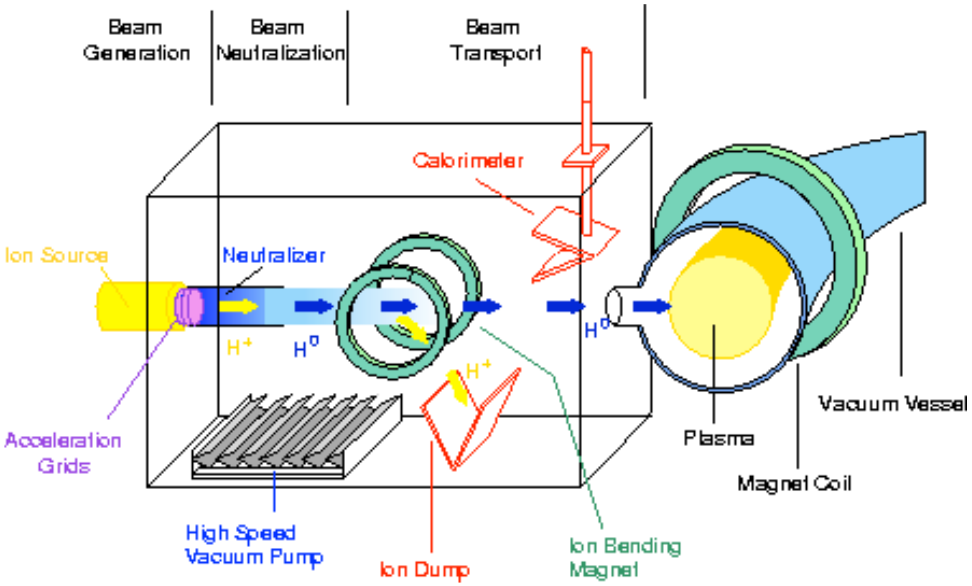

1. create energetic (fast) neutral ions
2. ionize the neutral particles
3. heat the plasma (electrons and ions) via Coulomb collisions

Negative ion source is preferred due to higher neutralization efficiency

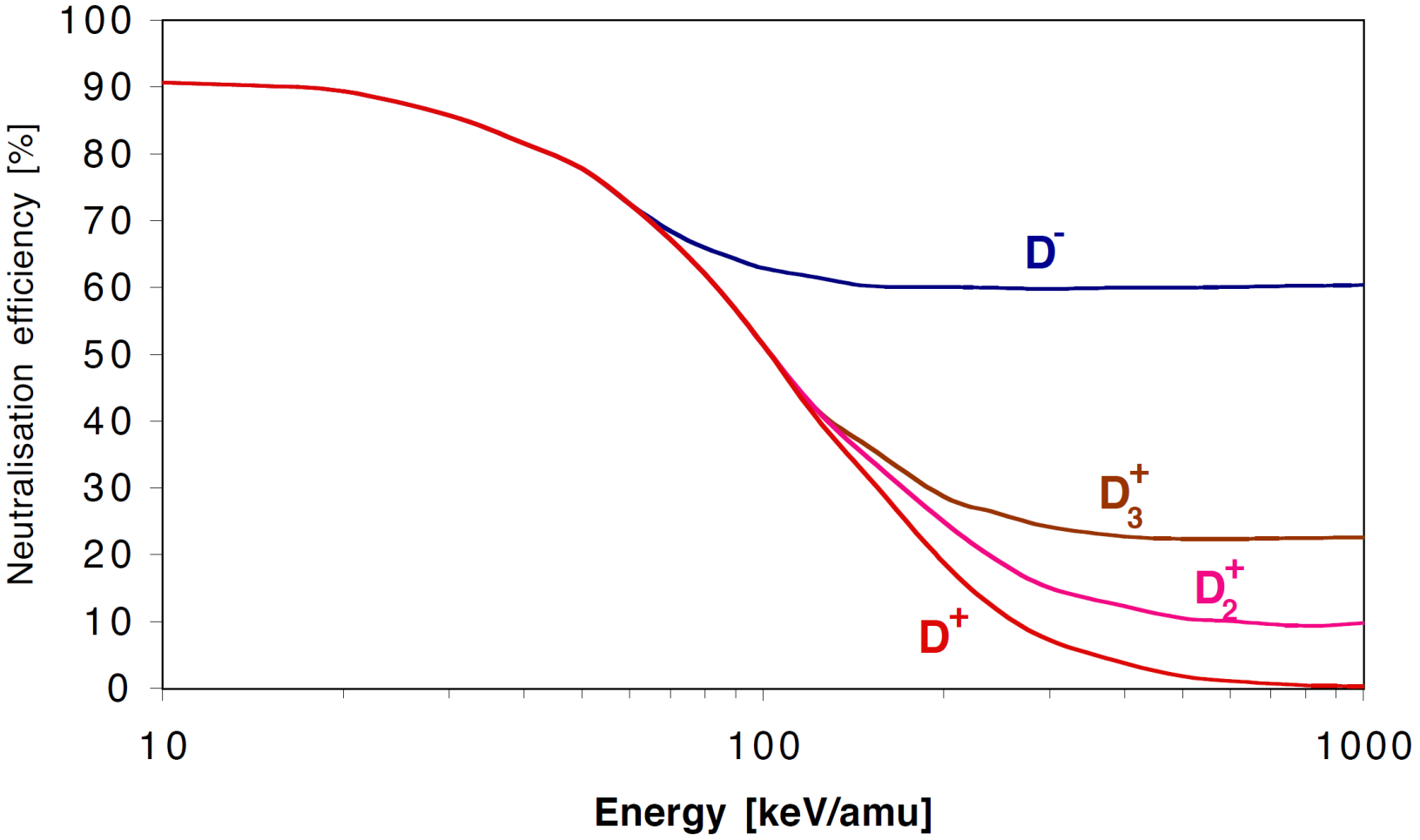

There are two ways to make negative ions – surface and volume production

- **Surface production, depends on :**
  - **Work function Φ**
  - **Electron affinity level, 0.75 eV for H^-**
  - **Perpendicular velocity**
  - **Work function can be reduced by covering the metal surface with cesium**

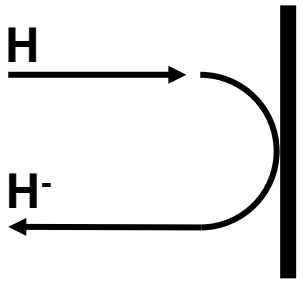

$$H + e^- \longrightarrow H^-$$

$$H^+ + 2e^- \longrightarrow H^-$$

- **Volume production:**

$$H_2 + e_{fast}(>20\ \text{eV}) \rightarrow H_2^*(\text{excited state}) + e_{fast},$$

$$H_2^*(\text{excited state}) + e_{slow}(\approx 1\ \text{eV}) \rightarrow H^- + H.$$

Two-chamber method of negative ions in volume production with a magnetic filter

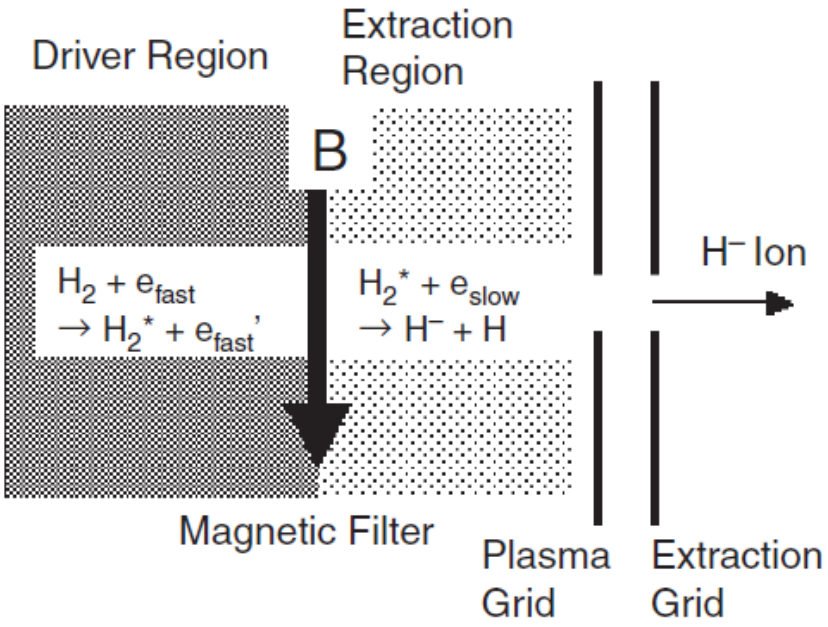

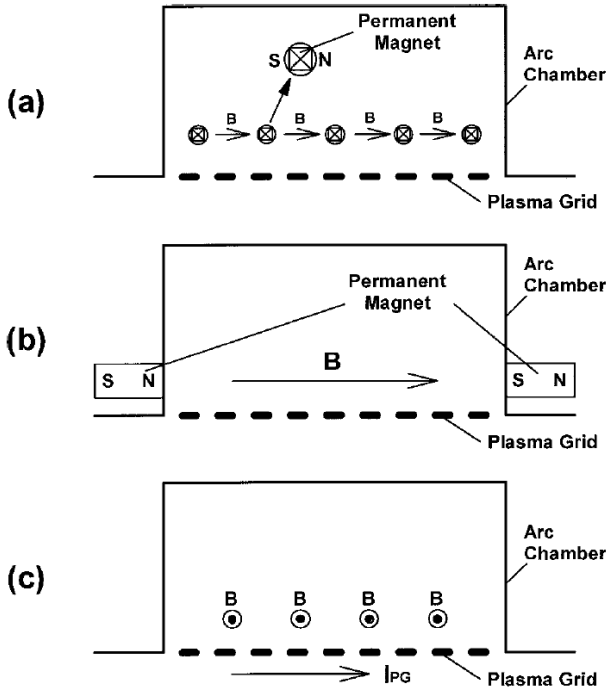

Adding cesium increases negative ion current

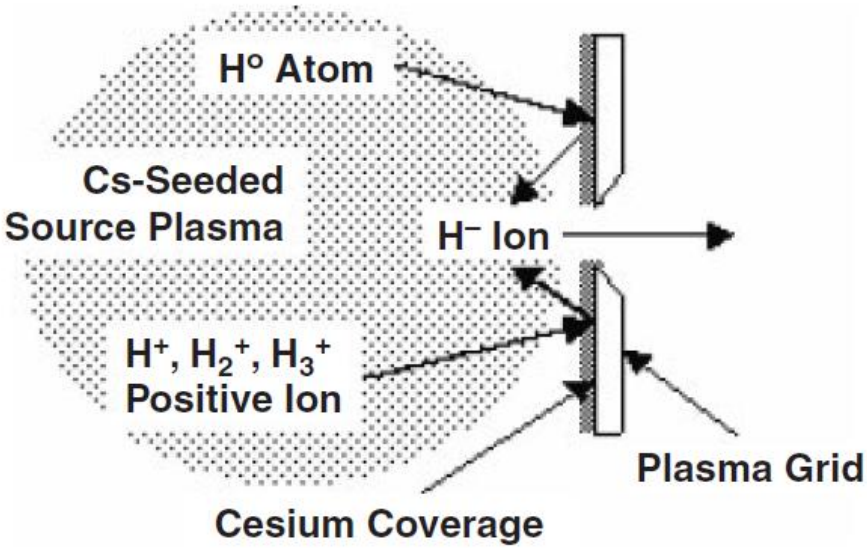

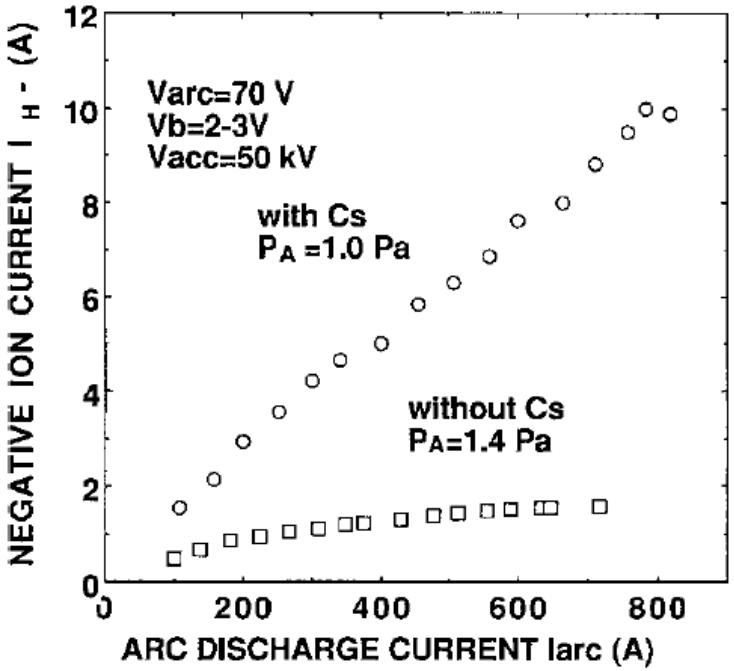

Electrons need to be filtered out since they are extracted together with negative ions

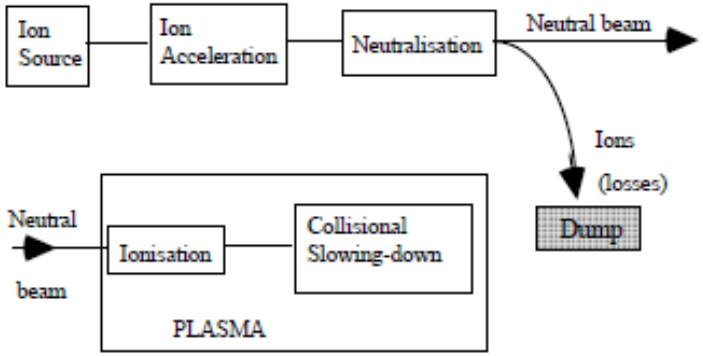

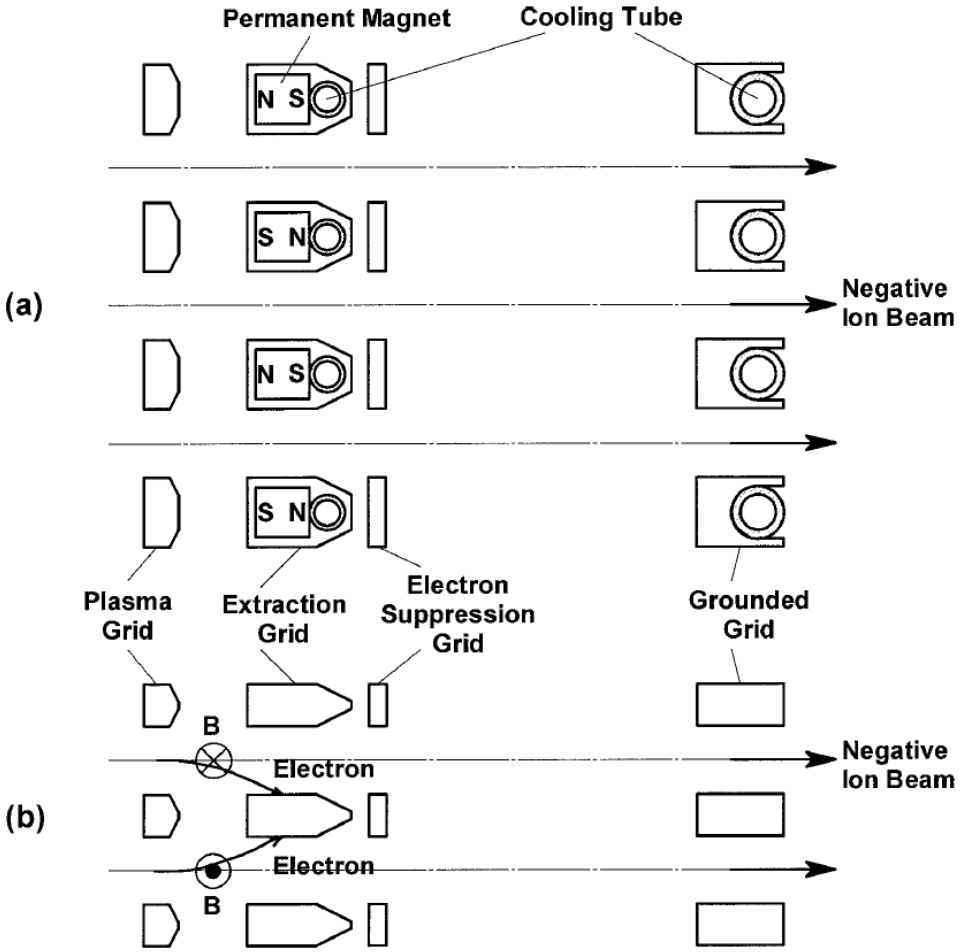

Acceleration

- **Multi-stage acceleration**
- **Single-stage acceleration**

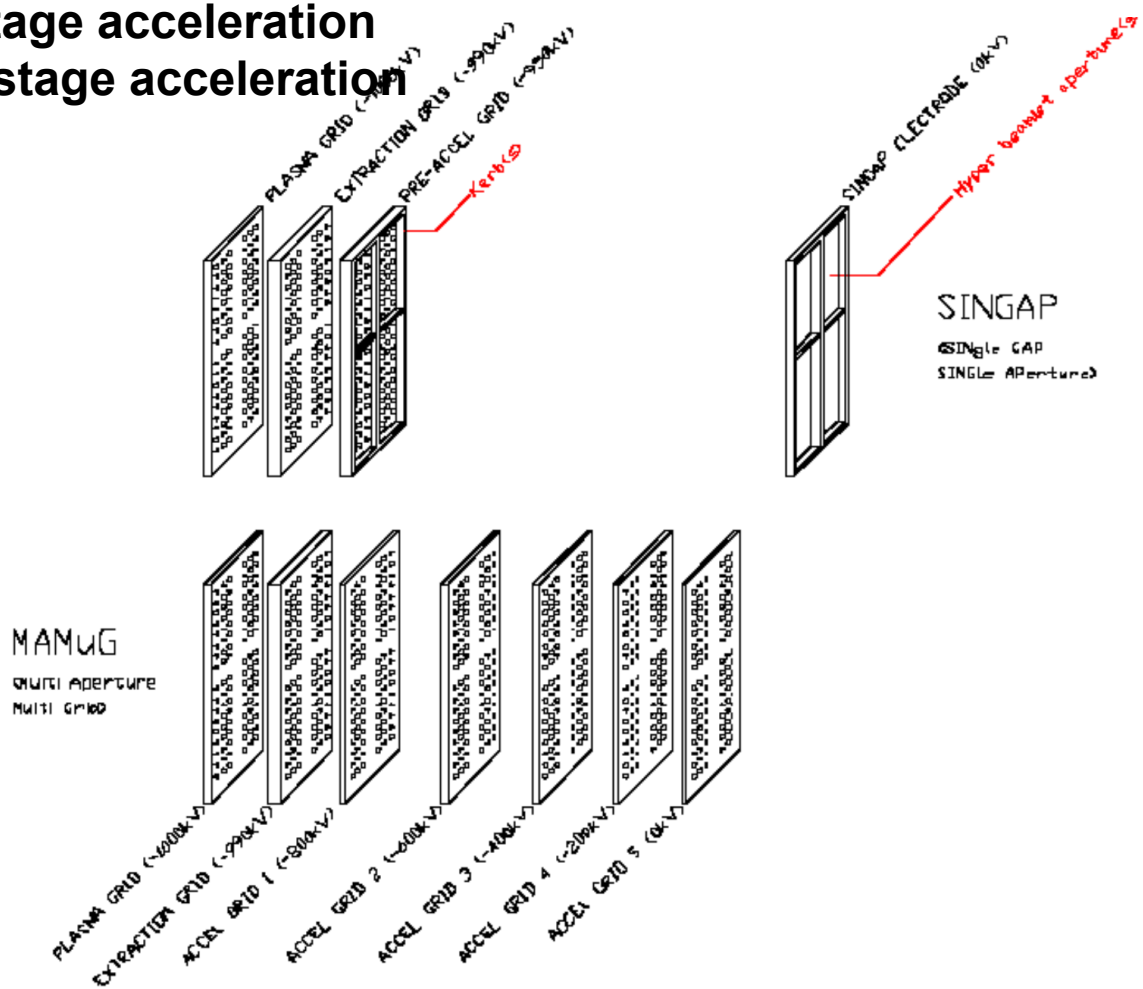

The ITER neutral beam system: status of the project and review of the main technological issues, presented by V. Antoni

NBI system of the LHD fusion machine

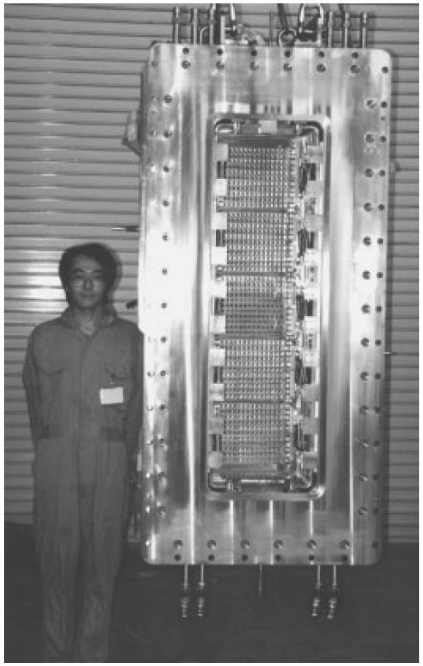

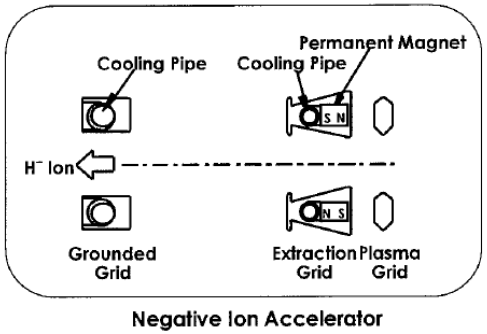

Negative Ion Accelerator

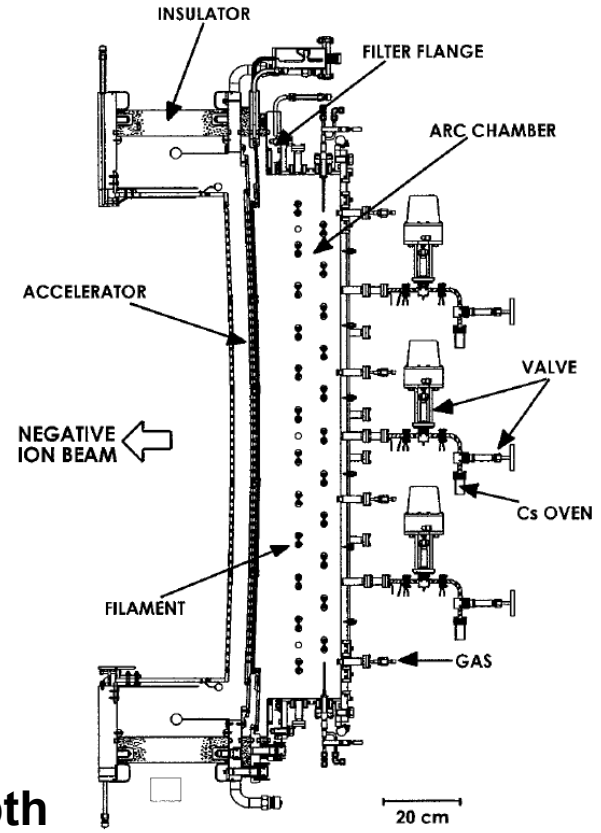

- **180 keV and 30 A**
- **Arc chamber: 35 cm x 145 cm, 21cm in depth**
- **Single stage accelerator**

Y. Takeiri, etc., Nucl. Fusion, 46, S199, 2006

JT60U NBI system

- JT-60 (Japan-Torus) is a tokamak in Japan.
- 550 keV, 22A
- 2m in diameter and 1.7 m in height
- 3-stage accelerator

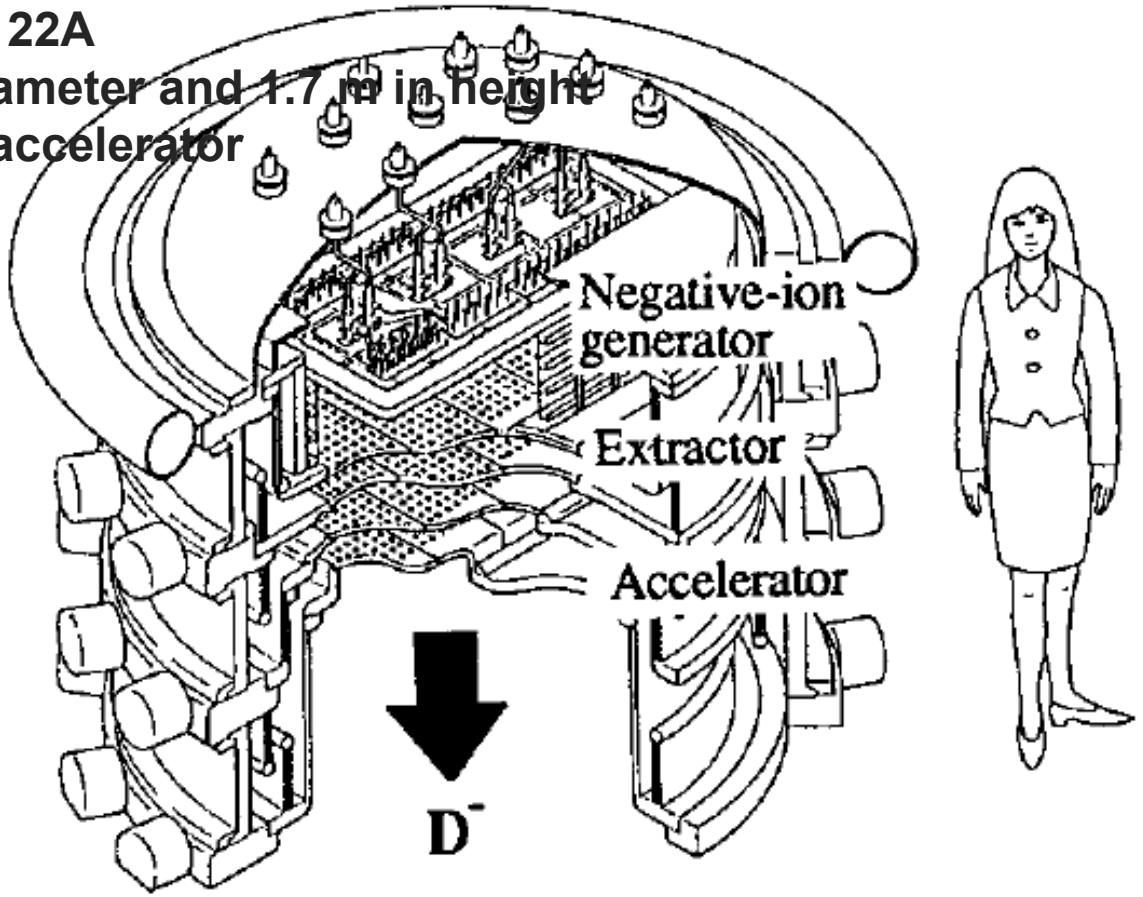

Neutralization

- **Gas neutralization**
  - **Collisions between fast negative ions and atoms**

$$H^- + H_2 \longrightarrow H + H_2 + e^-$$

  - **Fast ions can lose another electron after neutralized**

$$H + H_2 \longrightarrow H^+ + H_2 + e^-$$

- **Plasma neutralization**
  - **Collisions with charged particles in plasma**

$$H^- + X\left(e, \mathrm{Ar}, H^+, {H_2}^+\right) \longrightarrow H + X + e^-$$

  - **The efficiencies reach up to 85% for fully ionized hydrogen plasma**

Beam dump

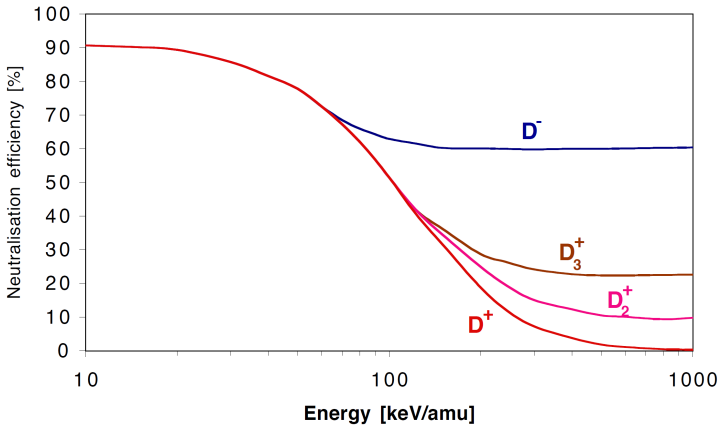

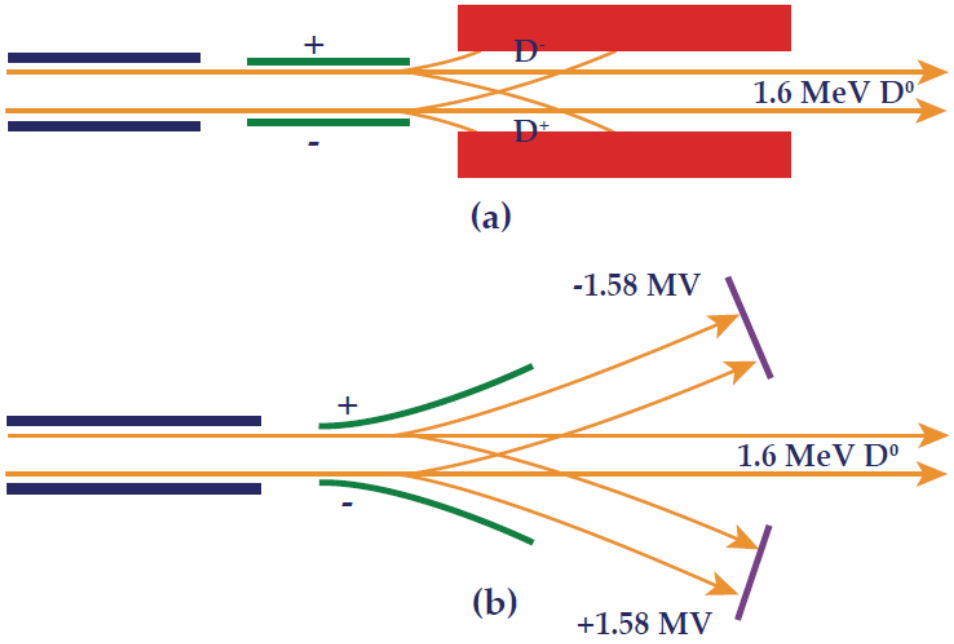

R. W. Moir, Fusion Technology, 25, 129, 1994

NBI for ITER

- **beam components (Ion Source, Accelerator, Neutralizer, Residual Ion Dump and Calorimeter)**
- **other components (cryo-pump, vessels, fast shutter, duct, magnetic shielding, and residual magnetic field compensating coils)**

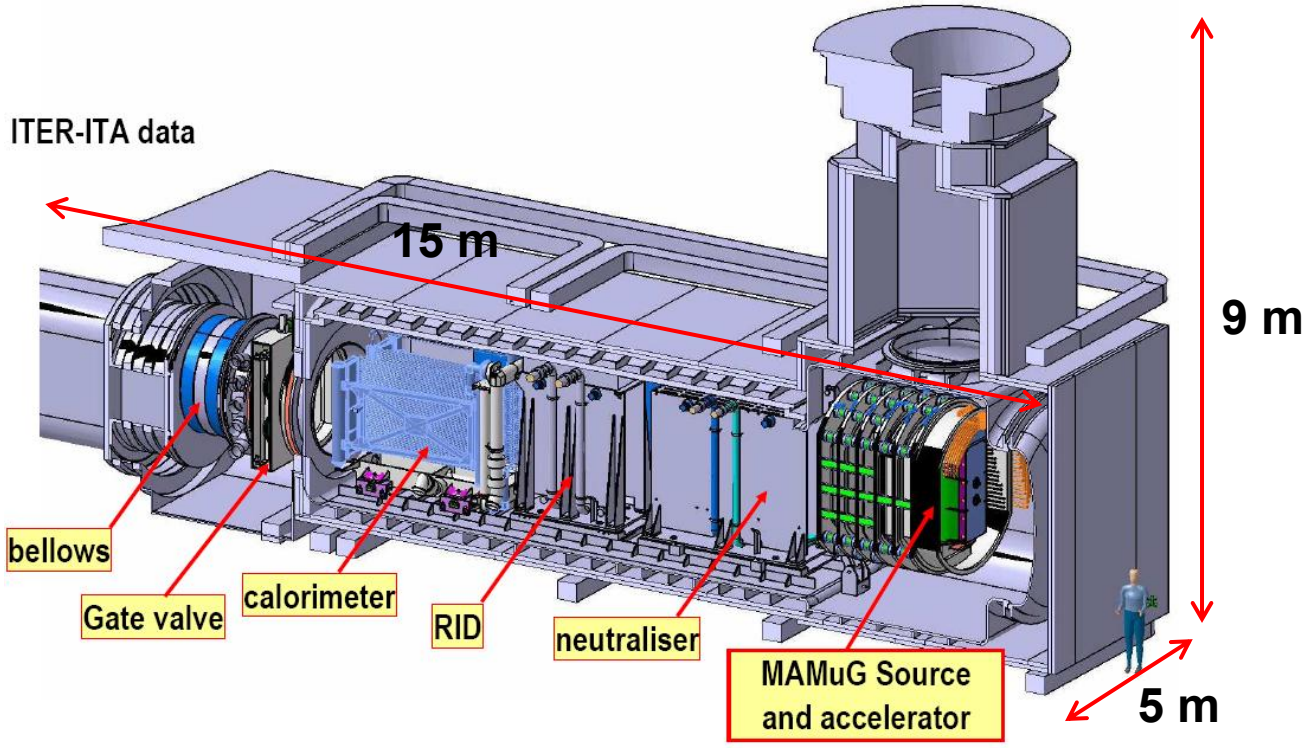

The ITER neutral beam system: status of the project and review of the main technological issues, presented by V. Antoni

Neutral beam penetration

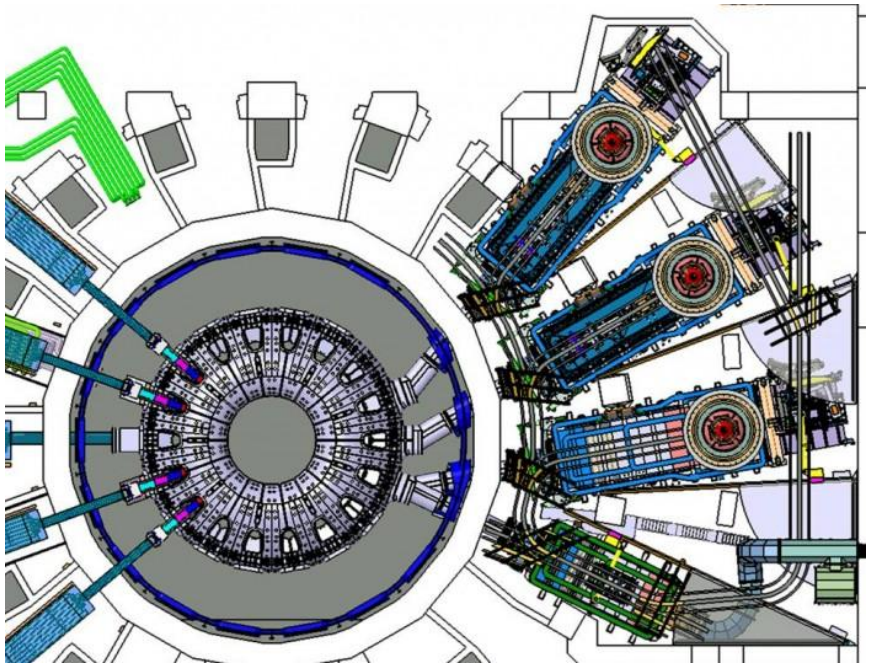

- Parallel direction
  - Longest path through the densest part of the plasma
  - Harder to be built
- Perpendicular direction
  - Path is short
  - Larger perpendicular energies leads to larger losses
  - Easier to be built

https://www.iter.org

Temperature of 100 eV is the threshold of radiation barrier by impurities

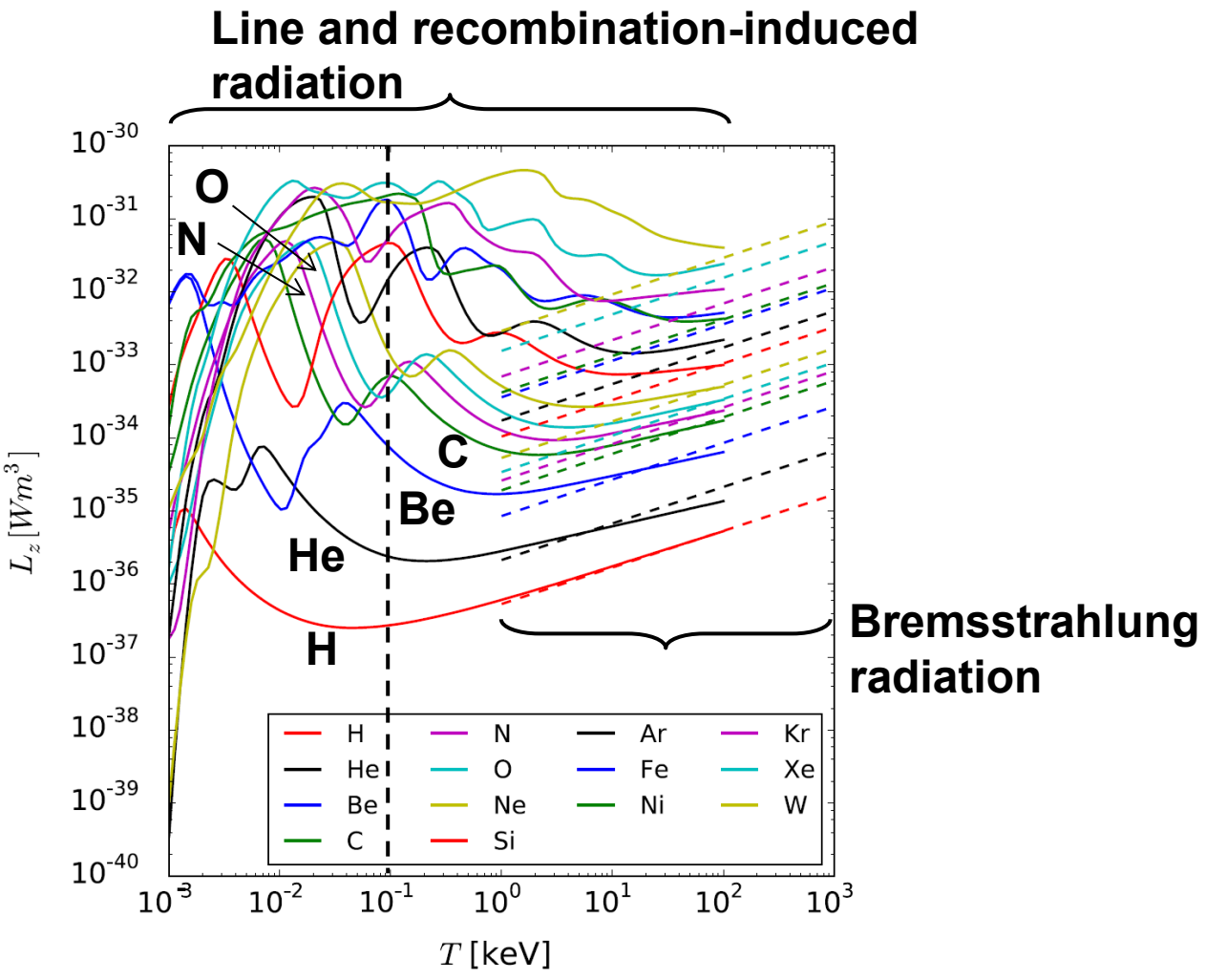

H. Lux, etc., Fusion Eng. Des. **42**, 101 (2015)

A banana current is generated when there is a pressure gradient in the plasma

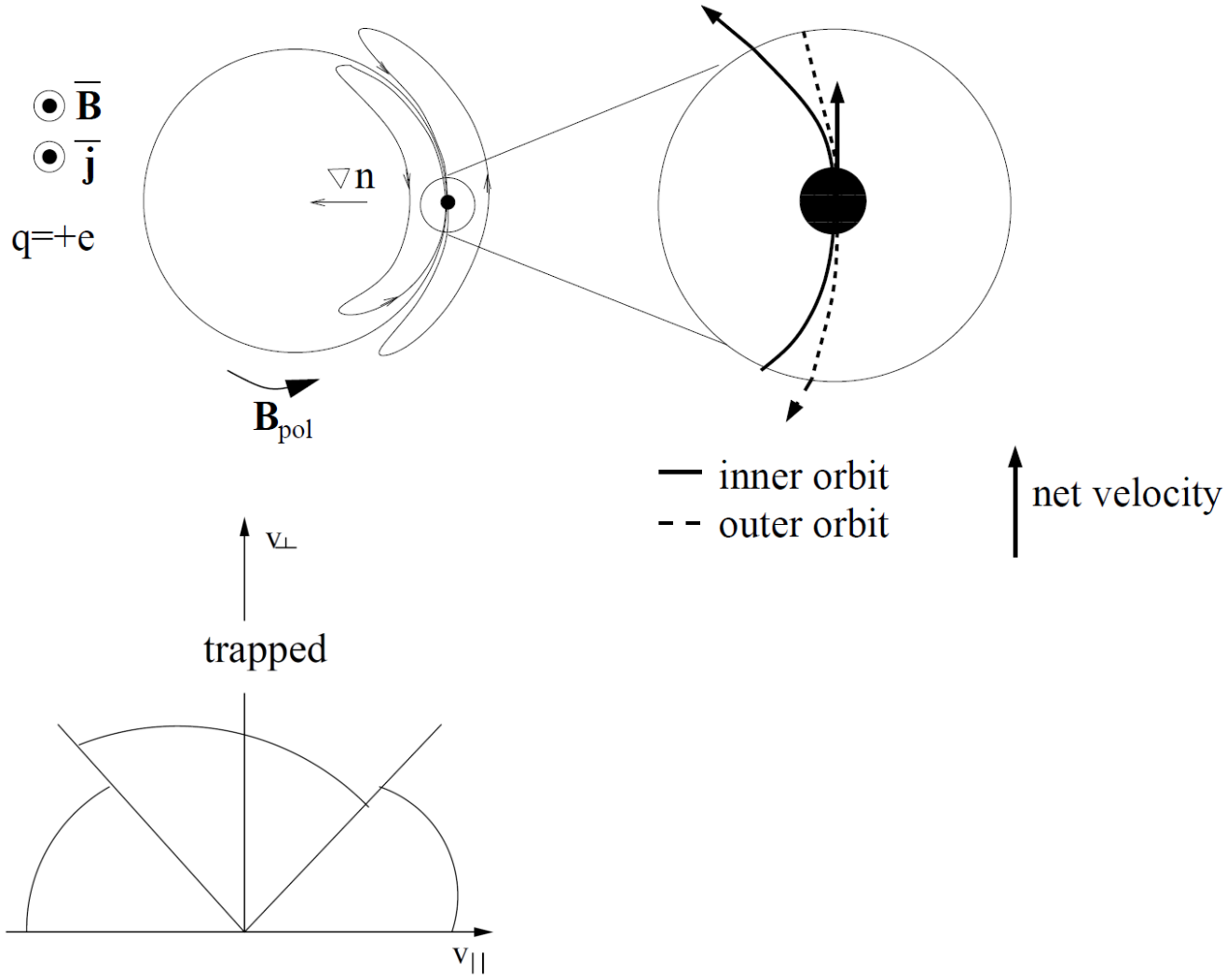

Samuli Saarelma, Helsinki University of Technology, PhD Thesis 2015

Bootstrap current is generated when passing particles are scattered by the trapped particles

- **Scattering smooths the velocity distribution and shifts it in the parallel direction, i.e., a current is generated. It is called the bootstrap current.**

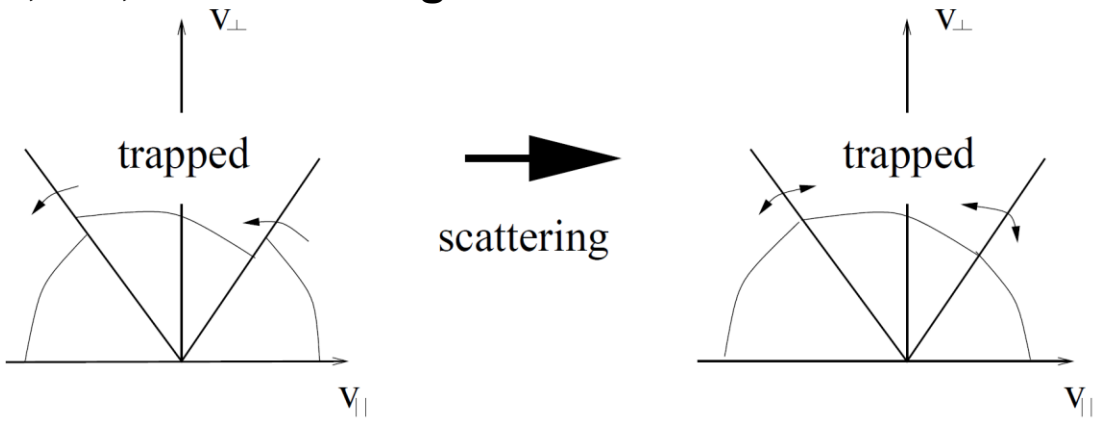

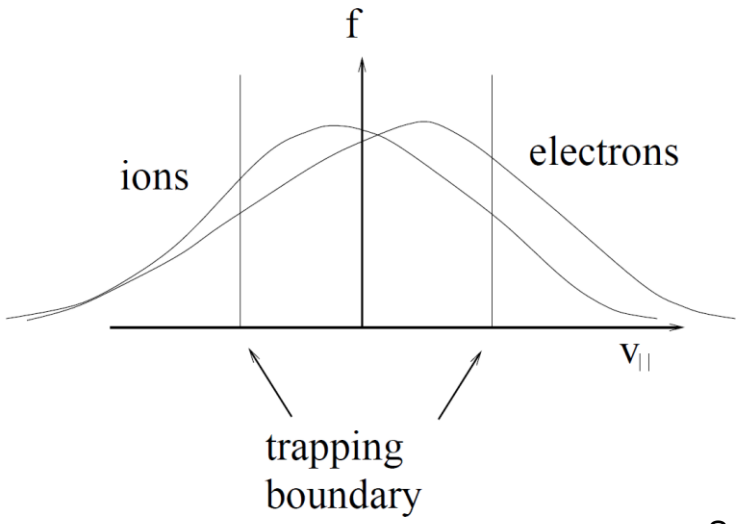

$$j = -enu_{||e} + enu_{||i} = 4\epsilon^{3/2}\frac{1}{B_p}T\frac{dn}{dr}$$

- **The bootstrap current is vital for steady-state operation.**

Samuli Saarelma, Helsinki University of Technology, PhD Thesis 2015

Momentum exchange may be needed to drive plasma current

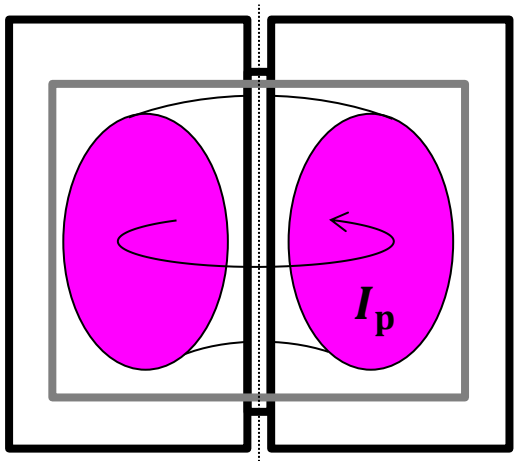

$$\vec{j}_p = \Sigma qn\,\vec{v} = -en_e\,\vec{v}_e + en_i\,\vec{v}_i$$

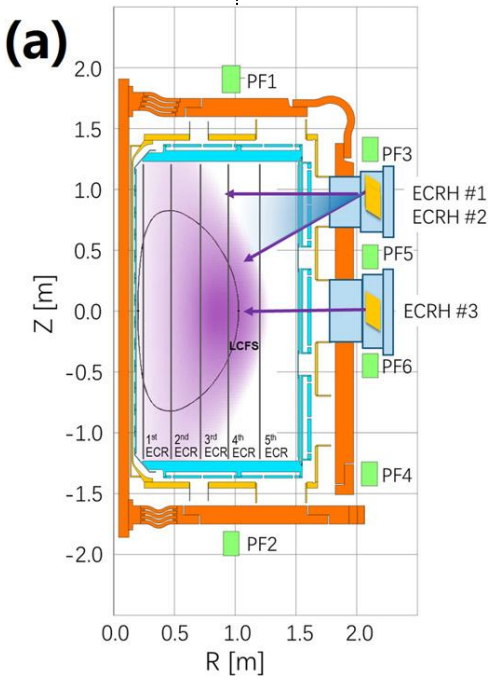

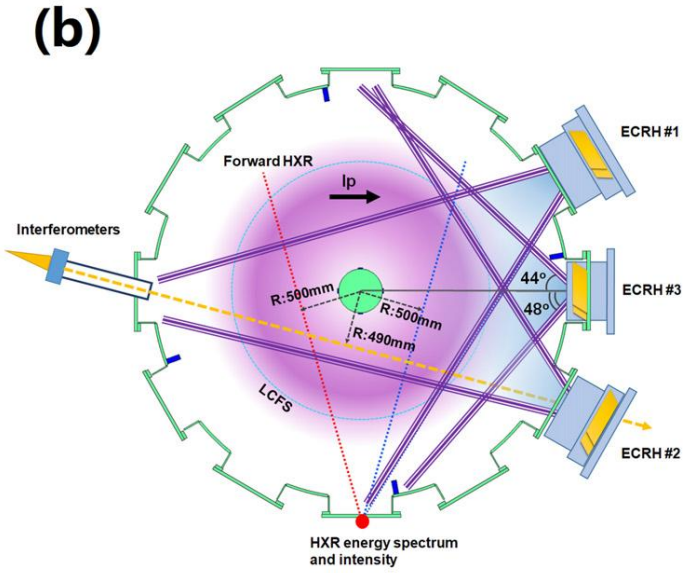

Yuejiang Shi et al, Nucl. Fusion **62**, 086047 (2022)

The collisional re-distribution of the ECRH-driven anisotropy in $E_\perp$ causes some parallel momentum to flow from e^- to ions

- **Coulomb collisions are more efficient at lower energies.**

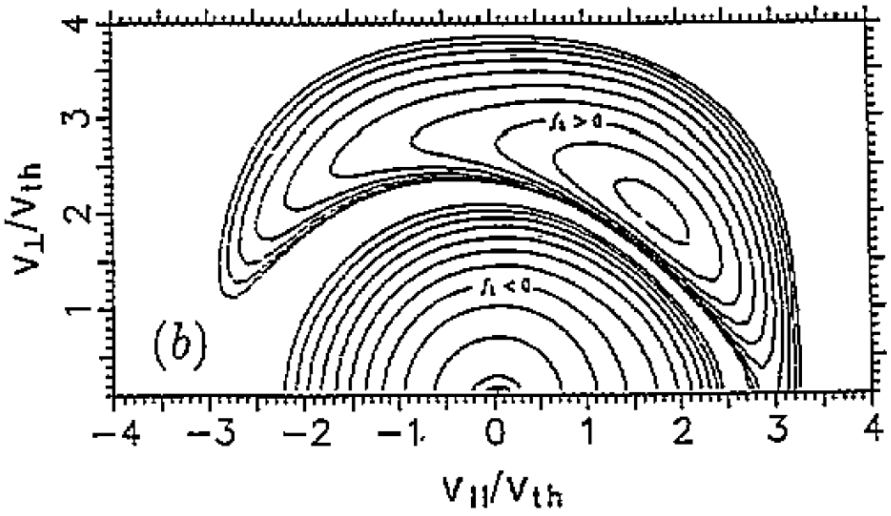

Velocity: $v_2 > v_1$

Collisions: $v_2 < v_1$

- **Electron cyclotron current drive:**

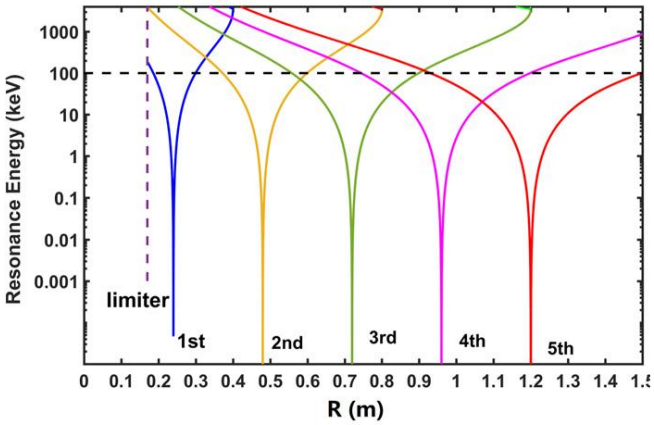

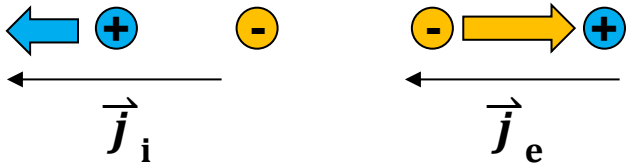

$$\vec{j}_p = -en_e\vec{v}_e + en_i\vec{v}_i$$

$$\vec{P} = n_e m_e \vec{v}_e + n_i m_i \vec{v}_i \approx 0$$

V. Erckmann and U. Gasparion, Plasma Phys. Control. Fusion **36**, 1869 (1994)
Yuejiang Shi et al, Nucl. Fusion **62**, 086047 (2022)

Passing electrons can be trapped if the $v_\perp$ is increased by heating

$$\omega - k_\parallel v_\parallel = \frac{neB}{\gamma m_e}$$

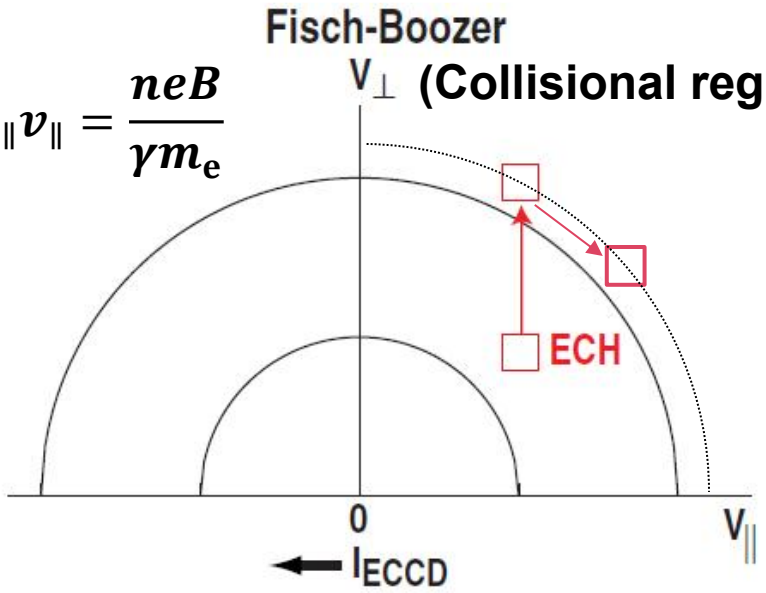

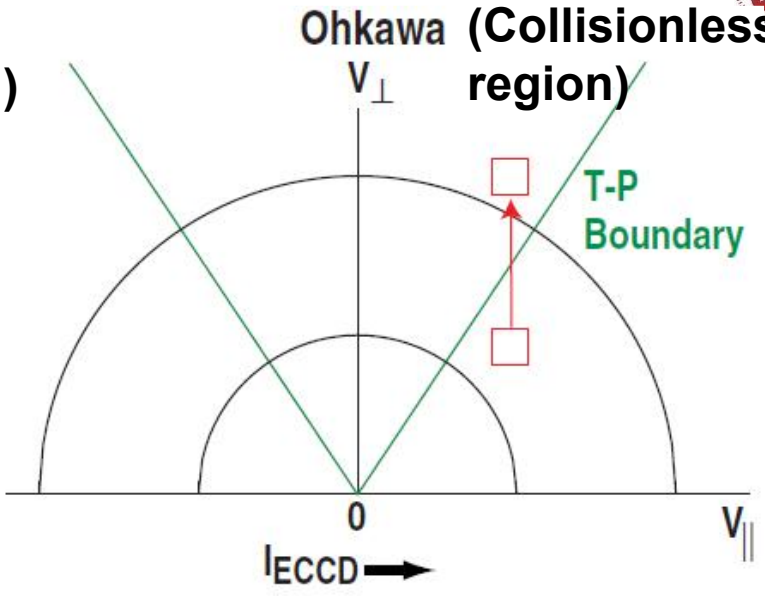

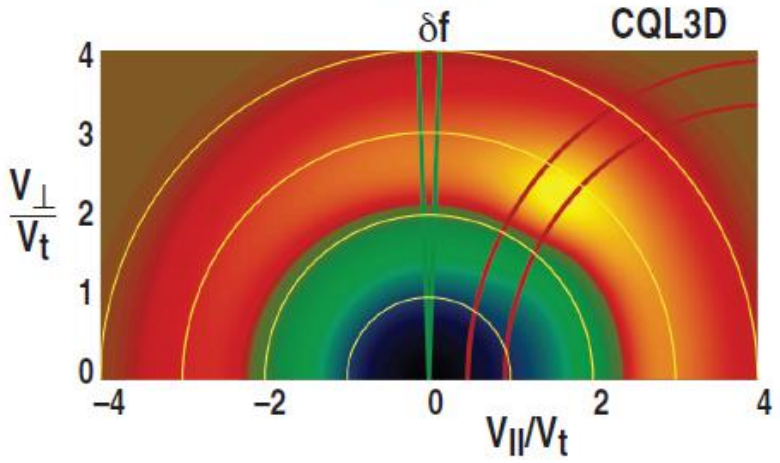

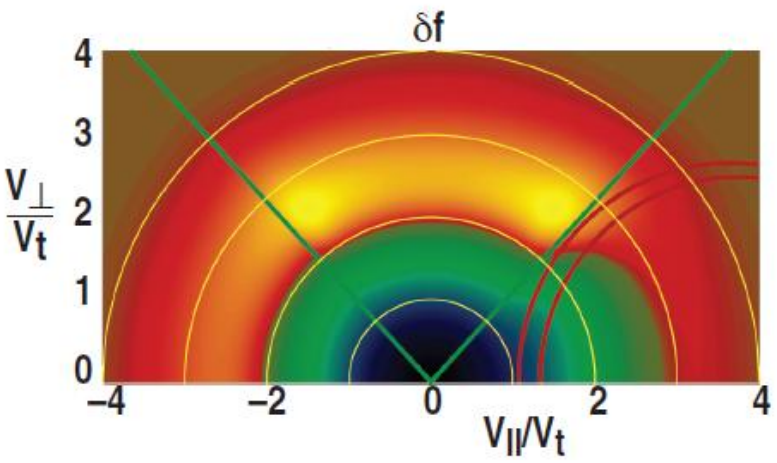

Lecture note "Physics and Applications of Electron Cyclotron Heating and Current Drive" by R. Prater from GA at 6th ITER International School 2012, Institute for Plasma Research, Gandhinagar Ahmedabad, India, December 2-6, 2012

Charged particles can be partially confined by a magnetic mirror machine

- Charged particles with small $v_{||}$ eventually stop and are reflected while those with large $v_{||}$ escape.

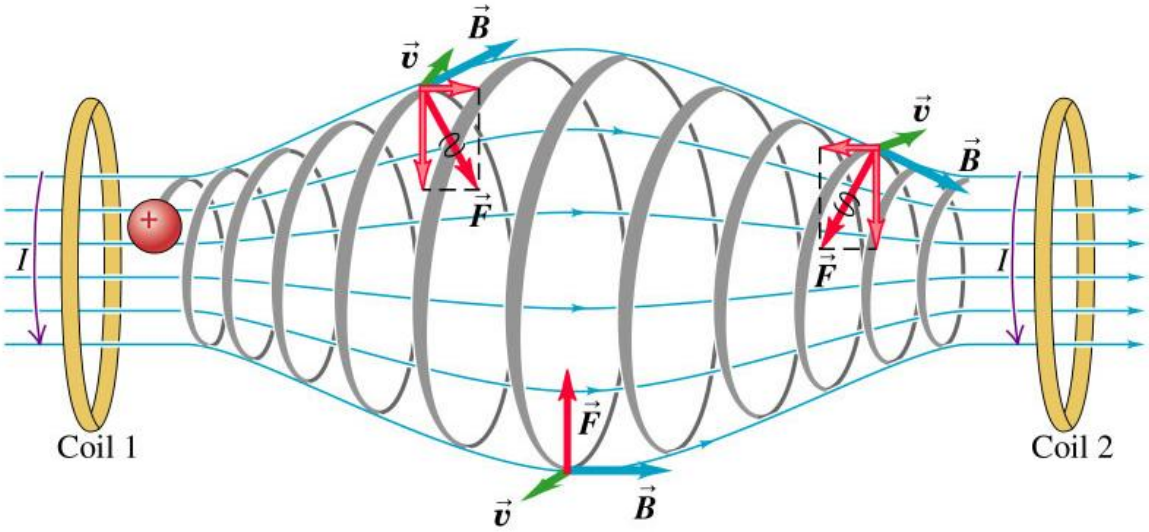

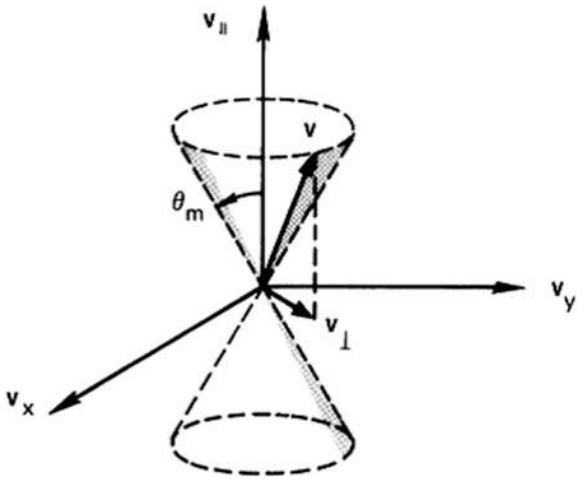

$$\frac{1}{2}mv^2 = \frac{1}{2}mv_{||}^{\ 2} + \frac{1}{2}mv_{\perp}^{\ 2} \qquad \textbf{Invarient: } \mu \equiv \frac{1}{2}\frac{mv_{\perp}^{\ 2}}{B}$$

$$v'_{\perp}{}^2 = v_{\perp o}{}^2 + v_{||o}{}^2 \equiv v_o{}^2$$

$$\frac{B_o}{B'} = \frac{v_{\perp o}{}^2}{v'_{\perp}{}^2} = \frac{v_{\perp o}{}^2}{v_o{}^2} \equiv sin^2\theta$$

$$\frac{B_o}{B_m} \equiv \frac{1}{R_m} = sin^2\theta_m$$

- Large $v_{||}$ may occur from collisions between particles.
- **Those confined charged particle are eventually lost due to collisions.**

https://i.stack.imgur.com/GlzGZ.jpg

The trajectories of charged particles follow the toroidal field lines

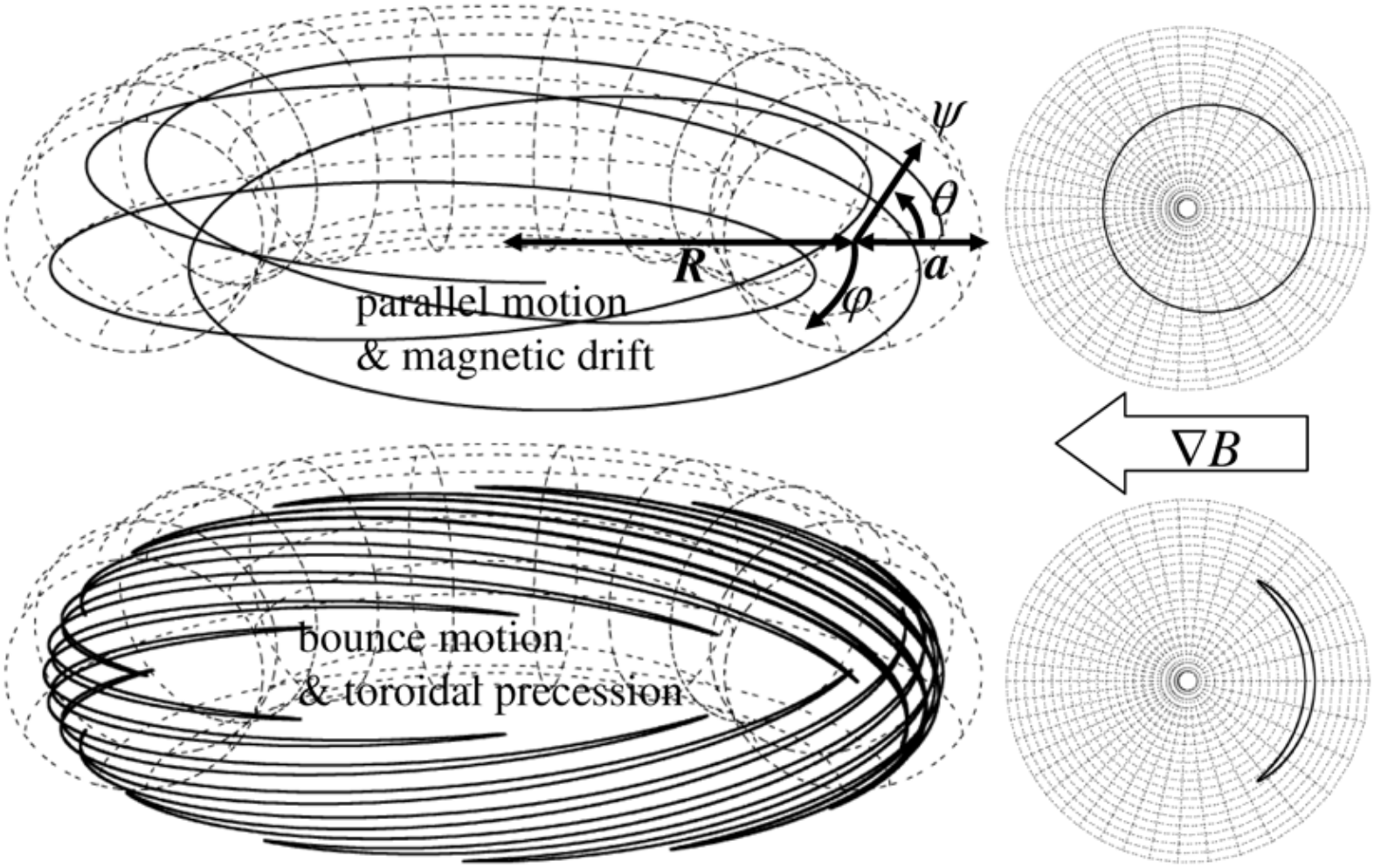

X. Garbet et al, Nucl. Fusion **50**, 043002 (2010)

Comparison of Fisch-Boozer Mechanism and Ohkawa Mechanism

Aspect	Fisch–Boozer Mechanism[1]	Ohkawa Mechanism[2]
Physical Process	Asymmetric heating of passing electrons with subsequent collisional momentum transfer	Selective de-trapping of barely trapped electrons into passing orbits (collisionless mechanism)
Requires collisions?	Yes (collisional mechanism)	No (collisionless pitch-angle scattering)
Key Particle Population	Passing electrons	Trapped (or barely trapped) electrons
Wave absorption location	Depends on Doppler-shifted resonance; typically near magnetic axis or mid-radius	Usually near edge where barely trapped particles are abundant

1 N. J. Fisch and A. H. Boozer, Phys. Rev. Lett. 45, 720 (1980).
2 T. Ohkawa, “Steady state operation of tokamaks by rf heating,” General Atomics Report No. GA-A13847 (1976).

Temperature of 100 eV is the threshold of radiation barrier by impurities

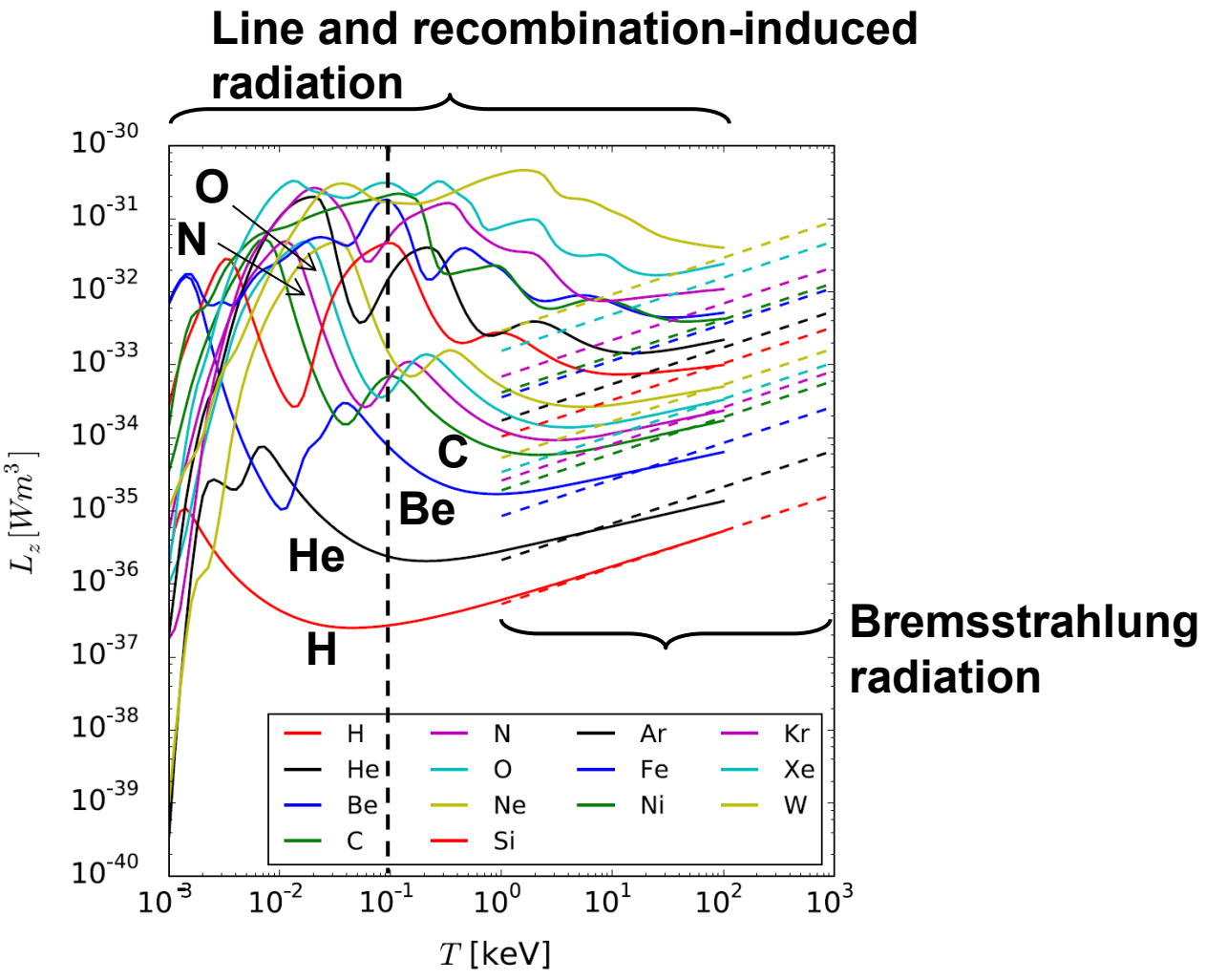

H. Lux, etc., Fusion Eng. Des. **42**, 101 (2015)

Reference for MCF

- **Jeffrey P. Freidberg, Ideal Magnetohydrodynamics**
- **John Wesson, Tokamaks**
- **Tokamak Physics by 陳驊 院士**